

Capacity-Demand Relationships in One-Legged Balance: Biomechanical Analyses

by

Payam Mirshams Shahshahani

A dissertation submitted in partial fulfillment
of the requirements for the degree of
Doctor of Philosophy
(Mechanical Engineering)
in the University of Michigan
2020

Doctoral Committee:

Professor James A. Ashton-Miller, Chair
Assistant Professor Clive R. D'Souza
Professor Andrzej T. Galecki
Professor C. David Remy
Professor James K. Richardson

Payam Mirshams Shahshahani

mirshams@umich.edu

ORCID iD: 0000-0001-6930-6225

© Payam Mirshams Shahshahani 2020

DEDICATION

To my parents, for their love, support, and guidance

ACKNOWLEDGMENTS

First and foremost, I would like to thank my mentor and advisor, Professor James A. Ashton-Miller for his constant support and encouragement in all my years as a graduate student. In addition to his vast knowledge of the biomechanics field, his kind and level-headed presence provided a nourishing environment in the Biomechanics Research Lab where all opinions are heard and considered. My appreciation extends to all my committee members whose comments and help enlightened me and greatly improved this dissertation.

This dissertation would not be possible without the generous support from the Biomechanics Core of the Claude D. Pepper Older Americans Independence Center at the University of Michigan, Graduate Student Instructor appointments from the Mechanical Engineering department at the University of Michigan, and the graduate student research assistant award from the U-M Injury Prevention Center. I also greatly appreciate the friendly and helpful environment that is the Mechanical Engineering department. The work of many staff members from various groups including ME-IT, ME-ASO, ME graduate machine shop, and the ME main office allowed me to focus mostly on my research while all the logistical details involved in research were perfectly handled.

I would like to thank all members of the Biomechanics Research Lab throughout these years, who made our office a friendly and inclusive environment: Mr. Ali Attari, Ms. Sasha Kapshai, Dr. Jinyong Kim, Dr. Mark Gordon, Dr. Hogene Kim, Dr. Yunju Lee, Dr. David Lipps, Dr. Jiajia Luo, Dr. Youkeun Oh, Dr. Melanie Beaulieu, Mr. Nicholas Groeneweg, Mr. Dan Imaizumi Krieger, Ms. Kayla Curtis, Dr. Paige Tracy, Ms. Mariana Masteling, Ms. So Young Baek, Ms. Natalie Deering, Mr. Zizheng (Fred) Zhang, Mr. Ryan Kassel, and Ms. Annalise Lane. Thank you all for the pleasant times we have had together.

Transitioning to life in a new country with a new language was a hard undertaking for me. But my friends from both inside and outside Ann Arbor made it much easier by encouraging me and helping me out in times of need. There are too many to mention. Suffice it to say, thank you all for your friendship and companionship.

Finally, my deepest thanks goes to my parents and sister. I love you all and know that I can never thank you enough for your unconditional love and support during all my life. This dissertation is entirely dedicated to you.

TABLE OF CONTENTS

DEDICATION	ii
ACKNOWLEDGMENTS	iii
LIST OF FIGURES	vii
LIST OF TABLES	xvi
LIST OF APPENDICES	xx
ABSTRACT	xxi
CHAPTER	
1. Introduction and Literature Review	1
1.1 Motivation	1
1.2 A Literature Review of Studies of One-Legged Balance	2
1.3 Knowledge Gaps and Dissertation Overview	12
2. The Feasible Balance Region, a Theoretical Measure of the Physical Strengths Required for Quasistatic One-Legged Balance in Young and Older Adults	14
2.1 Introduction	14
2.2 Methods	17
2.3 Results	23
2.4 Discussion	31
2.5 Conclusions	41
3. One-Legged Balance Experiment and Validation of the Feasible Balance Region	42
3.1 Introduction	42
3.2 Methods	44
3.3 Results	62

3.4 Discussion	69
3.5 Conclusions	82
4. Effect of Age, Gender, and Lower Extremity Strengths on Maximum Voluntary Frontal Plane Acceleration of the Stance Foot during Volitional Unipedal Shuffle Stepping	83
4.1 Introduction	83
4.2 Methods	86
4.3 Results	96
4.4 Discussion	102
4.5 Conclusions	106
5. General Discussion	107
5.1 Dissertation Part I: How do Chapters 2 & 3 Address KG1?	107
5.2 Dissertation Part II: How does Chapter 4 Address KG2?	110
5.3 Comparison of the Effectiveness of Ankle, Hip, and HTS Strategies in Recovering OLB	111
5.4 How May the Lower Extremity Weakness, Shorter UST, and Falls be Related?	113
5.5 Can We Predict Use of the HTS Strategy during an OLB Trial Based on the Methods Used in this Dissertation?	114
5.6 Recommendations for Physiatrists and Physical Therapists	115
5.7 Limitations	117
6. Conclusions	124
7. Suggestions for Future Research	126
APPENDICES	127
REFERENCES	154

LIST OF FIGURES

- Figure 1- Conceptual Model for One-Legged Balance. 6
- Figure 2- Changes to mean normative values for UST across all age groups with (a) eyes open, and (b) eyes closed. Plot copied from [22]. 7
- Figure 3- OLB is one of the common tests of balance in the clinic. However, a UST less than 5 seconds does not reveal which factors are contributing to the poor balance performance. 8
- Figure 4- Transition of the state of COM during a B-U transition. Photo copied from [27]. 10
- Figure 5- Free Body Diagram of quasistatic double inverted pendulum. Maximum ankle inversion/eversion, and maximum hip abduction/adduction moments were found from the literature [20, 38, 39]. For a description of other parameters, please refer to Figure 6 and Figure 7. 17
- Figure 6- Modeling OLB with a double inverted pendulum model in the frontal plane. In this chapter, and the next, the stance foot is assumed to be stationary. **(a)** The links in the double inverted pendulum model are stance leg and the rest of the body. The spine is assumed to be straight without any lateral bending, and the contralateral leg is kept at a neutral abduction angle. **(b)** Parameters of the double inverted pendulum model are from a 50th percentile man ($M_1 = 14$ Kg, $M_2 = 67$ Kg, $l = 57$ cm, $h = 88$ cm, $r = 19$ cm, $\alpha = 56^\circ$) [40]. **(c)** Two independent states are required to describe the double inverted pendulum model for quasistatic OLB (please refer to Figure 7 for more details). 18
- Figure 7- Angles describing the orientation of M_2 in the frontal plane. α is considered constant in this chapter and equal to 56 degrees. Considering the degrees of freedom, only two states are required to uniquely describe the orientation of the double inverted pendulum. It is clear that 19
- Figure 8- Maximum lateral bending of the COM of the HAT due to the lateral bending in lumbar vertebrae (θ_4). Thorax was considered rigid because of the added stiffness due to the rib cage. 22

Figure 9- Calculated quasistatic Feasible Balance Region (FBR) for healthy young (green + yellow + red regions), healthy older adults (yellow + red regions), and older patients with diabetic peripheral neuropathy (red region) for men and women. A point on the plot represents a quasistatic state for the double inverted pendulum model of OLB with a fixed foot link, where θ_1 is the angle that the stance leg makes with the vertical line and θ_2 is the stance leg's hip abduction angle (for more detailed description of the states, please refer to Figure 6 & Figure 7). By definition a quasistatic OLB can only be maintained for the states inside the FBR. The dashed-dot line in the middle is the locus of states for which the COM is in the same vertical plane as the ankle, so no ankle torque is required ($T_1 = 0$). The top boundary for all groups is the locus of points where the pelvic inclination angle is raised a nominal 20° . While in healthy young men and women, and healthy old men the bottom boundary is the locus of points where the pelvic inclination angle is dropped a nominal 20° , in the other groups (healthy old women, and old patients with peripheral neuropathy) it is the maximum hip abduction strength that constrains the lower end of the FBR. The left and right side boundaries are always determined by the medial and lateral margins of the functional base of support, respectively. Please refer to Table 3 for quantification of the FBR for each group. 24

Figure 10- Quasistatic transition from bipedal to unipedal stance. Point P_1 is the state of the person standing on both legs. This state cannot be maintained on one leg because it falls outside the FBR. If the person slowly transitions to one leg, she could take three different general routes. P_1 - P_2 shows a sample trajectory of quasistatic states where the pelvic inclination angle is kept level during the transition, P_1 - P_3 is when it is raised, and P_1 - P_4 is when it is sagged. 27

Figure 11- Predicted effect of $\pm 10^\circ$ medio-lateral bending of the lumbar spine on the FBR of the 50th percentile healthy old man. We can see that a medial (lateral) bending of the lumbar spine shifts the FBR to the right (left). The width of the FBR stays essentially unchanged. Medial bending of the lumbar spine increases the required hip abduction moment for OLB. If the hip abductor muscles are not strong enough, this results in shortening of the FBR. Conversely, lateral bending of the lumbar spine decreases the hip abduction moment and could increase the length of the FBR in the case of weak abductor muscles. 28

Figure 12-Definition of θ 30

Figure 13- Effect of reducing the ankle strength, BOS, and coefficient of friction on the “Feasible Region”. Photo copied from [49]. 31

Figure 14- Joint Specific Endurance Time Plots for Sustained Isometric Loads at Different Intensities (%MVS) (copied from [15]). We can see that a decrease in intensity will increase the endurance time ($ET = b_0(\%MVS)^{b_1}$). Since there are not enough experiments on the fatiguing of the hip abductors, we will instead use the published parameters for the fatiguing of the knee joint in young subjects for our estimations ($b_0 = 19.88$, $b_1 = -1.88$). 34

Figure 15- Effect of Hip Strategy on Extending the Width of the FBR. The yellow region shows the FBR for the 50th percentile old woman. While we predict that quasistatic OLB can only be maintained within the FBR, using maximum abduction and adduction moments in addition to the ‘Ankle Strategy’, we predict that quasistatic OLB can also be ‘recovered’ from the green regions on the two sides of the FBR. The bottom line of the FBR and the recoverable quasistatic OLB states is determined by the maximum hip abduction strength in this Figure. For details of the simulations and criteria for successful recovery of balance, please refer to Appendix II. 36

Figure 16- Effect of limited rate of torque development (RTD) in ankle and hip joints on the predicted recoverable quasistatic OLB states. The blue area shows the quasistatic OLB states that become unrecoverable due to enforcing a limited RTD. We enforced RTD by using a 90 ms rise time for reaching half of the maximum torque from a resting moment [44]. The area with the dashed line is the predicted FBR for the 50th percentile older woman, added here for reference. 39

Figure 17- Effect of latency, in initiation of the predetermined maximum COM acceleration strategy, on the predicted recoverable quasistatic OLB states: No latency (Blue + Green + Red region), 250 ms latency (Green + Red regions), and 500 ms latency (red region). The area with the dashed line is the predicted FBR for the 50th percentile older woman, added here for reference. 40

Figure 18- Overview of the sequence of measurements and experiments for each participant 45

Figure 19- A five link model was used to determine the mass distribution for each subject: one link per shank and foot (m_1), one link per thigh (m_2) and one link for the pelvis, trunk, arms, and head. 52

Figure 20- COG calculated from the force plate and the kinematics of the mass-link model derived from motion capture recordings for a single subject during eyes open OLB trial.

The root mean square error between the two methods for all subjects ranged from 1.5 mm to 14 mm with a mean value of 5 mm. 53

Figure 21- Assuming the body mass to be distributed symmetrically around the sagittal plane, the non-stance ankle is in the same vertical plane as the hip on the same side, and the pelvis is kept at a level inclination angle, the hip abduction moment demand (T_{Abd}) during quasistatic OLB can be estimated as the total body weight times half the inter-acetabular distance.

Please see text for the calculations. 57

Figure 22- Unipedal Stance Time (UST) boxplot for men and women in the young and older groups. 9 out of 10 women and 6 out of 10 men in the young group stood on one leg for four minutes (maximum length of the trial). Only one subject in the old category reached 4 minutes. The black line in the middle of each box is the group median. In this and any following boxplots, the lower and upper hinges correspond to the first and third quartiles (the 25th and 75th percentiles). The whisker extends from the hinge to the largest and smallest value no further than 1.5 times the interquartile range. The data beyond the end of the whiskers are plotted individually. 62

Figure 23- FBR (regions within the green border) and trajectory of the states of the double inverted pendulum model (cloud of pink points) for four different subjects during their OLB trial with eyes open. Opacity of the pink cloud points are related to the frequency of the states where the more transparent points indicate less frequency of occurrence. The blue lines indicate locus of states where the required abduction moment is equal to a constant percentage of the maximum adjusted hip abduction moments for each participant (3.2.2.1). For more details on how FBR is drawn and how each capacity constricts the length and width of the FBR, please refer to Figure 9. S11, S21, S26, and S40 are an older woman, young man, young woman, and an older man respectively. 63

Figure 24- Sample time-series for hip abduction moment (top) and intensity of hip abduction moment demand (bottom) during OLB trial for subject S11. The red line in both plots is the linear model fitted to the time-series to capture the general trend of change over time. The trimmed mean value without 20% of the outliers, the slope of the trend line, and the root mean square of error between the trend line and the data were extracted from both time-

series for each subject (please see 3.2.4.3 for more information on our feature extraction method for time-series). 65

Figure 25- Measured Unipedal Stance Time (UST) vs. measured endurance time at half of each subject's measured maximum voluntary hip abduction strength. If subjects were using more than 50% of their maximum hip abduction muscle strength during OLB trial, then we would expect all the points to fall below the diagonal line with zero intercept and slope equal to one. 68

Figure 26- Measured UST vs. anticipated max UST based on the calculated intensity of the hip abduction moment demand for each subject and the isometric exertion endurance time model parameters for knee and trunk [15, 17]. Knee and trunk fatigue models were used because there are not enough endurance time studies for the hip abductor muscles in the literature. If all the hip abduction moment demand was coming from the hip abductor muscles, then the fatiguing of these muscles would have to keep the points below the diagonal line with zero intercept and slope equal to one. 68

Figure 27- Inman's setup for measuring maximum hip abduction strength with the subject standing and needle and surface EMG data being recorded from the tensor fascia femoris, and gluteus medius and gluteus minimus muscles (Copied from [24]). 74

Figure 28- EMG Action Potential vs. Hip Abduction Torque in Inman's experiment. He noticed that raising the pelvic inclination angle on the non-stance hip side increased EMG activity while letting it drop reduced it to virtually zero activity at about 15-20 degrees. (Copied from [24]) 75

Figure 29- Muscles of the thigh and hip. Picture copied from Sobotta Atlas of Human Anatomy [76]. 76

Figure 30- Demonstrations of load sharing between muscles of the hip and the IT band in bearing the OLB moment demand (A) Equilibrium of moments in the frontal plane due to OLB demand (M_{OLB}), muscles of the hip ($M_{aBd.}$ for abductor muscles and $M_{aDd.}$ for adductor muscles), and the IT mechanism (M_{ITM}) determines the pelvic inclination angle. M_{OLB} and M_{ITM} are mostly functions of γ and θ_2 respectively (please see Figure 7 for their demonstration). On the other hand the muscular abduction and adduction moments are mostly determined by activations of the muscles which are voluntary (*aaBd. and aaDd.* respectively). For simplicity, we assumed the effect of muscles' length changes on their

force generating capacity is negligible in the range of lengths experienced during clinical OLB. **(B)** IT band can be modeled as a spring [78]; assuming no change in pretension from muscles inserting onto the IT band, the force in the IT band can change depending on its length (d) which in turn is determined as a function of hip abduction angle (θ_2). 77

Figure 31- Hip abduction moment demand of OLB for the double inverted pendulum model of OLB from Chapter 2 (blue line) and a hypothetical exponential curve representing the contribution of IT band in resisting the OLB demand moment (grey line). The exponential curve is not based on experimental data and was fitted mathematically based on Inman's observation that the abductor muscles' activity was close to nothing at -20 degree pelvic inclination sag and equal to the OLB demand moment at about 20 degrees pelvic inclination raise (Figure 28 [24]). The numbers on the grey curve show the hypothetical percentage of the OLB demand provided by the IT band. 77

Figure 32- Comparison of the stress-strain curves of young and old specimens and the related regression curves (dotted lines). Copied from [78] 78

Figure 33- Predicted effect of 60% loss of maximum voluntary hip abduction strength (MVS) on the FBR of the 50th percentile man used in Chapter 2. **(A)** Variation of different hip abduction moments during OLB as a function of pelvic inclination angles. All moments were calculated assuming zero ankle torque ($T_1 = 0$ curve in B). The hypothetical contribution of iliotibial mechanism (ITM) to hip abduction moment is the same as Figure 31. We can see that between -10 to 15 degrees of pelvic inclination angle, the sum of ITM and muscle strength moment are not enough to resist the OLB demand. **(B)** The FBR shows two distinctive regions where OLB is possible (green areas). The top portion is for the higher pelvic inclinations angles where the OLB demand is smaller (right side of the thick blue line in (A)), while the bottom portion is for the angles where the passive tissues resist most of the hip abduction moment demand. 80

Figure 34- Heel-Toe Shuffle experiment setup during a lateral HTS trial. Subject starts on both feet with their left foot on the right edge of the force plate (from subject's view point). He first gains his balance on the left leg and then travels the width of the force plate to the other edge (~45 cm). The tester stands on the left side of the subject, prepared to catch him in case he loses his balance. 86

Figure 35- An example of a lateral heel-toe shuffle trial in shoes. The trajectory of the center of pressure (COP) of the stance foot (the red line) has the characteristic zig-zag shape travelling to the left. The local extrema of the COP trajectory were identified to find the times when the COP was closest to the toes (green dots) and the heel (purple dots). Same time points are identified on the ankle position and center of mass projections onto the floor. The range of x values seen here is the same as the width of the force plate. 90

Figure 36- Maximum estimated DTA (or $\Delta\theta AT$, secondary outcome measure of the experiment) for four subjects during their second and third HTS trials in the medial and lateral directions. DTA is the change in COM angular velocity due to torque at the ankle during a single HTS step. During a lateral (medial) HTS, a negative (positive) DTA is needed to arrest a lateral (medial) angular momentum of the body. Since we used maximum measured ankle inversion and eversion strengths as T_1 in the formula for $\Delta\theta AT (= T_1 t_{i+1} + 1 - t_{i1} + ML2)$ the variations within each subject represents the variations in step times ($t_{i+1} - t_i$). For more details on the calculation of DTA from recorded trials, please refer to 4.2.3 .The circle symbols are for the HTS steps where the COP was moving from toe to heel; the triangles are for the heel to toe. S02 and S27 are in the young group (man and woman respectively); S40 and S14 are in the older group (man and woman respectively). 91

Figure 37- Using a semi-periodic function between each consecutive pair of heel/toe time points to fit the trajectory of ankle positions in the medio-lateral position (x_s) for each HTS step. The period of the semi-periodic function for each step was set at $2(t_{i+1} - t_i)$. For more details on the shape of the fitted function and the boundary conditions please refer to the text in 4.2.4.1. 92

Figure 38- Estimated DTH (or $\Delta\theta HTS$, primary outcome measure of the experiment) for four subjects during their second and third HTS trials in the medial and lateral directions. DTH is change in COM angular velocity due to averaged change in velocity measured during a single HTS. During a lateral (medial) HTS, a negative (positive) DTA is needed to arrest a lateral (medial) angular momentum of the body. For more details on the calculation of DTH from recorded trials, please refer to text body in this section .The circle symbols are for the HTS steps where the COP was moving from toe to heel; the triangles are for the heel to toe. S02 and S27 are in the young group (man and woman respectively); S40 and S14 are in the older group (man and woman respectively). 94

Figure 39- Estimated DTH during the first two steps in the medial and lateral HTS experiments categorized by Age Group and Step Type (HT for heel-to-toe and TH for toe-to-heel). Lateral DTH values were multiplied by a negative so their value can be compared with the medial. No significant interaction between Step Type, Age Category, Sex, or Direction was observed. For the results of the linear mixed-effect model fitted to DTH values please refer to Table 13. The black line in the middle of each box is the group median. In this and any following boxplots, the lower and upper hinges correspond to the first and third quartiles (the 25th and 75th percentiles). The whisker extends from the hinge to the largest and smallest value no further than 1.5 times the interquartile range. The data beyond the end of the whiskers are plotted individually. 97

Figure 40- Estimated DTA for the first two steps in the medial and lateral HTS experiments categorized by Age Group and Step Type (HT for heel-to-toe and TH for toe-to-heel). Lateral DTA values were multiplied by a negative so their value can be compared with the medial. 98

Figure 41- Comparison of DTA and DTH during the first two steps in lateral HTS experiments categorized by Age Group and Step Type (HT for heel-to-toe and TH for toe-to-heel). A negative DTH shows that the subjects decelerated during the medial HTS step instead of accelerating. DTH mean is significantly higher than DTA mean across all groups except in the TH Old. For details of the comparisons using contrasts in the fitted LMM, please refer to Appendix VI. Both within-subject and between-subjects variations were significantly higher in the DTH measurements compared to the DTA ($p = 0.005$ and $p < 0.001$ respectively). 99

Figure 42- Maximum DTH value vs. Normalized Hip Internal - External Strength for all the subjects. Hip internal-external rotation strength was the only lower extremity capacity which showed significant correlation with maximum DTH ($p = 0.037$, $R^2 = 12\%$). 101

Figure 43- Maximum DTH measured during the first two steps in the lateral HTS trials vs Unipedal Stance Time (UST) for all subjects. The plot suggests that a long UST is a necessary but not sufficient condition for being capable of producing large DTH values. 103

Figure 44- Coefficient of Damping ($b(\theta_2)$) considered for calculating $TPassive = -b(\theta_2) \times \theta_2$, which enforced the end of hip ROM. Our choice of 1000 for the maximum b and 20 degrees for the start of the rise of b value was arbitrary. However, we checked for the sensitivity of

the recoverable OLB states to these choices (1000 vs 500, and 20 degrees vs 10 degrees) and did not observe a noticeable change in results. 141

Figure 45- Mean hip abduction moment demand (estimated from inverse dynamic calculations) vs. quasistatic estimate of the hip abduction moment (calculated from mean value of r , $\cos(\gamma)$, and M_2). We can see that both estimates are in close agreement with each other ($R^2 = 99\%$). Please see 3.2.3.1 for definitions of the parameters and 2.2.1 for the calculations that show why $M_2 \cdot r \cdot \cos(\gamma)$ is the quasistatic hip abduction moment). 142

Figure 46- Absolute value of the normalized residuals vs. the fitted values for the LMM fitted to DTH measurements in 4.3.2. 149

Figure 47- Experimentally measured DTH vs. the fitted values from the LMM in 4.3.2. 149

Figure 48- QQ-plot for checking the normality of the normalized residuals of the fitted LMM to DTH measurements in 4.3.2. 149

Figure 49- Absolute value of the normalized residuals vs. the fitted values for the fitted LMM to DT measurements in 4.3.4. 151

Figure 50- Experimentally measured DT values vs. the fitted values for LMM in 4.3.4. 151

Figure 51- QQ-plot for checking the normality of the normalized residuals of the fitted LMM to DT measurements in 4.3.4. 151

LIST OF TABLES

Table 1- Cost of injurious falls in the elderly (age > 65 Years) in 2010, in the U.S. Data derived from [1].	1
Table 2- Fall Risk Factors Identified in a Recent Review, Copied from [6].	2
Table 3- Predicted FBR sensitivity to reductions in functional base of support (BOS) and hip abduction strength for healthy young (HY), healthy older (HO), and older patients with peripheral neuropathy (PN) in men and women. A reduction in functional BOS reduces the width of the FBR (FBOS (-20%) column), while a reduction in maximum hip abduction strength may reduce the length (Hip ABd Strength (-20%) column). We define the Length as the length of the zero ankle torque curve. Width is calculated then by dividing the Area by the Length.	26
Table 4- Predicted sensitivity of the calculated α , r, and hip abduction moment to ± 10 degree changes in medio-lateral bending of the lumbar spine and -10° and 30° of contralateral hip abduction for the 50 th percentile man double inverted pendulum model. For the definition of r and α , please refer to Equation 1.	29
Table 5- Hip abduction moment demand of OLB as a percent of maximum voluntary hip abduction strength (% MVS) for healthy young (HY), healthy older (HO), and older patients with peripheral neuropathy (PN) in both men and women. The required hip abduction moment was calculated for point P ₂ in Figure 10 for a level pelvis and zero torque generated at the ankle. The force-length characteristic of the hip abductor muscle-equivalent was included in the calculations.	29
Table 6- Ankle-hip moment coordination for avoiding model medial and lateral falls during OLB	30
Table 7- Predicted extension of the Functional BOS by the Hip Strategy in quasistatic OLB states with a 'Level Pelvis'. The numbers in the 'functional BOS' column refer to the medio-lateral difference in COG position at points P ₂ and P ₅ in Figure 15. The values in the	

‘Extension of FBR width due to the Hip Strategy’ column are the same difference for COG positions between points P₂ and P₆. 38

Table 8- Age, weight, and height of the participants in the OLB experiments. The entries inside the parentheses are the standard deviation for each group. 45

Table 9- Effect of age and sex on the mean (SD) measured left leg isometric strength data without normalization (N.m), normalized by Weight (m), and normalized by Weight and Height (1). **PF**: Plantar-Flexion, **DF**: Dorsi-Flexion, **Inv**: Inversion, **Ev**: Eversion, **Abd**: Abduction, **Int Rot**: Internal Rotation, **Ext Rot**: External Rotation. Adjusted Abd refers to the adjustments made to the maximum hip abduction strength using the hip fatigue test. 49

Table 10- Predicted Feasible Balance Region (FBR) dimensions and success of its boundaries in containing the OLB states for healthy young and healthy older adults in our OLB experiment. The FBR Length, Width, and Area from our cohort of subjects can be compared with those from Chapter 2 which were derived for the anthropometry of a 50th percentile man with strengths extracted from the literature (please see 2.2.1.1 for more details). **The entries inside the parentheses in this Table and all the following indicate the group standard deviation.** The three right columns indicate what percentage of the OLB trial each subject spent within different boundaries of the his/her own FBR: “States inside FBR” includes all the boundaries, “States inside FBOS” includes the bounds set by the functional base of support (i.e. the two long parallel FBR boundary lines in Figure 23), and “States inside Hip Strength” includes the boundary set by the maximum hip abduction strength. OLB states for 4 out of 10 women in the older group and 1 out of 8 men in the young group were completely below the maximum hip abduction strength line in the FBR. In the Discussion we will explore the possible reasons for this observation. 64

Table 11- Descriptive statistics for the time-series of calculated hip abduction moment demand (normalized by weight and half the inter-acetabular distance), and intensity of the hip abduction moment demand (% of adjusted maximum voluntary hip abduction strength) during the eyes open trial for all subjects. The bolded entries are the mean values for the main outcome measure. For detailed description of Mean, Slope and RMSE please refer to Figure 24 and 3.2.4.3. The inter-acetabular distance was measured here by calculating the horizontal distance between the two hip joint centers (which were found functionally from motion capture data, please see 3.2.2.3) while the subject was quietly standing on both legs.

Mean intensity of the hip abduction moment demand during OLB is defined as the mean ratio of the hip abduction moment and the maximum available voluntary hip abduction strength. The difference in maximum voluntary hip abduction strength drives the highly significant age group difference in the calculated Mean and RMSE for Intensity. For a review of the adjustment to the maximum voluntary hip abduction strength please refer to 3.2.2.1. We can also see that the slopes of the hip abduction demand and its intensity are not significantly different from zero. This indicates that even for the long OLB trials, our participants were not alleviating the high hip abduction moment intensity. 66

Table 12- Descriptive statistics for the trend line passing through the time-series of “Pelvic Inclination Angle” and “Lateral Bending of the Trunk” during the eyes open trial for all subjects with UST > 20 s. UST > 20 s was chosen to include only the participant who stood on one leg long enough to feel the effects of muscle fatigue. “Initial Angle” refers to the intercept, Δ is the total change in the trend line value over the full OLB trial (please refer to Figure 24 for demonstration), and RMSE is the root mean square error between the time-series and the trend line. While we see that men in our cohort of participant started the trial at a slightly more raised pelvic inclination angle, the mean initial pelvis inclination angle is not different than level in a meaningful way ([1.5, 5.4 deg] Men and [-1.2, 2.2 deg] Women, 95% Mean Confidence Interval). Also, all four groups slightly dropped their pelvis inclination angle on average for the duration of the OLB trial ([-3.4, -1.5 deg], 95% Mean Confidence Interval). Mean lateral bending of the trunk at the start of the OLB trial was slightly bigger than zero for the Young subjects ([2.0, 4.9 deg] Young and [-0.8, 2.7 deg] Older Subjects, 95% Mean Confidence Interval). In addition, on average all groups laterally bent their trunk further in the duration of the OLB trial ([1.5, 3.5 deg], 95% Mean Confidence Interval). 67

Table 13- Linear mixed-effect model for DTH 98

Table 14- Linear mixed-effect model for the comparison of the DTH and DTA. Last four rows show the difference between DTH and DTA for each of the considered group (Age Category by Step Type interaction). 100

Table 15- Comparison of our estimate of m_2 (percent body weight of the mass balancing over the stance leg) in young men (YM) and young women (YW) with the literature. 144

Table 16- Comparison of the hip abduction strength measured in this study versus published data. If the reported strengths were not normalized by weight, we used the reported mean height and weight in each paper to change it to the normalized by weight format. 145

Table 17- Calculated effect of possible biases in estimation of m_2 , $r \cos(\gamma)$, and maximum voluntary hip abduction strength on the calculated intensity of the hip abduction moment demand. m_2 is the percent body weight of the mass being balance over the stance leg, $r \cos(\gamma)$ is the moment arm of m_2 . We can see that biases in the calculation of the moment arm can create the biggest change in the calculated intensity. The highlighted cells are the unlikely event that all three possible sources of bias act in the wrong direction at the same time. 146

LIST OF APPENDICES

APPENDIX

I. Deriving the Equations of Motion for the Double Inverted Pendulum Model	128
II. Simulation of the Planar Movements of a Double Inverted Pendulum Model with Range of Motion Constraints	140
III. Quantifying the Sensitivity of the Calculated Mean Intensity of the Hip Abduction Moment Demand to Potential Biases in the Calculations	142
IV. Deriving the Equations of Motion for a Single Inverted Pendulum with a Moving Base	147
V. Diagnostic Plots for the Linear Mixed-Effect Model Fitted to Primary Outcome Capacity of the HTS Experiment (DTH)	148
VI. Details of the Linear Mixed-Effect Model Fitted to the Combined Outcome Measures of the Lateral HTS Experiment	150
VII. Telephone Screening Form for Subject Recruitment	152

ABSTRACT

A common screening test of balance is the timed ability to stand on one leg for as long as possible. A balance time of 5 s or less is an indicator that the patient has an elevated risk for fall-related injuries. But why one has to put one's foot down early is not always obvious. The first part of this dissertation is a mechanistic theoretical and experimental study of the physical capacities underlying the ability to balance on one leg. The theoretical study points to the importance of maintaining both hip abduction and ankle inversion and eversion muscle strengths in order to maintain a large enough 'Quasistatic Feasible Balance Region'; the latter is shown to depend largely upon frontal plane ankle muscle strength. When the states get too close to the boundaries of that region, additional recovery strategies are required, including a hip strategy, corresponding to that used in maintaining bipedal balance, and also a different behavior that is termed a 'heel-toe shuffle' in this dissertation.

The dynamics of one-legged balance in the frontal plane were modeled by the equations of motion for a double inverted pendulum. Using published anthropometric and maximum muscle strength data, the model suggests that the hip abduction moment required to stand on one leg is substantial, ranging from 50% of maximum voluntary muscle strength in healthy young men to 82% of the maximum in healthy older women. These results were corroborated by our experimental results from tests of healthy young and older adults. Our analyses suggest that this hip abduction moment demand is not resisted by the abductor muscles alone, but also by the iliotibial mechanism, even for a level pelvis.

The second part of this dissertation concerns the heel-toe shuffle which was occasionally used by 14 of 38 subjects to extend the time they stood on one leg in eyes open or closed trials. We found that all 20 young subjects and the majority of older subjects (13 out of 18) succeeded in performing a heel-toe shuffle locomotion task. The inverted pendulum model suggests that amongst those subjects a single lateral shuffle step was, on average, 2 to 6 times more effective in changing the angular velocity of the body in the frontal plane than exerting maximum ankle inversion moment over the same time interval. So heel-toe shuffle strategy is also at least as effective as the 'Ankle Strategy' and the 'Hip Strategy' in recovering one-legged balance.

Lateral falls onto the greater trochanter are a known cause of hip fracture. It is clear from this dissertation that if one is to avoid a lateral fall while standing on one leg, one needs to be able to use the ankle invertor muscles to rapidly move the center of pressure as far laterally as possible. In addition, one needs to raise the pelvis to medially accelerate the center of mass, and initiate one or more lateral shuffle steps. The clinical implications of this dissertation are that one-legged balance could be tested in two ways: first, the prescribed method in which no arm or foot movements are permitted versus a second, freestyle, method in which any recovery motions are permissible. A good freestyle performance provides confidence in the ability of the patient to recover their balance outside the clinic.

CHAPTER 1

Introduction and Literature Review

1.1 Motivation

1.1.1 Cost of Falls in the Elderly

According to CDC's 2010 cost of injury report, falls in the elderly cost just under 54 billion dollars every year in medical expenses and work hours lost; fatal injury, nonfatal hospitalization, and emergency department treatment and release were the types of injury outcome considered in this report (Table 1). These costs accounted for 74% of all unintentional injury costs in the elderly [1].

Table 1- Cost of injurious falls in the elderly (age > 65 Years) in 2010, in the U.S. Data derived from [1].

Year 2010	Fatal Injury	Hospitalization (Non-Fatal)	Emergency Department Treatment and Release
Medical Cost	\$0.5 B	\$25.4 B	\$5.0 B
Work Loss Cost	\$2.3 B	\$18.4 B	\$2.2 B
Combined Cost	\$2.9 B	\$43.9 B	\$7.2 B
% of Fall Cost to All Injury Costs	45.4%	79.5%	62.6%

Costs of falls are not limited to medical expense and total work hours lost. Loss of independence can be another important consequence of experiencing falls. Both injurious and non-injurious falls are associated with functional declines in 'Basic Activities of Daily Living', and 'Instrumental Activities of Daily Living' in community-dwelling elderly [2]. Also, fear of falling can lead to avoiding exercise and social activities, which in turn will lead to weakening of the muscles involved in mobility and therefore increasing the risk of falls further [3, 4].

1.1.1 Risk Factors for Falls

In a review of 74 studies on fall risk factors, Deandra *et al.* identified 31 risk factors including sociodemographic, mobility, sensory, psychologic, and medical factors and medication

use [5]. Determining risk of falls is a complicated task for there are many factors and interactions involved. For a brief list see Table 2 below.

Table 2- Fall Risk Factors Identified in a Recent Review, Copied from [6].

Intrinsic risk factors for falls	Demographic	Age Gender Race
	Systems	Gait and balance Strength Vision Cognition
	Symptoms/diseases	Dizziness/vertigo Cardiovascular disease Dementia Depression
	Medications	
Extrinsic risk factors for falls	Home Footwear	

Many functional tests have been developed to assess the risk of falling: Timed Up and Go, Berg Balance Scale, the Dynamic Gait Index, and the Performance-Oriented Mobility Assessment, to name a few [6]. One of the most frequently used clinical tests of balance is the Berg Balance Scale [7]. One-Legged Balance Time (OLB) is one of important components of this test. Vellas *et al.* found, in a nursing home population, that the relative risk of injurious falls in people who cannot stand on one leg for more than 5 seconds is 2.1 compared to those who can ($p = 0.03$) [8]. Since the ability to balance on one leg is important for many activities of daily living, it is important to understand the underlying mechanisms that enable humans to perform this activity. At the present time, these mechanisms are not fully understood.

1.2 A Literature Review of Studies of One-Legged Balance

1.2.1 Studying Standing Balance

While ‘balance’ is a commonly used word, it is a vague one and hard to quantify. For example, there is no doubt a professional ballet dancer has better balance than a regular non-athletic person. But can we tell the difference if they are just standing in line to get an ice cream while wearing regular clothes? Probably not. After years of research on human balance, in his review of the literature, David Winter described balance as follows: ‘*Balance is a generic term describing the dynamics of body posture to prevent falling. It is related to the inertial forces acting on the body and the inertial characteristic of body segments (page 194, [9]).*’ So balance

is defined indirectly as one's ability to avoid falls. In the case of standing balance, this implies being able to arrest the whole body momentum in any given direction. Otherwise, the person would have to take a step to avoid falling and will no longer be standing. So we define standing balance as follows:

Standing Balance: *A person's current stance state is 'balanced' if they can reach a quasistatic state in any direction without taking a step.*

In the above definition, 'state' refers to the orientation and velocity of each segment in the human body, *e.g.* arms, legs, trunk, and the head. Then 'quasistatic state' is one where the velocities of the body segments are negligible.

Based on our definition, one's standing balance can only be measured when we make it harder to avoid stepping or falling. In our example, the difference between the standing balance of a professional dancer and a regular person is perhaps easier to see if we ask them both to stand on one leg. In that case the ballerina has many hours of training that allow her to stand stock still with adjustments that are so small that we cannot see them, while the regular person might seem wobbly in comparison because of all the large body segment adjustments they need to accomplish the task. In most biomechanical studies of standing balance, the task of standing is challenged in one of two ways:

1) Challenging Balance by an External Perturbation: An external perturbation is introduced *e.g.*, a sudden pull at the waist or acceleration of the platform on which the subject is standing [10, 11] and the subject's response to the perturbation is then studied. 'Balance performance' could then be quantified as the largest perturbation which the subject can withstand, or the difference between responses quantified at the same level of external perturbation.

2) Challenging Balance by Reducing Effective Strategies and Sensory Feedback: Balancing tasks of different degrees of difficulty are performed and the subject's balance is measured by quantifying various kinetic and kinematic quantities such as body sway and center of pressure movements under the feet. Some of these tasks include standing with eyes closed on firm and soft surfaces, tandem stance, one-legged balance, and balancing on a narrow ridge. For a

thorough review of different types of standing balance studies, please refer to David Winter's review article [9].

In both approaches for measuring balance, we can speculate that having more quasistatic states that can be maintained would make the task of standing balance easier.

Working Hypothesis: *The availability of more quasistatic states where balance can be maintained makes the task of standing balance easier.*

Indeed, it has been shown for bipedal standing that a wider stance decreases the medio-lateral sway of the center of pressure and muscle effort in both quiet standing and in response to different types of perturbations [12, 13].

Any quasistatic stance requires that the center of mass (COM) be kept over the base of support (BOS). It is easy to see why: during quasistatic stance all the inertial loads on the body are negligible except for the weight of the subject. Body weight has a resultant force downward in the direction of gravity and is exerted at the COM. This force is balanced by the resultant pressure force under the feet (COP). The COP can be taken close to the outer edges of the feet/shoes and not beyond them; this area constitutes the BOS. Should the trajectory of the COM on the floor cross the boundaries of the BOS, the body weight cannot be balanced by just the resultant vertical pressure force. Consequently, to keep an upright stance, the subject has to either take a step, in a way to extend the BOS, or has to create a shear force under the feet which can only be achieved by changing the angular momentum of the body [14]. Either way, the subject is no longer standing quasistatically.

Bipedal stance and OLB are similar in the sense that to maintain quasistatic balance, the COM should be kept over the BOS. But in OLB, the BOS is much smaller in the medio-lateral direction (*i.e.* width of the foot vs. the distance between the outer margins of the two feet during bipedal standing). In addition, since the weight of the body minus the stance leg stays medial to the stance hip, a large hip abduction moment is required for maintaining OLB. Such a large moment does not exist in bipedal standing. These differences warrant an independent view of OLB from bipedal standing. In the next sections, we will present a conceptual model of OLB and then review the literature.

1.2.2 What Factors Affect OLB?

When studying OLB, we can think of the human body as a mechanical system. The size and shape of the bones, muscles, organs, and fat in the body determine the mass distribution in this mechanical system. Meanwhile, the properties of muscles, passive tissues (tendons, ligaments, etc.), and their lines of action determine the motor capacities. Sensory systems provide feedback to the central nervous system (CNS) about the current state of the musculoskeletal system. The CNS acts as the control unit which integrates the sensory feedback signals into a decision on how to control this mechanical system in order to perform a task like standing on one leg. Figure 1 shows my simple conceptual model for OLB.

Like any other mechanical system, CNS has to control OLB within the limits set by the capacities of the human body, which in turn can be affected by many factors including age. Some of these limits include:

- 1) Range of Motion:** The range of motion of each joint in the body depends on the stretch limits of the muscles, tendons, and ligaments surrounding it.

- 2) Moment Generation:** Muscles around each joint can generate contractile forces which exert torques about that joint. The maximum torque that can be generated about each joint, and the rate at which it can be created, depend on the moment arm of each muscle, the maximum force that the muscles can exert, and the current position and velocity of the joint within the range of motion.

- 3) Endurance Time:** Muscles can generate moment about each joint for a certain length of time before they get fatigued and require rest. The greater the intensity of the load, the shorter time they can endure it. Endurance time vs. intensity curves have been studied extensively and are usually reported as an exponential or power model (Rohmert's Curve) [15–17].

- 4) Noise and Delay in Biological Signals:** Both sensory feedback and command signals in the body travel at conduction velocities about 50 m/s [18, 19], much slower than electrical signals in electromechanical systems. In addition, all these biological signals contain noise.

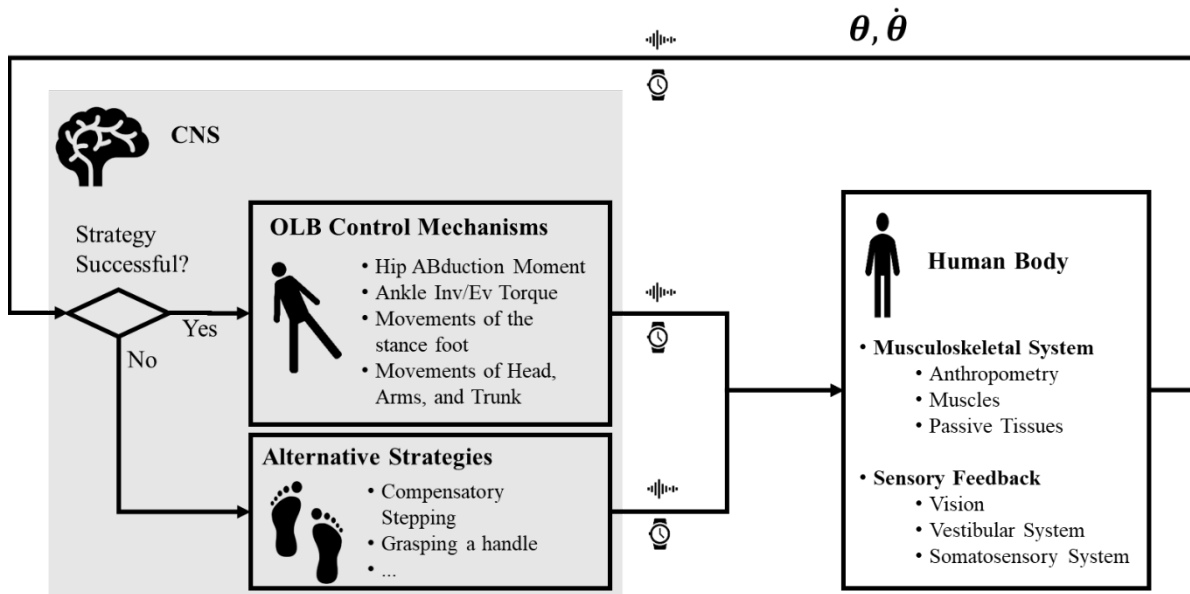


Figure 1- Conceptual Model for One-Legged Balance.

1.2.3 How is OLB Tested in the Clinic?

Currently, a patient's OLB is tested in the clinic by measuring the maximum time he/she can stand on one leg. Normative values for unipedal stance time (UST) decreases with age in adults especially with eyes closed (Figure 2). Regardless of age however, if $UST > 5$ seconds, then the patient has passed the test and is considered to have adequate unipedal balance. But $UST < 5$ seconds does not reveal the cause for failing the test (Figure 3). More importantly, if the clinician diagnoses an irreversible deficit in a patient, he/she would still need to know how much improving other factors can compensate for the deficit. For example, Allet *et al.* showed, in a cohort of patients with diabetic peripheral neuropathy, that hip abductor strength can compensate for imprecise ankle proprioception in predicting UST. Following up the same patients, they then showed that the ratio of hip rate of torque development (RTD) to minimum ankle proprioception angle was a significant predictor of injurious falls (pseudo- $R^2 = 0.38$) [20, 21]. But could we expect a given improvement of hip strength to help each patient's UST by the same amount? Probably not. To answer that question, we need to take a closer look at the mechanics of OLB.

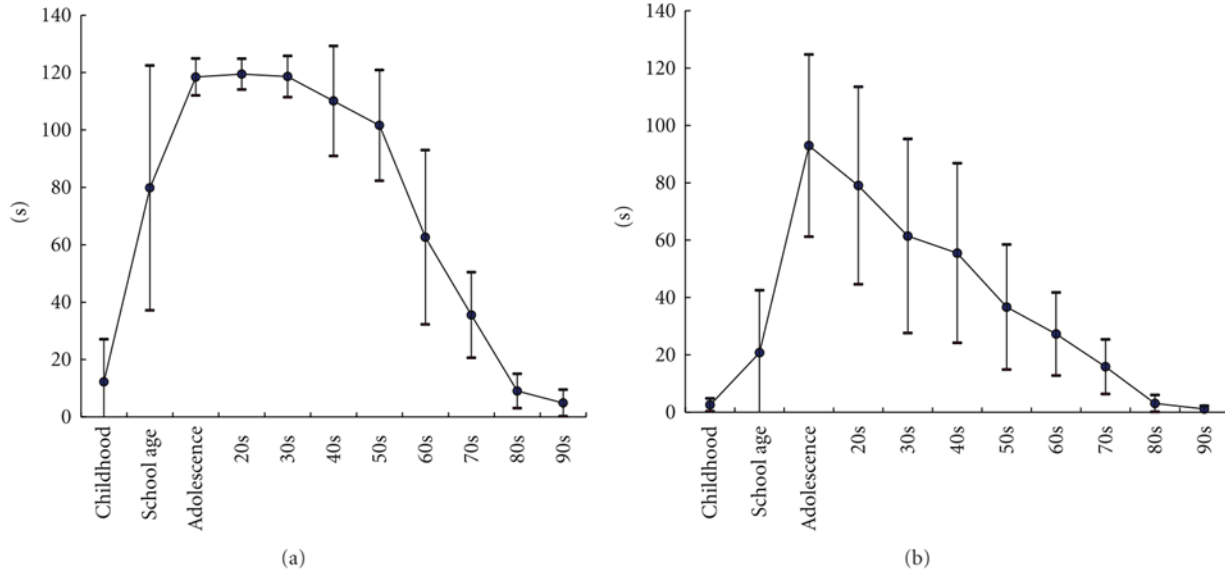


Figure 2- Changes to mean normative values for UST across all age groups with (a) eyes open, and (b) eyes closed. Plot copied from [22].

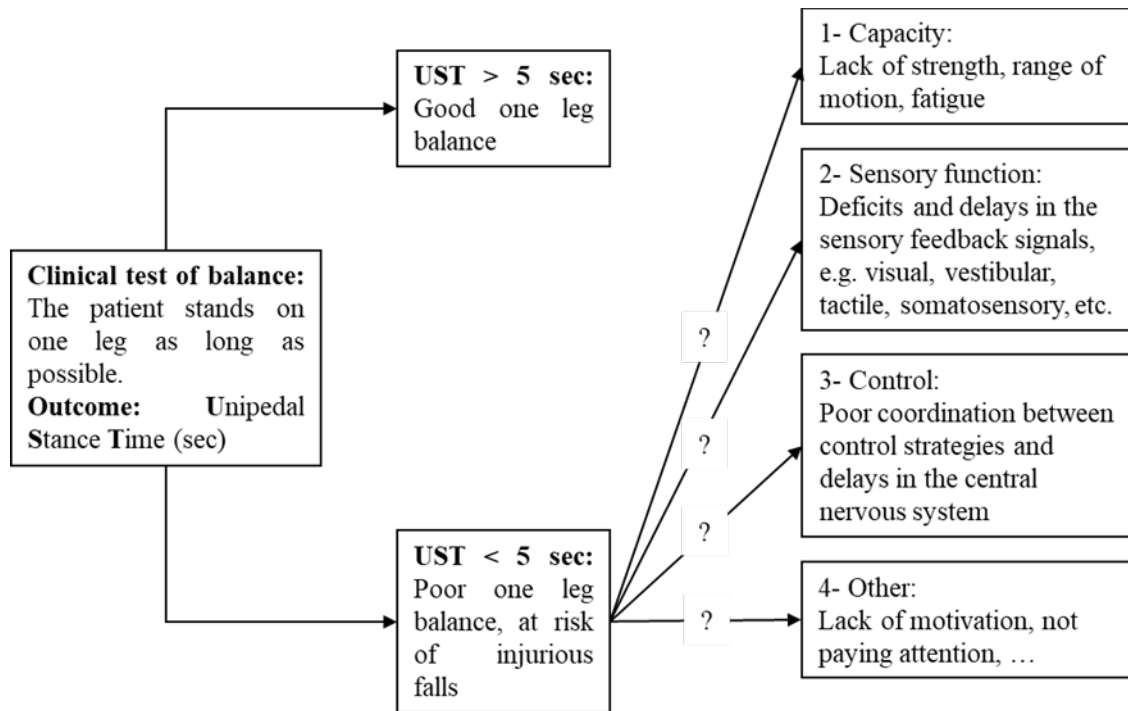


Figure 3- OLB is one of the common tests of balance in the clinic. However, a UST less than 5 seconds does not reveal which factors are contributing to the poor balance performance.

1.2.4 OLB and Lower Extremity Strength

On the one hand, OLB can be used as a functional test to predict injurious falls; on the other hand, in a review of 16 articles on fall risk factors, Rubenstein et al. identified lower extremity weakness as the most potent risk factor for falls amongst the elderly; it increased the odds of falling by more than four times (4.4, range: 1.5:10.3) [23]. But we do not have a measure of how leg strengths contribute to one's ability to balance on one leg.

In a seminal 1947 paper, Inman calculated the theoretical minimum hip abduction moment during OLB to be equal to *weight of the person times half the inter-acetabular distance* [24]. He measured maximum standing hip abduction moment in 35 subjects while measuring both surface and needle EMG of muscle activity in their main hip abductor muscles, namely tensor fascia femoris, gluteus medius, and gluteus minimus. In subjects who stood on one leg with a 'level pelvis', he observed that the empirical abduction moment calculated from the muscle activity was considerably lower than the theoretical moment that he calculated. In a follow up experiment he observed that letting the contralateral hip 'sag' by 15-20 degrees reduced the abductor muscle activity to almost zero, and reversely 'raising the pelvis' by the same amount would increase the muscle activity. This is contrary to the mechanical demands of

standing on one leg. Dropping the non-stance hip increases the moment arm of the head, arms and trunk over the stance hip while raising it would decrease the arm and therefore decrease the abduction demand. Inman concluded that only a ligamentous pull from the iliotibial band could explain the disparity.

In 1970 Charnley and McLeish made detailed calculations of the hip abduction moment during OLB in three subjects and showed that lateral bending of the torso, raising/sagging the pelvis, and holding out an arm can significantly affect the hip abduction demand of OLB [25]. While their calculations agree with Inman's, they refuted his theory of a ligamentous pull, arguing that people are nowhere near the end of their hip adduction range of motion while they are standing on one leg and therefore, there could be no passive tissue involved in providing the abduction moment. They cited the technological limitations in the measurements of muscle activity in Inman's time as a possible reason that he observed reduced muscle activity while subjects' non-stance hip sagged, but they did not conduct their own EMG study to confirm their hypothesis. In 2014, Prior *et al.* made the same observations as Inman's: while standing on one leg, dropping the non-stance hip decreased the abductor muscle activity measured by surface EMG (tensor fascia lata and gluteus medius in this case) while raising it would increase the activity [26].

1.2.5 Strategies for OLB

A successful OLB test requires a successful transition from both legs to one, and once on one leg, being able to maintain the unipedal stance. Let us take a closer look at these two phases.

1.2.5.1 Bipedal to Unipedal (B-U) Transition

In his dissertation, Son [27] showed that there are two dominant strategies for transitioning from two legs to one: 1) slowly shifting weight to the stance leg, by loading the stance hip abductors and reducing the weight on the contralateral foot down to zero, and 2) pushing off with the contralateral foot and using the momentum to land on the stance leg. Elderly subjects (age > 65 years) tended to use the first strategy more often; young subjects (age between 20 to 30 years) preferred the second. Both young and older subjects could fail during the transition, but the young usually made rapid adjustments, and succeeded in the very next trial, while the elderly needed a few more. Son then used a computational model of an inverted pendulum to study the B-U transition. He showed that both young and older subjects tried to bring the state of their COM in a diamond shaped controllable region in the velocity/position

space. The dimensions of this controllable region was determined by the maximum ankle inversion/eversion torques (Figure 3). He also found that COM velocity at the moment of lift off was enough for both young and older subjects to determine an impending failure of their B-U transition [27].

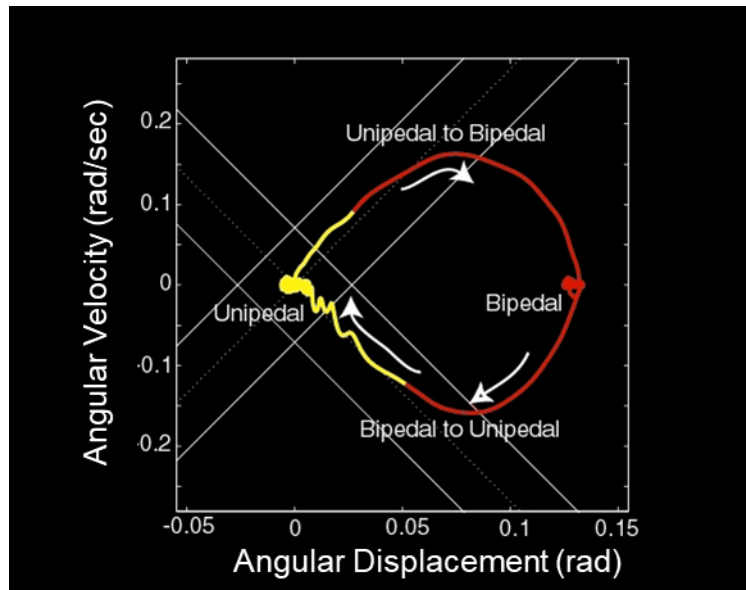


Figure 4- Transition of the state of COM during a B-U transition. Photo copied from [27].

1.2.5.2 Balancing on One Leg

Once already standing on one leg, the central nervous system (CNS) has to control the muscles around each joint to coordinate the generation of the right amount of moments to keep the body upright. Two control mechanisms have been identified for maintaining the upright stance during OLB: ‘Ankle Strategy’, and ‘Shear Force Strategy’. In what follows we take a closer look at each of them.

1) ‘Ankle Strategy’, Controlling COP of the Stance Foot by Ankle Inversion/Eversion Moments, the First Control Mechanism of OLB

Hoogvliet and Tropp *et al.* separately showed that ankle torque is the main mechanism that controls the position of the COP under the foot during OLB [28, 29], and therefore called this control mechanism the ankle strategy, a term used more often in the literature for control of bipedal balance in the sagittal plane [30]. During OLB a torque at the ankle, changes the position of the center of pressure (COP) within the BOS, which in turn controls the position of the COG

and keeps it away from the boundaries of the BOS. If the ankle muscles are strong enough, the subject can bring the COP close to the medial/lateral margins of the stance foot/shoe. On the other hand if the ankle muscles are weak, they cannot move the COP all the way to the medial/lateral margins causing them to act as if they had a smaller BOS. King *et al.* used the term “Functional Base of Support” to address the relationship between ankle strength and the area under the foot where the COP can be taken voluntarily [31]. Here is how we define it for OLB:

Functional Base of Support during OLB: *The area under the stance foot where COP can be taken while maintaining balance on one leg.*

Using the ‘Ankle Strategy’, we can closely regulate the position of the COG by small adjustments of the COP within the functional BOS. Therefore, while in quasistatic balance, ankle strategy can be used without the need for substantial dynamic movements of the limbs.

2) ‘Shear Force Strategy’, Modulating Shear Forces under the Stance Foot, the Second Control Mechanism of OLB

King *et al.* observed two different periods for the states of the ankle of the stance foot during OLB test of subjects with eyes closed: periods of extreme and non-extreme ankle displacements [32]. Extreme ankle displacements were defined as any instant when the ankle position was more than ± 2 SD away from the mean ankle joint position. They calculated almost the same ankle torque range being exerted in both scenarios, but observed a substantial increase in the range of shear forces measured under the stance foot during the extreme displacements. They concluded that in addition to the ankle strategy, subjects used the shear force accompanied by the extreme ankle displacements for maintaining their balance. However, they did not investigate the mechanism that created the shear force corrections.

In his experiment, Otten reduced the functional BOS by having the subjects stand on one leg on a narrow ridge oriented in the sagittal plane that was only 4 mm wide. He showed the COG went up to 40 mm beyond the edge of the ridge (which is the BOS in this experiment), while the subjects still managed to control their balance [33]. He concluded that ankle strategy is not the only available mechanism for OLB. He then showed that torques at joints other than the

stance foot ankle can create shear forces under the stance foot which regulate the movements of the COM. He also showed that the stance hip is the most effective joint for creating corrective shear forces under the foot.

Hof modeled standing balance in humans (one leg and two leg stance) with a general multi-segment mass-link system [14]. Using planar dynamic equations of motion, he identified 3 distinct methods available for controlling the balance during upright stance: 1) moving the COP under the feet, 2) counter-rotating other segments like arms, non-stance leg, the head, and the trunk to create shear forces under the feet, and 3) using external forces such as holding a hand rail, or a cane [14]. The third option is obviously not available during one leg stance. He measured the contribution of each of the first two methods from force plate measurements, and showed that the relative contribution of the second method can be substantial during OLB.

The shear force under the stance foot can only be generated as a result of a change in the angular momentum of the body. The larger the rate of change, the larger the shear force. Therefore, to use the ‘Shear Force Strategy’, the person standing on one leg has to make rapid dynamic movements of the body and the non-stance limbs. Clearly, ballerinas balancing on one leg do not need to use such strategies.

1.3 Knowledge Gaps and Dissertation Overview

1.3.1 KG1: Can strength and range of motion affect OLB time?

Physical capacities, such as lower extremity strength and range of motion, are modifiable risk factors for falls [34]. The same cannot be said about all risk factors of falling [35]. On the other hand, OLB has been shown to be a useful functional test for predicting injurious falls. Currently, there are no measures for the effect of physical capacities on one leg balance time other than the functional base of support. Such a measure could be used in determining if improving a certain physical capacity could compensate for other irreversible deficiencies in each patient with balance problems. (Chapters 2 and 3)

1.3.2 KG2: Are there any as yet unrecognized strategies for extending OLB time?

My simple calculations (Chapter 4) suggest that if one could move the stance limb medio-laterally, it might constitute a very effective way to maintain OLB. In early experiments on OLB that we conducted in volunteers, we realized that this very movement of the ankle was being used by individuals to recover their OLB - by shuffling their stance foot medially or laterally. This was especially pronounced with eyes shut trials. We called this the “heel-toe

shuffle” (HTS). One goal of this dissertation was to find out how effective the HTS could be in controlling OLB. We are not aware of any studies that identify the stance foot HTS as a possible mechanism for maintaining or recovering one-legged balance.

In Chapter 2 we derive the equations of motion for OLB and address KG1 by introducing the quasistatic Feasible Balance Region (FBR) as a theoretical tool for visualizing how ankle and hip strengths affect the states where a person can maintain OLB.

In Chapter 3, we will describe the OLB experiment with 38 subjects to a) measure the trajectory of each subject’s OLB states and determine how well they fits the theoretically driven FBR from Chapter 2, and b) examine the role of hip abductor fatigue on the FBR and the maximum OLB time.

In Chapter 4, we address KG2 by describing the heel-toe shuffle experiment and show that it can be at least as effective as the ‘Ankle Strategy’ in changing the lateral angular momentum of the body.

Chapter 5 is the general discussion for the entire dissertation. In Chapter 6 we present the concluding remarks, and in Chapter 7 we present suggestions for future research.

CHAPTER 2

The Feasible Balance Region, a Theoretical Measure of the Physical Strengths Required for Quasistatic One-Legged Balance in Young and Older Adults

2.1 Introduction

The ability to transfer weight from two legs onto one and then maintain so-called one-legged balance (OLB) for as long as possible is a common clinical test to assess a patient's balance and risk for falling. OLB not only is challenging because it has a narrower functional base of support (BOS) in the medio-lateral direction compared to bipedal stance, but also because it requires a significant hip abduction moment to be generated to maintain equilibrium. That demand for hip abduction moment stems from the center of mass of the head, arms, trunk, as well as the non-stance leg, being located medial to the stance hip during OLB. It is unclear when a patient loses OLB early which of the two demands was the more taxing or how those demands interact to end OLB. This raises two important questions:

1) How much hip abduction strength is required for maintaining an OLB posture?

This question has been addressed in the orthopedic literature by considering the hip abduction moment required to maintain OLB as a way of estimating the daily loads and stresses on the femoral head and acetabulum needed to design a hip prosthesis of adequate strength. For example, in 1947 Inman estimated the hip abduction moment demand during OLB when standing with a level pelvis and a straight trunk was equal to the weight force of the person times half the distance between the left and right hip joint centers [24]. In 1970, Charnley and McLeish meticulously verified Inman's calculations experimentally with three subjects, but also showed that the hip abduction moment demand greatly depended on the 'pelvis attitudes' [25]. By pelvis attitude they meant the inclination of the pelvis with respect to the horizon during OLB. However, they did not quantify the relationship between the pelvis attitude and the required hip abduction moment. Neither did they express the hip abduction moment required during OLB as a proportion of the maximum voluntary hip abduction isometric strength. Knowing the normative

values for this proportion could be helpful in guiding rehabilitation efforts for patients with balance problems stemming from lack of lower extremity strength [20, 34].

2) Might the unipedal stance time (UST) be affected by fatigue of the hip abductor muscles during OLB?

Muscle fatigue that develops as the result of a more-or-less constant external moment at a joint has been well-studied in the fields of ergonomics and physical therapy because of the propensity to develop musculoskeletal pain if the moment is too large [36, 37]. In general there is an inverse relationship between the ‘Intensity’ of the isometric load¹ and the ‘Endurance Time’ (ET) with Rohmert demonstrating this relationship to be nonlinear: he used a power curve to model it ($ET = b_0(\%MVS)^{b_1}$). In an extensive review of the literature Frey-Law *et al.* showed that fatigue is joint specific; the muscles about some joints like the shoulders fatigue sooner than those about other joints like the ankle [15]. One might anticipate that the hip abductor muscles might fatigue during OLB test because of the significant and more-or less constant hip abduction they have to generate. This should lead either to a change in posture to relieve the load, or a voluntary end of the OLB test. In this way hip abductor muscle fatigue could limit the UST. However, to our knowledge, such a relationship has never been studied in the literature, possibly because the intensity of the hip abduction has not been quantified (Question 1).

In this chapter, we address these two questions by using a modeling approach. To that end we invoked a 3-link double inverted pendulum computational model to represent a person standing on one leg for all our analyses with the frictionless joints in the model representing the stance ankle and hip articulations. The top link represents the body supported by the hip joint, the middle link represents the lower limb between the hip and ankle joint, and the lowest link represents the foot. In this chapter and the next, we will assume the foot link is stationary, essentially making our model a double inverted pendulum. We will first quantify all the postures in which one could maintain OLB by defining the quasistatic ‘Feasible Balance Region’:

Quasistatic Feasible Balance Region (FBR): *The set of all states in which quasistatic one-legged balance can be maintained.*

¹ Intensity is the proportion of the isometric load relative to the maximum voluntary strength (%MVS)

We will employ published mean values for capacities of three different populations to examine how age, sex, and disease affect lower extremity capacities, namely ankle and hip ranges of motion and isometric muscle strengths, and how they affect the boundaries of the FBR. To consider the effect of age, we will compare two groups, namely healthy young (20-30 years) and healthy older (65 - 80 years) adults. To consider the effect of disease in older adults we will compare healthy older adults with older patients with peripheral neuropathy. Then we examine the sensitivity of the FBR and the predicted hip abduction moment and intensity during OLB due to age- and disease-related losses of muscle strength in both men and women, the effect of changing the lateral bending configuration of the trunk, and different degrees of abduction of the non-stance leg. Subsequently, having predicted the intensity of the hip abduction moment demand during OLB for the young, healthy older adults and older adults with peripheral neuropathy, we touch upon the possible relationship between UST and the fatigue in the hip abductor muscles. We will examine this relationship in greater depth in Chapter 3 where we analyze the data from our OLB experiment with 38 subjects to examine age effects. Finally, in the Discussion we will examine the difference between maintainable and recoverable quasistatic states during OLB and discuss how relaxing some of the assumptions in the present chapter affect our predictions about the ability to maintain or recover OLB.

2.2 Methods

2.2.1 Quasistatic Equilibrium Equations for the Double Inverted Pendulum Model of OLB

In this chapter we start by making the simplifying assumption that the stance foot is stationary in order to consider what is needed to perform the task of OLB over a stable foot, something that someone who is highly skilled at OLB like a gymnast or ballet dancer tends to do. That simplifies the 3-link double inverted pendulum model of OLB into a double inverted pendulum model with a stationary ankle joint. The full state of the double inverted pendulum can be described by four variables: the angle of the stance leg with the vertical line and its derivative $(\theta_1, \dot{\theta}_1)$, and the hip abduction angle and its derivative $(\theta_2, \dot{\theta}_2)$. Since we are mostly studying the quasi-state phase of the OLB, we can also assume that the angular velocities of the two links are negligible. Therefore two variables (θ_1, θ_2) will be sufficient to describe all the states in our model (Refer to Figure 6 and Figure 7 for more details).

Using the free body diagram in Figure 5 and the dimensions and states in Figure 6, we can calculate the torques required for maintaining any quasistatic OLB state:

$$T_1(\theta_1, \theta_2) = -(M_1 l + M_2 h)g \sin \theta_1 + M_2 g r \cos(\alpha + \theta_1 + \theta_2) \quad (1)$$

$$T_2(\theta_1, \theta_2) = M_2 g r \cos(\alpha + \theta_1 + \theta_2) \quad (2)$$

$$T_{1min} \leq T_1 \leq T_{1max} \quad (3)$$

$$T_{2min} \leq T_2 \leq T_{2max} \quad (4)$$

$$-20^\circ \leq \theta_1 + \theta_2 \leq 20^\circ \quad (5)$$

Equation 1- Static Equations of a 3-link Double Inverted Pendulum

T_{1min} and T_{1max} are the maximum ankle inversion and eversion torques respectively, and T_{2min} and T_{2max} are the maximum hip abduction and adduction moments. θ_1 and θ_2 are also constrained by the physiological ranges of motion for the ankle and hip joints. We can combine equations (1) and (2) with the ranges defined in (3) and (4) to find all the combinations of θ_1 and θ_2 within the ROM, where maintaining a quasistatic OLB is possible. Equation (5) limits the range of pelvic

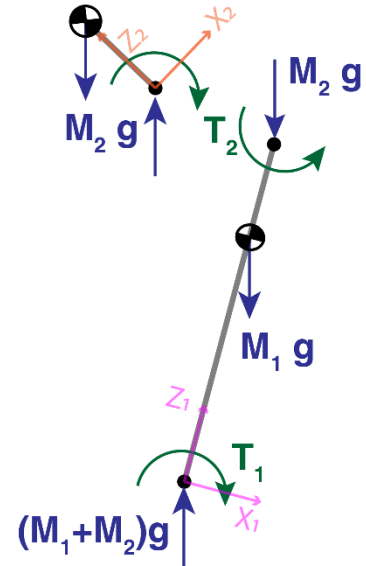


Figure 5- Free Body Diagram of quasistatic double inverted pendulum. Maximum ankle inversion/eversion, and maximum hip abduction/adduction moments were found from the literature [20, 38, 39]. For a description of other parameters, please refer to Figure 6 and Figure 7.

inclination angles between pelvic sag and raise encountered in the clinic (See Assumption A4 for more details). The resulting area defines the FBR for the double inverted pendulum.

2.2.1.1 Assumptions

A1- Parameters of the Double Inverted Pendulum Model:

Anthropometric measurements of a 50th percentile man were used in the model for the theoretical derivations of equilibrium equations and the equations of motion for the double inverted pendulum model (1.78 m, 81.4 Kg) [40]. Maximum ankle inversion/eversion, and maximum hip abduction/adduction moments were found from the literature [20, 38, 39]. The choice of two joints was a compromise between keeping the model as simple as possible while being able to include the major contributing balance strategies in the analysis.

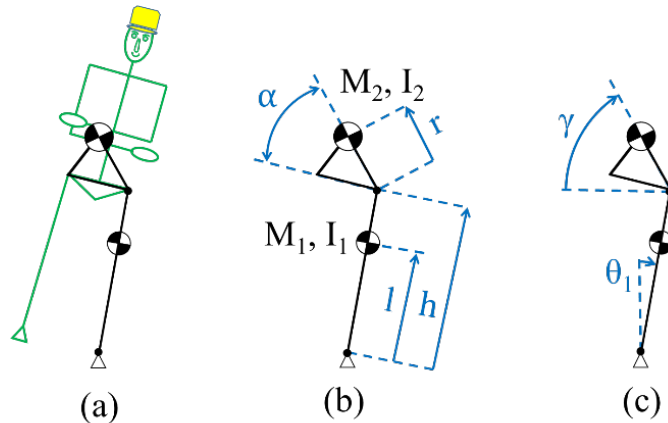


Figure 6- Modeling OLB with a double inverted pendulum model in the frontal plane. In this chapter, and the next, the stance foot is assumed to be stationary. (a) The links in the double inverted pendulum model are stance leg and the rest of the body. The spine is assumed to be straight without any lateral bending, and the contralateral leg is kept at a neutral abduction angle. (b) Parameters of the double inverted pendulum model are from a 50th percentile man ($M_1 = 14 \text{ Kg}$, $M_2 = 67 \text{ Kg}$, $l = 57 \text{ cm}$, $h = 88 \text{ cm}$, $r = 19 \text{ cm}$, $\alpha = 56^\circ$) [40]. (c) Two independent states are required to describe the double inverted pendulum model for quasistatic OLB (please refer to Figure 7 for more details).

A2- Choice of states for representing the double inverted pendulum model:

We assume the non-stance hip is kept at neutral abduction and extension angles and the head and neck are kept straight and not bent in any direction. We also assume no lateral bending of the torso and arms crossed. With these assumptions we are considering the parts of the body balancing on the stance hip to be rigid and therefore only need one variable/state to uniquely describe its orientation in the frontal plane. γ is the angle between the horizontal line and the line connecting the stance hip to the COM of the rest of the body (M_2 in Figure 7). α is the angle between a line connecting the left and right ASIS, and the line connecting the stance hip to M_2 . The rigid body assumption makes α constant, calculated to be equal to 56 degrees for the 50th percentile male model. In all our demonstrations we use θ_2 as the state describing the orientation of M_2 . In deriving the equations of motion ([Appendix I](#)) we will use γ instead to account for the between-subject differences for choice of OLB posture.

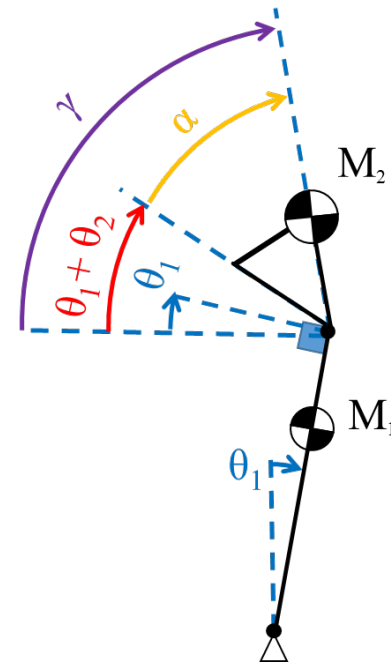


Figure 7- Angles describing the orientation of M_2 in the frontal plane. α is considered constant in this chapter and equal to 56 degrees. Considering the degrees of freedom, only two states are required to uniquely describe the orientation of the double inverted pendulum. It is clear that

$$\gamma = \alpha + \theta_1 + \theta_2.$$

A3- Muscle-equivalent force-length characteristics of the maximum isometric hip abduction moment

Since a large range of possible hip abduction angles can be expected during OLB, we have to account for how the force-length characteristics of hip abductor muscles affect the maximum voluntary isometric hip abduction moment. So we scaled the data from Neuman *et al.* to the 50th percentile male model, by both weight and height, to account for the change of maximum isometric hip abduction moment with the hip abduction angle [41]. We also assumed that the maximum isometric hip abduction moment will stay constant after -10 degree of hip abduction; this was because we couldn't find any data for the lower angles.

A4- Functional range of pelvic inclination angles during OLB

While a professional dancer or gymnast can maintain their OLB in highly extreme postures such as a '[standing split](#)', in the clinic a patient's OLB is tested at pelvic inclination

angles close to neutral, which is defined as when the line connecting the left and right ASIS is horizontal. In addition, due to the difficulty of measuring the stance hip abduction angle, reports often describe a ‘sagging’ or ‘raising’ of the contralateral hip or pelvis during OLB instead [42]. For example, Inman allowed a 15-20 degree pelvic ‘sag’ and ‘raise’ in his experiment when he calculated the contribution of the abductor muscles to the abduction moment during OLB [24]. In this study, we consider a 20 degree pelvic sag and raise will include most people’s OLB posture in the clinic. The angle the pelvis makes with the horizon can be described by $\theta_1 + \theta_2$ in our model (Figure 7).

A5- Applying the physical capacities of different populations to the 50th percentile male model:

To theoretically estimate the effect of sex, age, and peripheral neuropathy on the FBR, we first found the physical capacities of each of the three populations (young, older adult, and older adults with peripheral neuropathy) in the literature [21, 38, 39]. We then normalized the maximum isometric strengths by the reported mean mass and height values for each population, and then applied it to the mass and height of the 50th percentile male.

A6- No noise or time delays:

The inherent time delays and noise in the human sensorimotor system make the task of balancing harder [43]. For simplicity, in the analysis we assumed there are no time delays or noise in the double inverted pendulum model. This assumption will cause the estimates of the FBR size to be exaggerated, however, since most of the analyses are during quasistatic OLB, we predict that this exaggeration is not substantial. In the Discussion, we will relax this assumption to an extent and examine how a latency in executing the response to an unexpected perturbation from OLB equilibrium can limit the initial quasistatic states for which OLB is recoverable.

A7- Ideal moment generation in muscles around stance leg ankle and hip joints:

We assumed that the muscles around the ankle and hip joints can generate moments within their capacity range with no variation. We also assumed that the ankle maximum invertor/evertor moments stay constant within the usual ankle angles employed during OLB. Finally, we considered that the rate of moment generation to be very high. In the Discussion, we will relax this assumption by introducing a 90 ms rise time from zero to half of the maximum strength in both ankle and hip joint moments. This is because Thelen *et al.* showed that

normalizing the maximum rate of torque development by the corresponding strength removed the sex and age group differences [44]. On average, it took 90 ms for their subjects to reach half of their maximum torque from resting.

2.2.2 Dynamic Equations of Motion for the Double Inverted Pendulum Model of OLB

Following the same assumptions used for deriving the quasistatic equilibrium equations, the dynamic equations of motion for the 3-link double inverted pendulum model were derived and can be seen in [Appendix I](#). Since in this chapter we assume the stance foot is stationary at all times, we can simply set the medio-lateral position of the ankle (x_S) to be zero in all the derived equations.

2.2.3 Sensitivity of FBR to Lateral Movements of the Contralateral Leg during OLB

Given the high mass of the contralateral leg, the subject can deploy their contralateral hip abduction angle to affect their OLB and therefore FBR. To calculate the sensitivity of the FBR to this degree of freedom, we allowed a -10 to 30 degrees abduction angle at the contralateral leg in our sensitivity calculations for the FBR.

2.2.4 Sensitivity of FBR to Lateral Bending of the Spine during OLB

Given the high mass of the head, arms, and trunk we can expect the FBR to be highly sensitive to any lateral bending of spine. We used published data on the maximal lateral bending of the vertebrae in the lumbar spine to estimate the maximum lateral bending that M_2 could experience relative to the pelvis ($\theta_4 \sim 20$ degrees in Figure 8) [45]. In our calculations for the sensitivity of the FBR to lateral bending of the spine, we used half of this value as a reasonable range to expect during normal OLB.

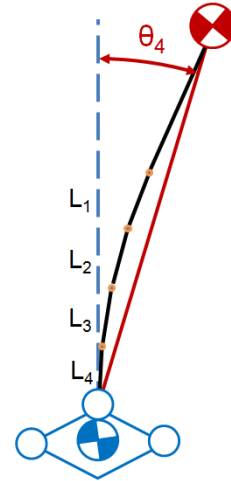


Figure 8- Maximum lateral bending of the COM of the HAT due to the lateral bending in lumbar vertebrae (θ_4). Thorax was considered rigid because of the added stiffness due to the rib cage.

2.3 Results

All the results that are presented here in this chapter are predictions based on my computational double inverted pendulum model of the OLB. The parameters for this model were extracted from the literature. For more details, please see the Methods Section.

2.3.1 Characteristics of the Quasistatic Feasible Balance Region

Figure 9 shows the predicted FBR for healthy young, healthy older adults, and older patients with peripheral neuropathy for both men and women. By definition *a quasistatic OLB can only be maintained for the states inside the FBR*. The lateral and medial margins of the functional BOS are always active constraints and determine the width of the FBR. The top line in all six groups is set by the maximum pelvic inclination angle ('pelvic raise') that we expect during clinical test of OLB. The length of the FBR is then set by the bottom constraint which is determined either by the minimum pelvic inclination angle ('pelvic sag') or the maximum hip abduction strength. The cross-sectional area, length, and width of the FBR for each of the six groups are reported in Table 3.

Note: We can see that for a person with strong enough hip abductors, only considering the medio-lateral margins of the functional BOS is sufficient for assessing the quasistatic OLB. On the other hand, if the hip abductors are weak, then the FBR gets shorter from the bottom. For the person standing on one leg, this means having fewer poses for which they can maintain a quasistatic OLB.

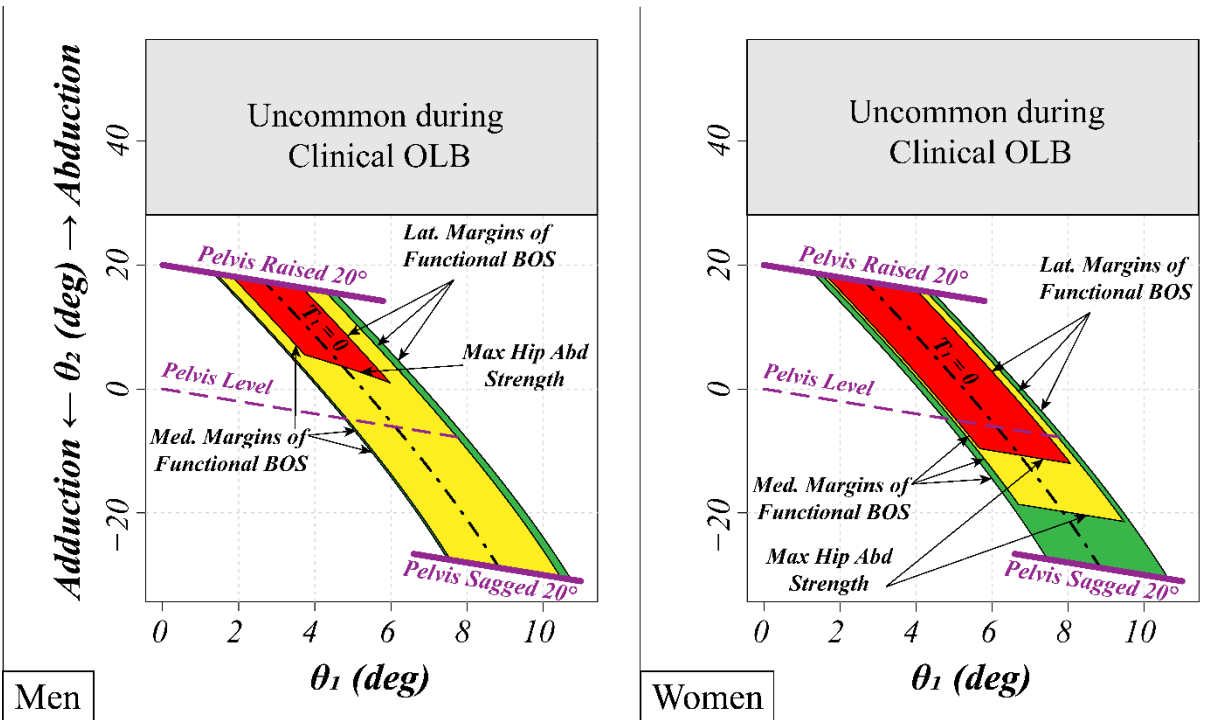


Figure 9- Calculated quasistatic Feasible Balance Region (FBR) for healthy young (green + yellow + red regions), healthy older adults (yellow + red regions), and older patients with diabetic peripheral neuropathy (red region) for men and women. A point on the plot represents a quasistatic state for the double inverted pendulum model of OLB with a fixed foot link, where θ_1 is the angle that the stance leg makes with the vertical line and θ_2 is the stance leg's hip abduction angle (for more detailed description of the states, please refer to Figure 6 & Figure 7). By definition a quasistatic OLB can only be maintained for the states inside the FBR. The dashed-dot line in the middle is the locus of states for which the COM is in the same vertical plane as the ankle, so no ankle torque is required ($T_1 = 0$). The top boundary for all groups is the locus of points where the pelvic inclination angle is raised a nominal 20° . While in healthy young men and women, and healthy old men the bottom boundary is the locus of points where the pelvic inclination angle is dropped a nominal 20° , in the other groups (healthy old women, and old patients with peripheral neuropathy) it is the maximum hip abduction strength that constrains the lower end of the FBR. The left and right side boundaries are always determined by the medial and lateral margins of the functional base of support, respectively. Please refer to Table 3 for quantification of the FBR for each group.

2.3.2 Predicted Sensitivity of the FBR Area to Loss of Strength and ROM in Ankle and Hip

Table 3 shows the quantification of FBR area and examines its sensitivity to loss of functional BOS and maximum hip abduction strength. Base of support (BOS) refers to the cross-sectional area under the stance foot. In Chapter 1 we defined the functional BOS as follows:

Functional Base of Support during OLB: *The area under the stance foot where COP can be taken while maintaining balance on one leg.*

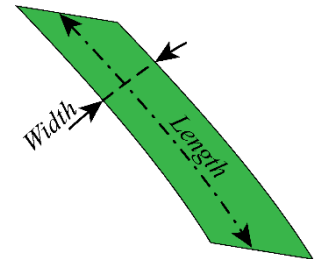
Loss of Ankle Inversion/Eversion Strength: Any loss of functional BOS will reduce the width of the FBR. However, a loss of functional BOS is not synonymous to loss of ankle inversion/eversion strength. BOS during OLB is determined by the area under the stance foot. If a healthy young individual is standing on a narrow ridge, or wearing narrow shoes, they are automatically reducing their BOS and therefore their functional BOS, but they still have their strong ankle muscles. Alternatively, if the ankle muscles are too weak to tilt the stance foot so as to move the center of pressure between the lateral and medial margins of the BOS while standing on one leg, then any further loss of ankle inversion/eversion strength will shrink the functional BOS more and thereby shrink the width of the FBR.

Loss of Hip Abduction Strength: If the hip abductors are strong enough, the maximum hip abduction strength will not become an active constraint in determining the bounds of the FBR. For example, consider healthy young and healthy older men in Table 3; the maximum hip abduction strength is not active for either group. However, we can see that a 20% reduction in strength reduces the FBR length by 24% in the healthy older men while not affecting the young men at all. A similar trend can be seen in the healthy women groups. Finally, both PN groups show high FBR sensitivity to any further reductions in hip abduction sensitivity.

Loss of Ankle and Hip ROM: The range of ankle and hip abduction angles that we expect during a clinical test of OLB can easily be seen in Figure 9. If the stance foot does not tilt, a positive θ_1 is approximately the same as the ankle eversion angle; θ_2 is defined as the hip abduction angle. We assumed mean reported ROM in arriving at the FBR for our six groups, none of which became limitations on the FBR (11° ankle eversion, 31° hip adduction, and 48° hip abduction [46, 47]). However, losses of ankle eversion and hip adduction ranges of motion seem to be closest to becoming active constraints and thereby reducing the available FBR area.

Table 3- Predicted FBR sensitivity to reductions in functional base of support (BOS) and hip abduction strength for healthy young (HY), healthy older (HO), and older patients with peripheral neuropathy (PN) in men and women. A reduction in functional BOS reduces the width of the FBR (FBOS (-20%) column), while a reduction in maximum hip abduction strength may reduce the length (Hip ABd Strength (-20%) column). We define the Length as the length of the zero ankle torque curve. Width is calculated then by dividing the Area by the Length.

Group		FBR			% Reduction in FBR Area	
		Area (deg ²)	Length (deg)	Width (deg)	FBOS (-20%)	Hip ABd Strength (-20%)
<i>HY</i>	<i>Men</i>	122	44	3	20	0
	<i>Women</i>	121	44	3	20	7
<i>HO</i>	<i>Men</i>	110	44	3	20	24
	<i>Women</i>	82	34	2	20	46
<i>PN</i>	<i>Men</i>	24	15	2	20	65
	<i>Women</i>	58	28	2	20	69



2.3.3 Quasistatic Transition of Bipedal to Unipedal Stance

Figure 10 shows three hypothetical quasistatic transitions from bipedal to unipedal stance. Point P_1 is the state of the person standing on both legs. It is clear that this state cannot be maintained quasistatically since it lies outside the boundary of the FBR set by the medial margin of the functional BOS. Indeed, the COM of the body without the stance leg (M_2) stays more medially than the medial margin of a regular shoe during bipedal stance. During the transition, the subject can either keep their pelvic inclination angle level (e.g. P_1 - P_2), raise it (e.g. P_1 - P_3), or let it sag (e.g. P_1 - P_4). Raising the pelvic inclination angle will reduce the hip abduction moment required for OLB because it reduces the moment arm of M_2 on a cosine curve approaching 90 degrees (please see (2) in Equation 1). Conversely, letting it sag will increase the hip abduction moment.

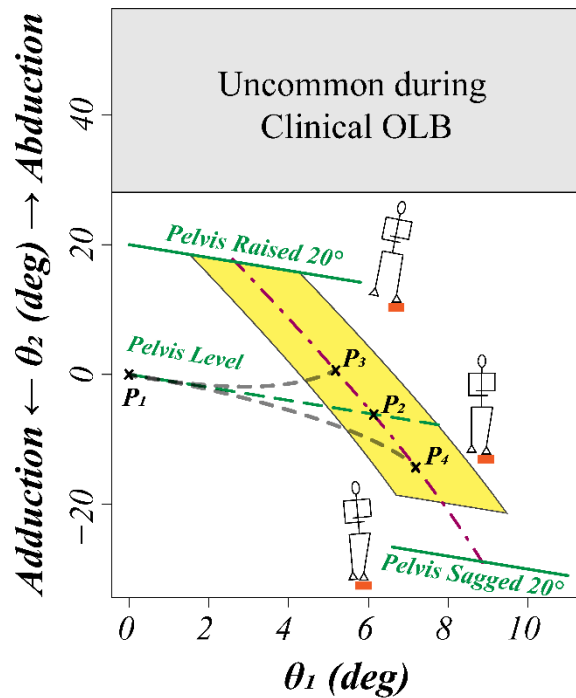


Figure 10- Quasistatic transition from bipedal to unipedal stance. Point P_1 is the state of the person standing on both legs. This state cannot be maintained on one leg because it falls outside the FBR. If the person slowly transitions to one leg, she could take three different general routes. P_1 - P_2 shows a sample trajectory of quasistatic states where the pelvic inclination angle is kept level during the transition, P_1 - P_3 is when it is raised, and P_1 - P_4 is when it is sagged.

2.3.4 Predicted Sensitivity of FBR and Hip Abduction Moment to Medio-Lateral Bending of the Lumbar Spine and Movements of the Contralateral Leg in the Frontal Plane during OLB

Table 4 shows the effect of $\pm 10^\circ$ of medio-lateral bending of the lumbar spine and a variation from -10° to 30° of contralateral (Cont.) hip abduction on the parameters determining the effective moment arm of M_2 for the model of the 50th percentile man ('r' and ' α ' in Equation 1 and Figure 6). We can see that laterally bending the spine and adducting the contralateral leg decrease the effective moment arm, while medially bending the spine and abducting the contralateral leg increase it.

Figure 11 shows the effect of $\pm 10^\circ$ degree of medio-lateral bending of the lumbar spine on the FBR for the 50th percentile healthy old man. The width of FBR is unaffected because it is determined by the width of the functional BOS. On the other hand, the increase in the demand for hip abduction moment due to medially bending the spine shortens the FBR. If the hip abduction strength was high enough, the medial (lateral) bending of the spine would just shift the FBR to the right (left) between the two parallel lines set by $\pm 20^\circ$ pelvic inclination angle raise and sag.

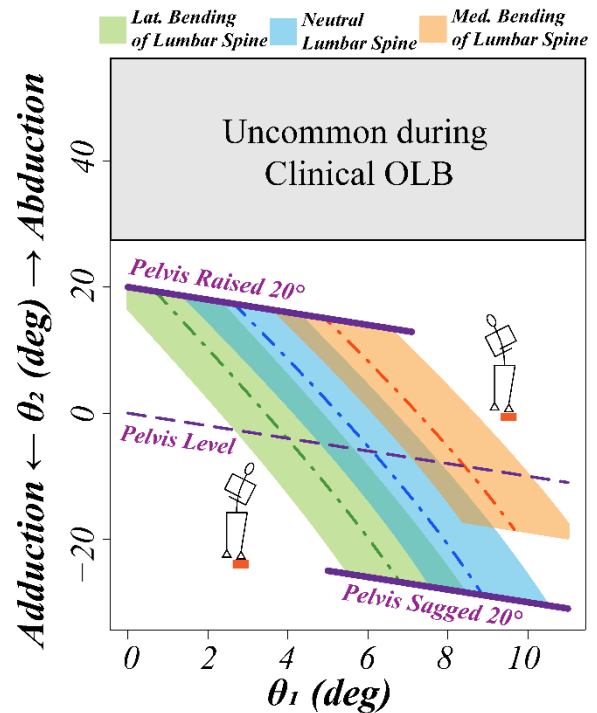


Figure 11- Predicted effect of $\pm 10^\circ$ medio-lateral bending of the lumbar spine on the FBR of the 50th percentile healthy old man. We can see that a medial (lateral) bending of the lumbar spine shifts the FBR to the right (left). The width of the FBR stays essentially unchanged. Medial bending of the lumbar spine increases the required hip abduction moment for OLB. If the hip abductor muscles are not strong enough, this results in shortening of the FBR. Conversely, lateral bending of the lumbar spine decreases the hip abduction moment and could increase the length of the FBR in the case of weak abductor muscles.

Table 4- Predicted sensitivity of the calculated α , r , and hip abduction moment to ± 10 degree changes in medio-lateral bending of the lumbar spine and -10° and 30° of contralateral hip abduction for the 50th percentile man double inverted pendulum model. For the definition of r and α , please refer to Equation 1.

	Case 1	Case 2	Case 3	Case 4	Case 5
Lumbar Spine Medio-Lateral Bending Angle (deg)	0	10° Lateral	10° Medial	0	0
Contralateral Hip Abduction Angle (deg)	0	0	0	30	-10
r (cm)	19	17	21	22	18
α (deg)	56	66	46	49	59
OLB Hip Abduction Moment Demand (N.m)	70	44	96	95	61
% Increase in OLB Hip Abd Moment	-	-37	37	36	-13

2.3.5 Predicted Intensity of the Hip Abduction Moment Demand for the Clinical OLB Test

Table 5 shows the demand of the hip abduction moment during OLB for each of the six groups standing with a level pelvic inclination angle. This assumption is close to the clinical test of OLB where a noticeable pelvic sag (Positive Trendelenburg Sign) or a lateral bending of the spine accompanied by raising of the pelvic inclination angle (Negative Trendelenburg Sign) are considered signs of severe hip abduction weakness [42]. In Table 4 we showed that a half maximal bending of the lumbar spine can reduce the intensity of the hip abduction moment demand by 37%.

Table 5- Hip abduction moment demand of OLB as a percent of maximum voluntary hip abduction strength (%MVS) for healthy young (HY), healthy older (HO), and older patients with peripheral neuropathy (PN) in both men and women. The required hip abduction moment was calculated for point P_2 in Figure 10 for a level pelvis and zero torque generated at the ankle. The force-length characteristic of the hip abductor muscle-equivalent was included in the calculations.

	HY		HO		PN	
	Men	Women	Men	Women	Men	Women
Hip Abduction Moment Demand of OLB (%MVS)	50	57	66	82	106	95

2.3.6 Ankle and Hip Moment Coordination for Creating the Maximum Medial/Lateral Acceleration of the COM

For any state of OLB one might need to maximize COM acceleration in the lateral direction ($\ddot{\theta} > 0$ in Figure 12), then we would need to rapidly increase ankle torque (take the COP to the medial margin of BOS) and decrease hip abduction moment (decrease the pelvic inclination angle). Conversely, in order to develop the maximum medial acceleration of the COM ($\ddot{\theta} < 0$), e.g. avoiding lateral falls, one would need to rapidly decrease the ankle torque (take the COP to the lateral margin of BOS), and increase the hip abduction moment (increase the pelvic inclination angle).

It should be noted that the suggested strategies in Table 6 only apply when the goal is to create maximum possible accelerations of the model COM in a given direction. During regular OLB, many different control schemes could be applied to successfully control OLB.

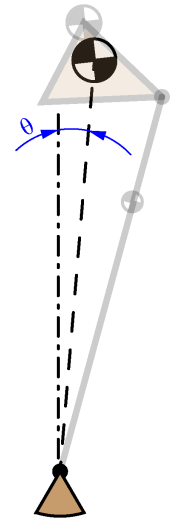


Figure 12- Definition of θ

Table 6- Ankle-hip moment coordination for avoiding model medial and lateral falls during OLB

Avoid OLB Falls		<i>Laterally</i>	<i>Medially</i>
Moment Direction	Ankle	Inversion	Eversion
	Hip	Abduction	Adduction

2.4 Discussion

One-legged balance (OLB) is one of the most common tests of balance in the clinic. To our knowledge, this is the first time that the effect of limited lower extremity capacities (namely ankle and hip strength and ROM) on the possible OLB postures (states) has been quantified. Using our simple double inverted pendulum model, we showed that even quietly standing on one leg requires a healthy individual of any age to generate at least half their maximum hip abduction moment, and that demand increases markedly with age and especially PN. The need for such a large constant abduction moment of course does not exist in bipedal standing. We also introduced in this Chapter the quasistatic feasible balance region (FBR) as the combination of all poses for which a subject can maintain OLB. We then used the size of the FBR area as a measure to quantify the sensitivity of OLB to reductions in lower extremity capacities. We showed that the natural reduction in maximum hip abduction strength due to aging made the size of the FBR for the elderly more sensitive to any further reduction in hip strength compared to the case for the young. Since the intrinsic noise in physiological feedback loops and force generation in the muscles, make one's OLB states follow a random Brownian motion [48], a reduction in FBR size makes maintaining quasistatic OLB a more difficult task.

How does this chapter and the concept of FBR extend the current literature on OLB? In the next two paragraphs we consider this question. The clinically relevant question, “how much lower extremity strength and ROM is required for OLB?” has not received much attention in the biomechanics literature. This is perhaps due to the assumption that the strength requirements of OLB and bipedal stance are similar except for the smaller BOS in OLB. Even then, the literature on the effect of lower extremity capacities on bipedal balance is

sparse. In a computational modeling study of rising from a chair, Pai *et al.* used a single inverted pendulum model with a foot link to study all the combinations of COM position and velocity from which a person could come to rest while maintaining their balance [49]. They referred to

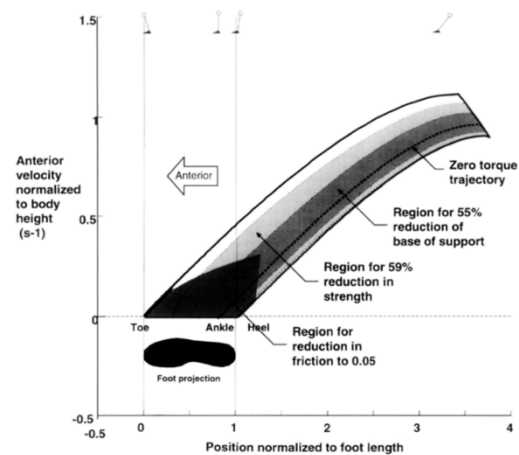


Figure 13- Effect of reducing the ankle strength, BOS, and coefficient of friction on the “Feasible Region”. Photo copied from [49].

this area in the space of COM position-velocity the ‘Feasible Region’ (Figure 13). They also established the sensitivity of the ‘Feasible Region’ area to reductions in BOS and ankle strength. Such an approach could be implemented for OLB as well [50]. However, since our model shows that the limiting stance hip ROM and muscle strength also limit possible OLB poses, we would have to find the ‘Feasible Region’ in a four dimensional space $(\theta_1, \theta_2, \dot{\theta}_1, \dot{\theta}_2)$. While this is computationally interesting and possible, it does not provide much insight into the effect of limited lower extremity on OLB due to the added complexity for interpretation of the results. Instead we resorted to considering only the quasistatic states where maintaining OLB was possible. This is relevant because any dynamic OLB maneuver in the frontal plane has to be brought to rest momentarily before changing speed to the opposite direction. So having a large enough FBR area is then a necessary condition for balancing on one leg.

Many biomechanical studies of OLB, usually conducted with healthy young subjects, have naturally overlooked the role of limited hip abduction [29, 32]. But in clinical studies with elderly it has been recognized as being an important factor in determining a patient’s OLB pose (*i.e.*, Trendelenburg signs for OLB) and unipedal stance time (UST) [20, 42]. The negative Trendelenburg sign during OLB is a term used to refer to patients with severe hip abductor weakness who have to resort to extreme lateral bending of their spine in order to reduce the hip abduction moment demand during OLB. Our double inverted pendulum model showed that even using half of that maximum possible lateral bending of the lumbar spine could decrease the hip abduction demand by 37%. So, we can see that, even with a quasistatic analysis, our calculations provide useful clinical insights into the capacity requirements for maintaining OLB.

While our study quantifies the effect of lower extremity capacities on the possible OLB postures, we still have not established a relationship between the limited lower extremity capacities and the unipedal stance time (UST). It is obvious that having enough lower extremity strength and ROM is a necessary but not sufficient condition for achieving a long UST. A possible connection between the two is that the fatiguing of the stance hip abductors can change the subject’s strategy in order to maximize UST. We will explore this further in Section 2.4.1.

What are the limitations in our analyses? One obvious limitation is that our analysis has been concerned with quasistatic OLB. During quasistatic OLB, hip abductors keep the pelvis from sagging, and the ankle moments move the center of pressure under the stance foot to finely control OLB. But the hip abductor muscles could also be effective in creating a corrective

acceleration of the center of mass. In Section 2.4.2 we will examine how rapid torque development at the stance hip could extend the boundaries of the FBR that are constrained by the medio-lateral margins of the functional BOS. Finally, in Section 2.4.3 we consider what would happen to our predictions if we relaxed two important assumptions, namely infinite RTD and no latency in detecting and reacting to a hypothetical perturbation to OLB.

Amongst the most important limitations of this chapter are modeling errors and extracting anthropometric and capacity related parameters of the model from published mean values in the literature. *First*, we used a double inverted pendulum model for all our analyses. This required considering the arms, head, non-stance leg, and particularly the spine to be always kept rigid. Such simplification was a compromise for finding the simplest model that could still capture the importance of the stance hip joint during OLB. In Section 2.3.4 we presented the sensitivity of our findings to this assumption. *Second*, we used published mean muscle capacity data from the literature, normalized those values to the mean reported height and weight of their subjects, and then rescaled them to the height and weight of our 50th percentile man model. Unfortunately, this approach neglects the between-subject differences in mass distribution, anthropometry, strengths and ROM. In the next Chapter, we address this limitation by bringing in 38 human volunteer subjects (groups of young and older men and women) to the Biomechanics Research Lab, measuring their relevant muscle capacities, and testing their OLB using standard motion capture and force measuring equipment. *Finally*, the assumption that the maintenance of OLB is accomplished by movements completely contained within the frontal plane may not always be valid. For example, at the stance hip, we can redirect torso momentum in the frontal plane to the sagittal plane by engaging the hip internal or external rotator muscles. In addition, the stance foot is not glued to the floor. One can systematically shift the COP between the heel and toes in such a way as to shuffle the foot medially or laterally, a behavior that we study in Chapter 4. However, since in this chapter all our results were for quasistatic OLB, we considered out-of-frontal plane movements to be negligible.

2.4.1 Predicted Effect of Hip Abductor Muscle Fatigue on Unipedal Stance Time

As discussed in Chapter 1, the usual outcome measure for the clinical OLB test is the maximum UST. We showed that standing on one leg with a level pelvis takes between 50%-106% of the maximum hip abduction strength, depending on which of the six subject groups are considered. At a level of demand in excess of 50% of maximum, and if all the hip abduction moment is being provided by the abductor muscles, we can anticipate that fatigue of the abductor muscles could well limit UST. What would be the magnitude of this effect and how would it affect UST?

We can model the fatiguing of the hip abductors as a loss of maximum strength over time. Let us assume the patient is trying to keep a level pelvic inclination angle during a 30 s timed clinical OLB test. As the test continues, the hip muscle strength decreases and now we know that results in the length of the FBR decreasing from the bottom. We hypothesize that when the FBR has shrunk past the ‘Pelvis Level’ line, the patient can no longer maintain their OLB in the same state as before. He (she) then either has to decrease the hip abduction demand by bringing the quasistatic state to a higher region inside the FBR, or ending the OLB test by putting his (her) foot down because the state passes outside the FBR.

We can use Rohmert’s curve (Figure 14) to estimate an upper limit for UST, given the intensity of the hip abduction moment demand of OLB. Since fatigue due to isometric load has been shown to be joint specific [15] and there are not many studies of hip abduction fatigue we instead used the knee, as the closest joint to the hip, for our estimations of how the hip abductors will fatigue. We calculated that achieving a 30 s UST with a level pelvis is only possible if the hip abduction moment demand is not larger than 61% of the MVS. To achieve a two minute UST, the hip abduction moment has to be less than 35% MVS. It is noteworthy this is smaller than the value we calculated for the parameters of our

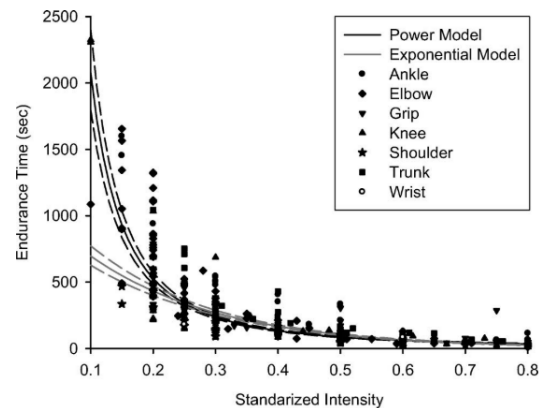


Figure 14- Joint Specific Endurance Time Plots for Sustained Isometric Loads at Different Intensities (%MVS) (copied from [15]). We can see that a decrease in intensity will increase the endurance time ($ET = b_0(\%MVS)^{b_1}$). Since there are not enough experiments on the fatiguing of the hip abductors, we will instead use the published parameters for the fatiguing of the knee joint in young subjects for our estimations ($b_0 = 19.88$, $b_1 = -1.88$).

strongest group, the healthy young men. This result is unexpected given population norms for recorded UST values. For example, Morioka *et al.* found that in a “two-minute” OLB test, the mean UST for people in their 20s and 30s was close to two minutes (Figure 2 from [22]). This suggests that many of their subjects probably could stand for even longer times.

The discrepancy between the predicted fatigue time for the stance hip and the observed mean normative values for UST could be due to two reasons:

a) Estimation error in our calculation of the hip abduction moment demand during OLB: All the limitations that we mentioned for this chapter could contribute to potential overestimation errors in our calculation of the hip abduction moment demand.

b) Contribution of passive elements to the necessary hip abduction moment during OLB: There is evidence that suggests there could be ligamentous tension that contributes some of the hip abduction moment during OLB. For example, in patients with severe gluteal damage, sometimes a marked sagging of the pelvis is observed during OLB (Positive Trendelenburg Sign) [42]. There are also studies that measured the hip abductor muscles activity during OLB using surface and needle EMG. They showed that dropping the pelvic inclination angle decreases abductor muscle activity, while raising it increases it [24, 26]. But a sagging of the pelvis increases the hip abduction moment demand of the OLB. This suggests that something other than the abductor muscles could be sharing the load.

In Chapter 3, we will test the validity of our estimations by testing human volunteer subjects doing OLB tests. That will allow us to estimate the intensity of the hip abduction moment demand for each individual, and compare his/her hip muscle fatigue time with their UST. Should the UST be significantly longer than the estimated fatigue time, then we could conclude the existence of a load sharing mechanism between the hip abductor muscles and passive elements.

2.4.2 Maintainable vs. Recoverable Quasistatic States during OLB

It is important to point out that being able to maintain a quasistatic state (all points within the FBR) and being able to recover balance from an initial quasistatic OLB state are not the same. To maintain quasistatic balance, the only option is to use the ‘Ankle Strategy’ [28, 29] while using isometric hip abduction moment to prevent the pelvis from sagging. However, to control OLB, one does not have to remain quasistatic. The ‘Shear Force Strategy’ [33, 51] can also exert considerable control over OLB². In our double inverted pendulum model, considerable shear force under the stance foot can only be generated by rapid increase or decrease of hip abduction moments. *We will call this the ‘Hip Strategy’ [33] from now on.* As we have seen, exerting maximum hip abduction (adduction) moment along with bringing the COP to the lateral (medial) margin of the BOS, can create a large medial (lateral) acceleration of the COM. This acceleration is substantial but limited in duration because exerting maximal hip abduction / adduction will inadvertently cause the hip to reach its end of ROM. At that point, a reverse moment is exerted by the ligaments surrounding the hip to stop damage to the joint.

Figure 15 shows the effect of ‘Hip Strategy’ on extending the width of the FBR, while observing the limits of ROM of the stance hip and ankle. We can see that in this particular case, we are predicting the width of the recoverable quasistatic states area to be almost twice as much

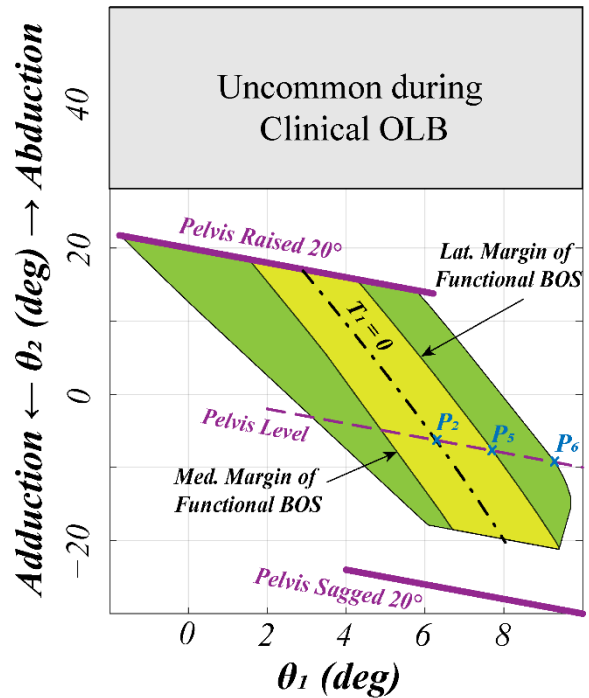


Figure 15- Effect of Hip Strategy on Extending the Width of the FBR. The yellow region shows the FBR for the 50th percentile old woman. While we predict that quasistatic OLB can only be maintained within the FBR, using maximum abduction and adduction moments in addition to the ‘Ankle Strategy’, we predict that quasistatic OLB can also be ‘recovered’ from the green regions on the two sides of the FBR. The bottom line of the FBR and the recoverable quasistatic OLB states is determined by the maximum hip abduction strength in this Figure. For details of the simulations and criteria for successful recovery of balance, please refer to [Appendix II](#).

² For a review, please refer to Balancing on One Leg in Chapter 1.

as the width of the FBR. For details of the simulation and the criteria for successful recovery of balance, please refer to [Appendix II](#).

2.4.2.1 Extension of Functional BOS Lateral Margin by Using the Hip Strategy in Quasistatic OLB States with a Level Pelvis

In Figure 15 we showed how using the ‘Hip Strategy’ can extend the side boundaries of the FBR to include more quasistatic states from which OLB can be recovered. Previously, we showed that the side boundaries are set by the medio-lateral margins of the functional BOS. So in a way, using the hip strategy is extending the margins of the functional BOS. In his experiment, Otten reduced the functional BOS by having subjects stand on one leg on a narrow ridge (4 mm wide). This forced the subjects to use the hip strategy for maintaining their OLB. He showed that the COG could go up to 4 cm beyond the BOS and still recover OLB [33]. For comparison, we consider the locus of initial states for which the pelvis is kept level (‘Pelvis Level’ line in Figure 15). Starting from the $T_1 = 0$ point (P_2) we travel to the right (laterally) until crossing the boundaries of the FBR (P_5) and the recoverable quasistatic states (P_6). Then we calculate the location of the COG relative to the stance ankle³. Table 7 shows the predicted location of the COG relative to the stance ankle at P_5 and P_6 for healthy young and healthy older men and women. We predict that the COG can be more than 2 cm away from the lateral margin of the functional BOS and the subject is still able to recover his (her) OLB balance. This number is less than Otten’s observation. However, it should also be noted that his observation is for all the states during OLB (both dynamic and static), while ours only include the initial quasistatic states. In addition, in our calculations, we have assumed the subject has their arms crossed and their torso is rigid. We predict that allowing the movements of arms and the trunk can increase the effectiveness of the ‘Shear Force Strategy’ in extending the functional BOS.

³ We chose the lateral direction because a lateral fall during OLB is more likely to cause an injury compared to a medial fall [86]; should one feel oneself falling medially, one simply put the contralateral foot down.

Table 7- Predicted extension of the Functional BOS by the Hip Strategy in quasistatic OLB states with a ‘Level Pelvis’. The numbers in the ‘functional BOS’ column refer to the medio-lateral difference in COG position at points P_2 and P_5 in Figure 15. The values in the ‘Extension of FBR width due to the Hip Strategy’ column are the same difference for COG positions between points P_2 and P_6 .

Group		COG offset relative to stance ankle at the lateral margin of	
		Functional BOS (cm)	Extension of FBR width due to the ‘Hip Strategy’ (cm)
<i>HY</i>	<i>Men</i>	2.0	4.5
	<i>Women</i>	2.0	4.5
<i>HO</i>	<i>Men</i>	2.0	4.2
	<i>Women</i>	2.0	4.2

2.4.3 Predicted Sensitivity of Recoverable Quasistatic OLB States to Physiological Delays

In this chapter, we assumed that there are no neuromuscular delays in the human body (assumptions A6 and A7 in the Methods section). This was mainly because our focus was on quantifying both the effect of changes in ankle and hip strengths and of ranges of motion on OLB capacity, without making assumptions on the control strategy and the state estimation scheme that the CNS uses for controlling OLB [52, 53]. On the other hand, it is obvious that being slow in executing corrective actions for quasistatic balance recovery, will make the task harder. Next, we examine two different sources of physiological delay in reacting to recover OLB in a hypothetical scenario:

One Hypothetical Scenario for Recovering OLB: Our 50th percentile model of healthy older woman is standing on one leg at a quasistatic state on the $T_1 = 0$ locus of points (for example point P_2 , P_3 , or P_4 in Figure 10). Now, while she maintains a constant hip abduction moment, we deviate her quasistatic state away from her current state with zero ankle torque. In the following two cases, we consider if she can create enough corrective acceleration to recover from the initial deviation.

2.4.3.1 Case I: Predicted Effect of Limited Rate of Torque Development on the Recoverable Quasistatic OLB States

In this case, we assumed our hypothetical woman instantly realizes that she needs to take corrective action. Then we consider the effect of delay in developing her maximum ankle and hip moments in the correct direction. Figure 16 shows the predicted effect of enforcing rate of torque development on the recoverable quasistatic OLB. First we assumed there is no delay in developing maximum ankle and hip moments. Then we made both ankle and hip joints in our model to have limited rates of torque development. So, starting from zero ankle moment and constant hip abduction moment, we found all the initial quasistatic states that we predicted could be recovered during OLB. As expected, we see that enforcing a limited rate of torque development shrunk the area of recoverable quasistatic OLB states.

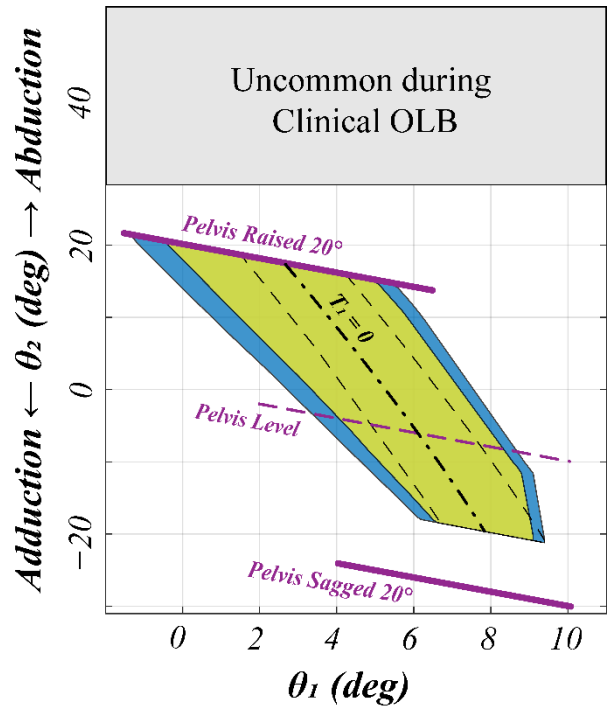


Figure 16- Effect of limited rate of torque development (RTD) in ankle and hip joints on the predicted recoverable quasistatic OLB states. The blue area shows the quasistatic OLB states that become unrecoverable due to enforcing a limited RTD. We enforced RTD by using a 90 ms rise time for reaching half of the maximum torque from a resting moment [44]. The area with the dashed line is the predicted FBR for the 50th percentile older woman, added here for reference.

2.4.3.2 Case II: Predicted Effect of Latency on Initiating the Predetermined Maximum COM Acceleration Ankle-Hip Recovery Strategy

What happens if the rate of torque development used in Case I is maintained, but the woman did not instantly initiate her corrective ankle-hip response? This could be the case if the subject was dual-tasking or not paying attention to their OLB but then, after a latency, realized that a balance correction was necessary. We considered a 250 ms latency, which has been shown to be the average time required for a recognition reaction time in the simple task of deciding whether or not to catch a falling stick depending on whether a light cue was present or not [54]. We then considered what would happen if we increased the latency to 500 ms. Figure 17 shows the recoverable quasistatic OLB states for each considered latency. We see that even enforcing the 250 ms latency in initiation of the corrective ankle-hip strategies shrunk the quasistatic recoverable OLB states past the FBR!

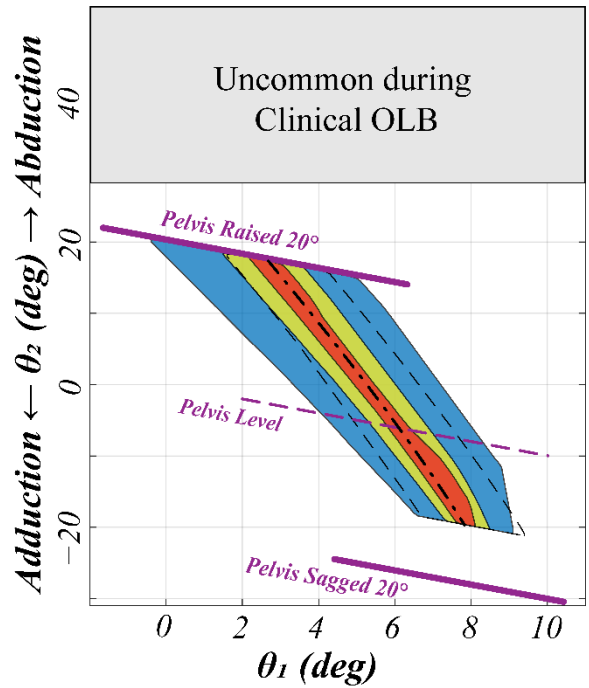


Figure 17- Effect of latency, in initiation of the predetermined maximum COM acceleration strategy, on the predicted recoverable quasistatic OLB states: No latency (Blue + Green + Red region), 250 ms latency (Green + Red regions), and 500 ms latency (red region). The area with the dashed line is the predicted FBR for the 50th percentile older woman, added here for reference.

2.5 Conclusions

- The FBR can be used to demonstrate the effect of limited ankle inversion-eversion (FBR width) and hip abduction moment (FBR length) on OLB postures.
- Effect of restrictions on muscular capacities and range of motion due to aging, disease, or injury, can be shown as reductions in FBR width and length. Conversely, we can show the effect of rehabilitation as an increase in FBR width and length.
- The model makes it clear that the hip abduction moment required to stand on one leg is substantial, ranging from 50% of maximum voluntary muscle strength in healthy young males to 82% of the maximum in healthy older women. If there is no muscle fatigue then UST is likely not limited by lower extremity muscle strengths.
- In patients with moderate peripheral neuropathy, the demand for hip abduction strength likely exceeds their capacity leading one to expect brief UST times. This effect is amplified by a lack of proprioception which makes the OLB states more variable and more likely to cross out of the width of the FBR as well.
- Because of the OLB demand for 50% or more of maximum hip abduction strength, fatigue of the hip abductor muscle will almost certainly limit UST beyond ~1 minute, particularly in older women, and severely limit UST in those with peripheral neuropathy (73 s and 57 s for healthy young men and women respectively, 55 s and 34 s for healthy older men and women respectively, and less than 10 s for both older men and women with peripheral neuropathy).
- The coordination necessary for creating a maximal medial or lateral acceleration of the COM during OLB is independent of the initial state. To avoid a lateral fall during OLB, the most effective recovery strategy is maximum available hip abduction combined with ankle inversion strength.

CHAPTER 3

One-Legged Balance Experiment and Validation of the Feasible Balance Region

3.1 Introduction

In Chapter 2 we used a modeling approach to quantify the strength requirements for one-legged balance (OLB). To accomplish that we used mean published anthropometric and lower extremity capacity data to arrive at two results:

- 1) Ankle and hip strengths and ranges of motion in the frontal plane defined a feasible balance region (FBR) in which we anticipate maintaining quasistatic OLB is physically possible (please see Section 2.3.1).
- 2) Hip abduction moment demand during OLB was, on average, calculated to be more than 50% of the maximum voluntary hip abduction strength in all adult groups (please see Section 2.3.5).

Based on the second result and knowledge of the fatigue behavior of muscles [15], we hypothesized that fatigue of the hip abductor muscles (mostly the gluteus medius, gluteus minimus, and tensor fasciae latae) may actually limit maximum unipedal stance time (UST). A limitation of this approach is that it was based on literature data extracted from different sources. In this chapter we address this limitation directly by conducting an OLB experiment in young and older adults. Our hypotheses are:

H₁: All experimentally measured quasistatic OLB states will fit inside the FBR derived from subject-specific anthropometry, and hip and ankle strengths and ranges of motion.

H₂: Measured endurance time at a 50% of maximum hip abduction strength exertion exceeds the measured UST for each subject. Alternatively, the calculated subject-specific hip abduction moment demand intensity will reliably predict the maximum UST for that subject.

Both hypotheses rely on the assumption that, in healthy adults, the hip abduction demand of OLB is completely resisted by only the abductor muscles. Rejections of these hypotheses would suggest that there is significant contribution from mechanisms other than the hip abductor muscles in resisting the hip abduction moment demand of OLB.

The Methods Section provides full details of the OLB experiment. In short, the anthropometry and ankle and hip strengths were first measured for each participant. Then they stood on one leg for as long as they could, up to a maximum time of four minutes, while their movements were recorded by a motion capture system. The *primary outcome* measures from the experiment were the *UST* and calculated *intensity* of the hip abduction moment demand of OLB for each subject. *Secondary outcomes* include the kinematic parameters such as *pelvic inclination angle* and *lateral bending of the trunk* during OLB. The secondary outcome measures are presented because they could reveal potential strategies that our participants used to change the intensity of their hip abduction moment during the experiment.

In the Results section we review our findings. These show that the calculations of the hip abduction moment demand in Chapter 2 were correct. Furthermore, the findings lead one to reject both the above hypotheses, indicating the existence of a load sharing mechanism between the abductor muscles and another structure or set of structure; we posit those involve the ipsilateral iliotibial band. The Discussion includes a further examination of the posited iliotibial mechanism and a discussion of how it affects our original hypotheses. Particularly, regarding the FBR, only a severe hip abductor muscle strength loss would cause the FBR length to be affected. In these cases, we anticipate that the change in FBR length will be in the form of a splitting in the middle showing that maintaining OLB with a level pelvis is not possible. This finding is corroborated by the Trendelenburg's test of function in the clinic in which patients with severe abductor muscle atrophy are asked to stand on one leg; they would either have a marked 'sagging of their pelvis' or maximally bend their torso to reduce the hip abduction moment demand.

3.2 Methods

3.2.1 Participants

Twenty young (20-30 yrs) and 21 older (65-80 yrs) healthy participants were recruited for this study. Each participant read and signed a printed copy of the informed consent form that was approved by the Institutional Review Board for human studies at University of Michigan (HUM00130970). Initial telephone screening can be found in Appendix VII. *Inclusion Criteria:* All subjects were considered healthy and exercised at least two times a week. To participate, subjects were required to be able to stand on their left foot for more than 10 seconds. *Exclusion Criteria:* Participants who regularly took sedatives or medicines with a combined 1+ anticholinergic burden score were excluded [55]. A foot vibration sensation test was conducted as an indicator for developing neuropathy in the participants [56]. A 128 Hz tuning fork was used to perform the test on the big toe of both feet. A perceived vibration sensation lasting under 10 seconds was considered “low sensitivity” and excluded the participant from the study. The results led to the exclusion of three older participants. None of the participants in this study were pregnant, had amputation or foot deformity, recent sprain or fracture of ankles, knees, hips, arms, spine, or head in the past year. Subjects with BMI over 35 kg/m² were excluded due to the potential for excessive movement of the surface markers relative to the bony landmarks which would have made interpretation of the motion capture data inaccurate. The data for two men (one in the young group) were excluded in the analyses due to markers sliding permanently on the skin after the digitization process. The data for another man in the young group were also excluded due to inaccurate strength measurements. These exclusions resulted in an effective sample size of 18 young and 17 older participants. All the subjects participated in both the OLB experiment and the heel-toe-shuffle (HTS) experiment on the same testing session. The details of the HTS experiment can be found in Chapter 4. The demographics of the participant pool can be seen in Table 8.

Table 8- Age, weight, and height of the participants in the OLB experiments. The entries inside the parentheses are the standard deviation for each group.

	Young (20-30 yrs)		Older (65-80 yrs)		p-value
	Men (n = 8)	Women (n = 10)	Men (n = 7)	Women (n = 10)	
Age (yrs)	25 (2.5)	26 (2.8)	70 (4.0)	69 (3.6)	< 0.001 ¹
Weight (Kg)	76.1 (11.4)	62.5 (6.6)	82.4 (5.3)	64.6 (8.1)	< 0.001 ²
Height (cm)	174 (5)	168 (6)	177 (5)	159 (5)	0.01 ³
BMI (Kg/m²)	24.9 (3.1)	22.2 (1.8)	26.4 (2.2)	25.4 (2.9)	0.007 ¹ 0.03 ²

¹Age main group effect

²Sex main group effect

³Age:Sex group interaction

3.2.2 Testing Sequence

Figure 18 shows an overview of the sequence of measurements and experiments for each participant. We have already covered Step 1. We will clarify the remaining steps in the remainder of the Methods section.

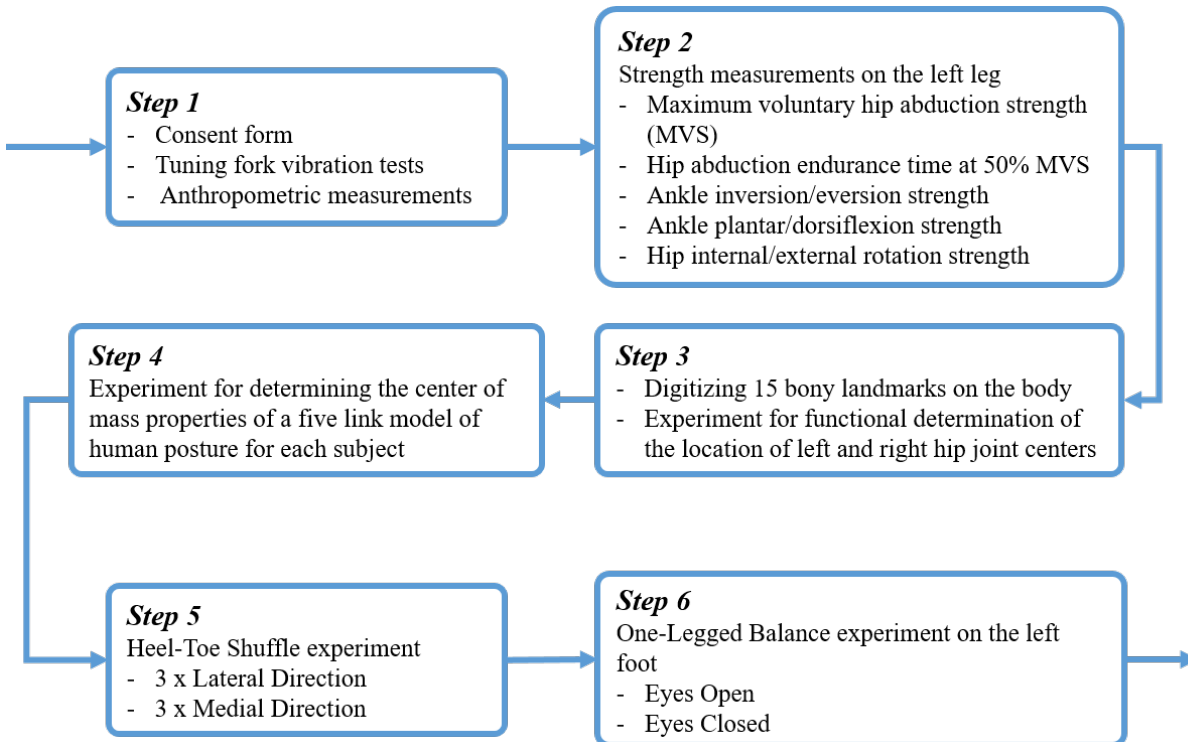


Figure 18- Overview of the sequence of measurements and experiments for each participant

3.2.2.1 Left Leg Muscle Strength Measurements (Step 2 in Figure 18)

In this section we will describe the procedure for measuring different lower extremity strengths and the hip abduction fatigue test which followed the measurement of the maximum hip abduction strength test. All the measurements were made on the left leg. A summary of the measured strengths with different normalization methods can be seen in Table 9.

Measuring Maximum Voluntary Isometric Hip Abduction Strength

Different methods have been reported in the literature for measuring maximum hip abduction strength [57, 58]. In this study, subjects laid supine on a padded cot with the left leg extended at a neutral abduction angle supported by padded bracket on a lever that was kept stationary. (If released, which it was not for this isometric part of the experiment, the lever could rotate about a vertical axis collinear with the axis of rotation of the left hip.) The right trochanter was supported by another bracket and a belt over the pelvis secured the subject to the test bed. Subjects were instructed to gradually reach their maximum hip abduction isometric strength against the bracket in about 3 seconds, and maintain it for two seconds before relaxing. Maximum strength was measured by recording the force on the bracket using a Lafayette Manual Muscle Tester and multiplying by its measured moment arm about the center of the left hip. Three trials were performed and the peak torque was chosen as the maximum voluntary isometric hip abduction moment. Testing the hip abduction strength in the horizontal plane eliminated any possibility of gravity affecting the measurements.

Measuring Hip Abduction Endurance Time at 50% MVS

We used the same test bed for measuring maximum hip abduction strength to measure hip muscle endurance behavior. This time the lever under the left leg was allowed to rotate freely about the left hip. Physical weights corresponding to approximately half the subject's maximum exerted force were connected to the rotating lever and bracket via a pulley mechanism. Subjects were then asked to develop an abduction moment to maintain the weight off the ground for as long as possible. The weight and the maximum time that each subject could maintain the weight off the ground were then recorded. A single trial was performed.

Adjusting the Maximum Isometric Hip Abduction Strength by the Fatigue Time

After testing the first 10 subjects, we noticed that some, especially older, subjects were having difficulty with the coordination required for exerting a maximum isometric abduction

effort in the supine position. Meanwhile, keeping the submaximal weight suspended was a more familiar task which they all had success accomplishing suggesting little or no learning was required. This could be readily observed because some of the subjects kept the weight suspended for a long time, up to five minutes in some cases when the tester had to halt the fatigue experiment. According to our inspection of the published leg muscle endurance literature (Rohmert Curve [15]), this would suggest that to maintain a muscle contraction for up to 5 minutes they had to be operating at a moment threshold that was significantly lower than their 50% MVS [15, 17]. Since we could only find a few published studies on the fatigue behavior of the hip muscles, and they were not as reliable as we hoped, we instead used the Rohmert curves for the knee joint for young and older subjects in order to estimate the hip abduction %MVS, a value we then used to back calculate what their maximum hip abduction strength must have been [15, 17]. The equations that were used follow:

$$ET = b_0 \times (\%MVS)^{b_1}$$

Equation 2- Power model for knee joint endurance time (ET) where $b_0 = 19.38$, $b_1 = -1.88$ for Young [15] and $b_0 = 22.04$, $b_1 = -2.21$ for old subjects [17].

$$\%MVS = e^{\left(\frac{\ln(ET/b_0)}{b_1}\right)}, MVS_{Fatigue} = \frac{(\text{Hip Fatigue Moment})}{(\%MVS)}$$

Equation 3- Estimating maximum hip abduction strength from endurance time and the fatigue moment during the endurance time test.

For the “adjusted” maximum hip abduction strength for each subject, we selected the larger of the two values between the measured hip abductor MVS and the value of MVS back-calculated and estimated from the endurance time test. Both measured maximum hip abduction strength and adjusted hip abduction strength can be seen in Table 9.

Measuring Ankle Inversion / Eversion and Plantarflexion / Dorsiflexion Isometric Strengths during One-Legged Stance

Different methods have been reported for measuring maximum ankle strengths in different directions for both sitting [46] and weight-bearing conditions [39]. However, since the effective maximum ankle strength during OLB depends on the dimensions of the base of support, we used maximum deviations of the center of pressure under the stance shoe multiplied

by the weight of each subjects to estimate the effective ankle strengths during OLB. Subjects stood on their left foot on a six-axis force plate (Optima HPS, AMTI Massachusetts). Waist-height safety hand rails were placed on both sides and could be used for balance as needed. Subjects lifted one leg, shifted their center of pressure under their stance foot as far lateral (inversion) as possible, and lifted their hands from the rails for three seconds. The test was repeated three times for the lateral, and then likewise repeated for the medial margin (eversion) of the stance foot. Maximum ankle inversion/eversion strength was estimated as the maximum one second averaged shift of the center of pressure in lateral/medial direction from the neutral position. The same method was used to estimate the ankle plantarflexion/dorsiflexion strength. Instead of asking the subjects to move the center of pressure to the lateral and medial margins of their stance foot, they were instructed to move it as far as possible towards the toes and backward to the heel.

Measuring Hip Internal / External Rotation Isometric Strengths

Isometric hip internal / external rotation strength is usually measured with a flexed knee with the subject sitting or lying prone on a bed [59, 60]. However, in both OLB test and the heel-toe shuffle test, the participants are standing with a straight knee. Additionally, the friction between the shoes of the subject and the floor limits how much internal / external rotation moment can be exerted by the subject. So in our test we used a functional method for measuring the maximum internal / external rotation moment that a subject could exert on the floor as a proxy for the maximum effective isometric hip internal / external rotation strength. Subjects stood on the force plate on their left foot while grabbing waist-height bilateral safety rails on both sides. To measure maximum hip internal / external rotation strength, subjects used the safety rails like a steering wheel to rotate themselves CCW / CW while resisting the rotation with their stance hip. Subjects progressively increased their effort from rest to maximum over a count of three, and maintained their maximum effort for two seconds before relaxing. Each subject performed three trials in each direction, and the maximum one second averaged Mz signal from the force plate was taken as the internal / external rotation strength.

Table 9- Effect of age and sex on the mean (SD) measured left leg isometric strength data without normalization (N.m), normalized by Weight (m), and normalized by Weight and Height (l). **PF**: Plantar-Flexion, **DF**: Dorsi-Flexion, **Inv**: Inversion, **Ev**: Eversion, **Abd**: Abduction, **Int Rot**: Internal Rotation, **Ext Rot**: External Rotation. Adjusted Abd refers to the adjustments made to the maximum hip abduction strength using the hip fatigue test.

		Measured Ankle Strengths											
		<i>PF (N.m)</i>	<i>PF (m)</i>	<i>PF (l)</i>	<i>DF (N.m)</i>	<i>DF (m)</i>	<i>DF (l)</i>	<i>Inv (N.m)</i>	<i>Inv (m)</i>	<i>Inv (l)</i>	<i>Ev (N.m)</i>	<i>Ev (m)</i>	<i>Ev (l)</i>
Young <i>(20-30 yrs)</i>	Men <i>(n = 8)</i>	98 (16)	0.132 (0.016)	0.076 (0.010)	64 (11)	0.086 (0.013)	0.049 (0.008)	28 (8)	0.037 (0.007)	0.021 (0.004)	19 (5)	0.026 (0.006)	0.015 (0.003)
	Women <i>(n = 10)</i>	74 (11)	0.122 (0.015)	0.073 (0.010)	49 (13)	0.078 (0.015)	0.047 (0.008)	19 (4)	0.031 (0.006)	0.019 (0.003)	15 (3)	0.024 (0.006)	0.014 (0.004)
Old <i>(65-80 yrs)</i>	Men <i>(n = 7)</i>	95 (16)	0.117 (0.016)	0.066 (0.009)	64 (11)	0.080 (0.014)	0.045 (0.007)	25 (4)	0.030 (0.004)	0.017 (0.002)	21 (3)	0.026 (0.003)	0.014 (0.001)
	Women <i>(n = 10)</i>	70 (10)	0.111 (0.019)	0.070 (0.012)	48 (10)	0.075 (0.011)	0.047 (0.007)	18 (4)	0.029 (0.005)	0.018 (0.003)	14 (2)	0.022 (0.004)	0.014 (0.003)
		Measured Hip Strengths											
		<i>Abd (N.m)</i>	<i>Abd (m)</i>	<i>Abd (l)</i>	<i>Adjusted Abd (N.m)</i>	<i>Adjusted Abd (m)</i>	<i>Adjusted Abd (l)</i>	<i>Int Rot (N.m)</i>	<i>Int Rot (m)</i>	<i>Int Rot (l)</i>	<i>Ext Rot (N.m)</i>	<i>Ext Rot (m)</i>	<i>Ext Rot (l)</i>
Young <i>(20-30 yrs)</i>	Men <i>(n = 8)</i>	115 (35)	0.157 (0.049)	0.090 (0.029)	115 (35)	0.157 (0.049)	0.090 (0.029)	18 (5)	0.024 (0.005)	0.014 (0.003)	16 (4)	0.021 (0.005)	0.012 (0.003)
	Women <i>(n = 10)</i>	81 (29)	0.131 (0.041)	0.078 (0.023)	93 (23)	0.152 (0.032)	0.090 (0.018)	15 (4)	0.025 (0.006)	0.015 (0.003)	13 (3)	0.022 (0.005)	0.013 (0.003)
Old <i>(65-80 yrs)</i>	Men <i>(n = 7)</i>	90 (41)	0.111 (0.050)	0.062 (0.027)	100 (29)	0.123 (0.035)	0.069 (0.018)	15 (8)	0.019 (0.009)	0.010 (0.005)	14 (7)	0.017 (0.009)	0.009 (0.005)
	Women <i>(n = 10)</i>	44 (15)	0.068 (0.022)	0.043 (0.014)	58 (14)	0.093 (0.025)	0.058 (0.015)	11 (4)	0.018 (0.007)	0.011 (0.005)	11 (3)	0.017 (0.007)	0.011 (0.004)

3.2.2.2 Motion Capture, Force Plates and Data Recording Setup during OLB Experiments (Step 3 in Figure 18)

Two motion capture cameras (one Optotrak Certus and one Optotrak 3020 from Northern Digital Inc.) were connected in series to view a floor area containing two 1000 lbf capacity AMTI force plates (one Optima HPS, and one OR-6) embedded into the floor of the lab. The volume of view was approximately 1.5 m on a side. The Optima force plate had a pattern of eight threaded holes which were used to temporarily fasten a custom calibration jig fixture outfitted with infrared (IRED) motion capture markers. By fixing the jig on top of the force plate, we reliably aligned the motion capture cameras' coordinate system with the Optima force plate coordinate system and set the center of the top surface of the force plate to be the origin of the lab coordinate system. Seven rigid bodies with three to four IRED motion capture markers were fixed to each subject: one on each shank and thigh, one on pelvis, one on sternum, and one on the head. Additionally, one marker was fixed on the heel of the stance foot shoe, and two more on top in the third and fifth metatarsal area. Location of the markers in the lab coordinate system were recorded at 90 Hz during the trials. The signals from the force plates were recorded at 500 Hz. All data were filtered by the "*filtfilt*" command in MATLAB © with a fifth order low-pass filter and cutoff frequency of 20 Hz.

3.2.2.3 Digitization and Functional Determination of the Hip Joint Centers (Step 3 in Figure 18)

Fifteen bony landmarks were found by palpation and digitized using a NDI manual digitizing wand: medial and lateral malleoli on both feet, medial and lateral points on both knees determining the axis of rotation (subject was sitting in a chair and asked to extend and flex each knee while the tester located the axis by hand), both left and right greater trochanters, both ASIS, the point between the two PSIS, and both shoulder acromia. The knee joint was defined as the mid-point between the lateral and medial digitized points. The ankle center of rotation in the frontal plane was assumed to lie 2 cm distally from the mid-point of the malleoli on a line connecting it to the knee joint center [61]. Due to sensitivity of the calculated stance ankle torques to the stance ankle joint center, we used an optimization algorithm that searched a 2 cm x 2 cm x 2 cm cube around the aforementioned point to minimize the magnitude of the mean ankle torque during the full duration of the OLB trial. This was based on the clinical observation that for a healthy foot, small adjustment at the ankle can be observed by looking at the small tilts of

the foot between the lateral and medial margins. This means that the direction of the ankle torque should keep changing between inversion and eversion which makes the assumption of zero mean ankle torque over the extended period of time plausible.

To locate the hip joint center on each side, the subject was asked to stand on the contralateral leg while holding onto a support chair on that side, while performing a series of five gross leg movements: extend the leg at the hip by ~30 degrees and bring it back to neutral, abduct the stance leg by ~30 degrees and bring it back, and complete a circumduction of the leg with a ~30 degree included angle. We then used the SCORE method to functionally locate the center of the hip joint, and to assess the accuracy of our estimation for the hip joint centers [62, 63]. The RMSE for left hip location during the functional trial was between 2 to 19 mm, with a mean value of 5 mm for all subjects. For the right leg this was 2 to 14 mm with a mean of 6 mm. During the OLB trial, the left hip location RMSE was between 2 to 20 mm, with a mean value of 10 mm.

3.2.2.4 Determining Subject Specific Mass Distribution (Step 4 in Figure 18)

To determine the mass distribution for each subject, we used a five link model (Figure 19). A total of eight variables are required to uniquely determine the mass distribution in this model:

- m_1 : mass of shank and foot on each side as a percentage of whole body mass.
- m_2 : mass of thigh on each side as a percentage of whole body mass.
- m_3 : mass of pelvis, trunk, arms, and head as a percentage of whole body mass.
- r_1 : location of m_1 on a line connecting the ankle to the knee as a percentage of the length of the aforementioned line.
- r_2 : location of m_2 on a line connecting the knee to the hip joint center as a percentage of the length of the aforementioned line.
- r_3 : location of m_3 on a line connecting mid-point between the two hip joint centers to the mid-point between the two shoulder acromia as a percentage of the length of the aforementioned line.
- r_x, r_y : location of m_3 on a plane perpendicular to the line connecting mid-point between the two hip joint centers to the mid-point between the two shoulder acromia at the r_3 location, given as a percentage of the aforementioned line length.

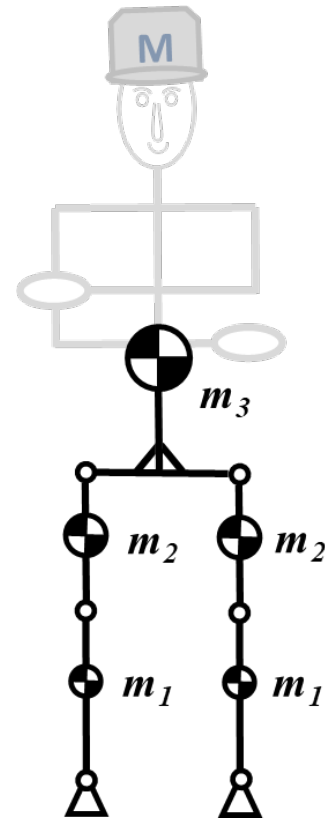


Figure 19- A five link model was used to determine the mass distribution for each subject: one link per shank and foot (m_1), one link per thigh (m_2) and one link for the pelvis, trunk, arms, and head.

To create the data for the optimization algorithm that determined the value of the above eight variables, each subject performed a series of movements as slowly as possible while both force plate and motion capture data were being recorded: the subject started in a neutral stance defined as standing on both feet with arms crossed. Then (s)he slowly shifted her/his weight to the left leg until the right leg lifts off the floor and then returned to neutral. Then the movements were repeated, this time shifting the weight onto the right leg. Next, the subject lifted their left leg by bending the left knee to 90 degrees and externally rotating the left hip to 45 degrees. After this

they returned to neutral and repeated the procedure for the other leg. Finally, while keeping the arms crossed and close to chest and the back straight, the subject slowly squatted until their knees were about 90 degree flexed after which they slowly returned to neutral. All the above movements were performed while the subject's feet rested on the force plate inside its perimeter.

We used Zatsiorsky's zero-point-to-zero-point integration method to find the location of the center of gravity from the force plate recordings in the trial described in the last paragraph [64]. Briefly, this method is based on the fact that the only source of horizontal force on the body of the person during the trial comes from the contact of the feet with the force plate. We can then calculate the horizontal acceleration of the center of mass of the body from the force plate recordings using Newton's second law ($\text{Force} = \text{Body Mass} \times \text{COM Acceleration}$). Assuming the center of pressure and center of gravity coincide when the shear force is zero, we can then double integrate the acceleration to find the time series describing the location of whole body center of gravity.

To find the value of the described eight variables for each subject, we used a Newtonian descent optimization algorithm (interior-point, *fmincon* function in MATLAB ©) that minimized the root mean square error between the COG calculated from the force plate and that calculated using the five link model. The initial value for the eight parameters were calculated from the literature [65]. To validate our COM calculations, we calculated the root mean square error between the COG from the force plate and the mass-link model

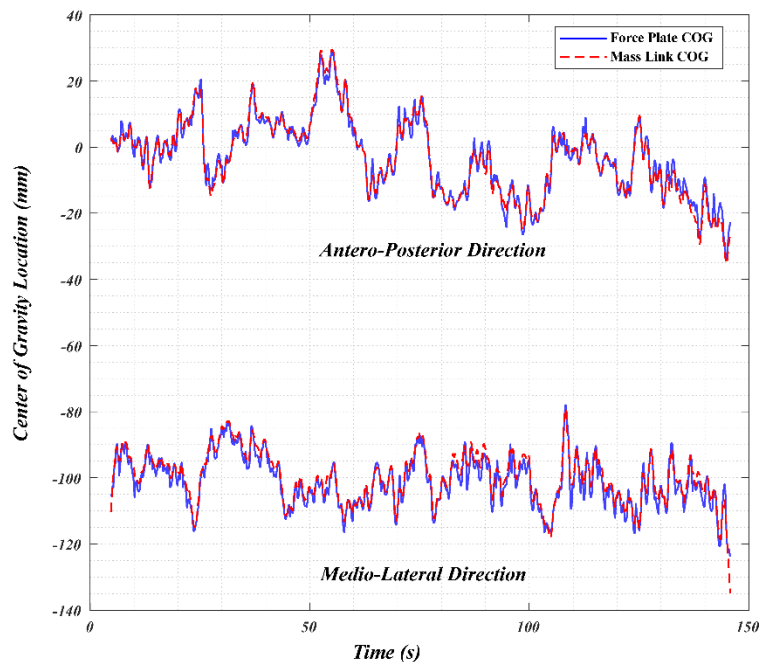


Figure 20- COG calculated from the force plate and the kinematics of the mass-link model derived from motion capture recordings for a single subject during eyes open OLB trial. The root mean square error between the two methods for all subjects ranged from 1.5 mm to 14 mm with a mean value of 5 mm.

during the eyes open OLB trial (Figure 20). The root mean square error between the two methods for all subjects ranged from 1.5 mm to 14 mm with a mean value of 5 mm.

3.2.2.5 Heel-Toe Shuffle Experiment (Step 5 in Figure 18)

A full description of this experiment and its results are presented in the next chapter where we examine how movements of the stance foot can affect the angular momentum of the whole body during OLB.

3.2.2.6 One-Legged Balance Experiment (Step 6 in Figure 18)

All OLB tests were performed on the left leg which allowed the lab motion capture setup to reliably track all kinematic markers during the trial. *All but five of the subjects wore New Balance 411 walking shoes provided by the Biomechanics Research Lab.* The exceptions were for the participants whose shoes size was not available in the lab on the day of testing. Before the testing started, each subject received the same instructions: try to keep your back straight and arms crossed at all times. The right leg should not touch any point on the left leg as for example with thighs or knees pressing against each other. The right foot should not lean against the left leg, as in the yoga “*tree pose*”, or against the left foot and ankle. Movements of the stance foot were allowed as long as the foot stayed entirely within the bounds of the force plate. If the right foot touched the ground, or the subject maximally bent their trunk in the lateral or anterior direction, the test was halted. Subjects were given clear instructions regarding these rules and were continuously monitored for compliance. Any violation led the trial being halted.

Each subject started the experiment in their neutral bipedal stance: feet were shoulder width apart, one on each force plate. After the start of the data recording, the subject was instructed to stand on their left leg. The first two trials were warm-ups; the subject was then instructed to go back to their neutral bipedal stance after a successful transition to one leg. On the third trial, the subject was instructed to stand on their left leg for as long as possible. The tester stopped recording data at the four minute mark or upon failure to stand on one leg under the conditions described in the previous paragraph. Each subject performed the three OLB trials both with eyes open and with eyes closed. Since OLB with eyes closed is more dynamic than OLB with eyes open, and our hypotheses are concerned with the strength requirements of quasistatic OLB, *in this chapter, we will only examine the data for the eyes open trials.*

3.2.3 Calculating the States, Moments, and Parameters of the Double Inverted Pendulum Model for the OLB Experiment

3.2.3.1 Definition and Calculation of Kinematic Parameters from Motion Capture Marker Data

Below is a list of the important variables that are used to describe the state of the double inverted pendulum model for each subject, or used in the inverse dynamics calculations for calculating the ankle and hip moments during the OLB experiment.

Note: *The origin of the lab coordinate system was set at the geometric center of the top surface of the force plate on which the subject stood during the OLB experiment. The z-axis (0, 0, 1) is the vertical direction increasing with the height from the floor. The subject stood on the force plate such that their frontal plane was aligned with the xz-plane, and the sagittal plane with the yz-plane.*

Height: The height of the subject was measured without shoes in Step 1.

Body Mass: The weight of the subject measured while standing still for 10 s on the force plate, divided by the gravity constant (9.819).

M_0 : The mass of the left foot, found from the regression formula in Clauser [66].

Location of M_0 : M_0 was considered to be at the same location as the stance foot ankle.

M_1 : The mass of the stance leg calculated as $(m_1 + m_2) \times \text{Body Mass} - M_0$ (Figure 6). m_1 and m_2 are the percentage body mass of the shank + foot and thigh, respectively, as calculated for each subject in 3.2.2.4.

Location of M_1 during the OLB Experiments: We assumed that M_1 lies on a line connecting the left ankle to the left hip (Figure 6). To calculate the location of M_1 from the mass-link model in 3.2.2.4, the center of mass of the stance leg $(m_1 + m_2)$ was calculated and projected onto the line connecting the left ankle and hip joints in the kinematic data.

l : The distance between the left ankle and M_1 in the lab xz-plane, averaged during the OLB experiment with eyes open (Figure 6).

I_1 : The subject-specific mass moment of inertia for the stance leg around its center of mass, based on the anthropometric measurements in Step 1 and using regression formulae in the literature [67, 68]

M_2 : The mass of the head, arms, trunk, pelvis, and the non-stance leg calculated as $(m_1 + m_2 + m_3) \times \text{Body Mass}$ (Figure 6). m_1 , m_2 , and m_3 were calculated for each subject in 3.2.2.4.

Location of M_2 during the OLB Experiments: In the motion capture kinematic recordings, we derived the location of M_2 as the center of mass of the right leg m_1 and m_2 , and m_3 from the mass-link model in 3.2.2.4.

r : The distance between the left hip joint center and M_2 in the lab xz-plane, averaged during the OLB experiment with eyes open (Figure 6).

I_2 : The mass moment of inertia M_2 around its center of mass, calculated for each person based on the anthropometric measurements in Step 1 and using regression formulae in the literature [67, 68]

h : The distance between the left ankle and hip joint center in the lab xz-plane, averaged during the OLB experiment with eyes open (Figure 6).

Pelvic Inclination Angle: The angle between the Left ASIS-Right ASIS line with the horizon $(-1, 0, 0)$ in the lab xz-plane minus the average of the same angle during a 10 s quiet bipedal standing trial.

θ_1 : The angle between the vertical $(0, 0, 1)$ and the Left Ankle- Left Hip line in the lab xz-plane (Figure 7).

θ_2 (*hip abduction angle*): The angle between Left Hip-Left Knee line and the Horizon $(-1, 0, 0)$ in the lab xz-plane + Pelvic Inclination Angle (Figure 7).

γ : The angle between Horizon $(-1, 0, 0)$ and the Left Hip- M_2 line the lab xz-plane (Figure 7).

α : The angle between Left ASIS-Right ASIS line and Left Hip- M_2 line in the xz-plane (Figure 7).

Lateral Bending of the ‘Trunk’⁴: The angle between Mid Hip-Mid Acromia line and Left ASIS-Right ASIS line in the xz-plane minus the average of the same angle during a 10 s quiet bipedal standing trial.

Contralateral Hip Abduction Angle: The angle between the Right ASIS-Left ASIS line and the Right Hip-Right Knee line in the xz-plane

⁴ Since this technically is a line extending between approximately T3 and S4, we have termed this the ‘trunk’ rather than the thoracolumbar spine.

3.2.3.2 Numerical Calculation of Derivatives in the States' Time-Series

We needed to calculate the first and second derivatives of the states (θ_1, γ) as inputs to the inverse dynamics algorithm for calculating ankle and hip moments during OLB experiments (please see Appendix I). After a survey of literature, and experimenting with our data, we decided that fitting a quintic smoothing spline to the states and calculating the derivatives from the spline was best suited for our data and calculations [69]. Doing so ensured continuous second derivatives. We used the “*spaps*” command in MATLAB © to fit the splines to the states which were in radians, and set the tolerance at 0.5 degree, also in radians (tolerance = $0.5 \pi / 180$).

3.2.3.3 Simple Theoretical Calculation of Hip Abduction Moment

Demand during OLB

We can estimate the hip abduction moment demand for quasistatic OLB, if we make three simplifying assumptions:

- 1- The body mass is distributed symmetrically about the sagittal plane.
- 2- The pelvis is kept close to a level inclination angle.
- 3- The non-stance ankle is kept in the same vertical plane as the hip joint center on the same side.

In case the above three assumptions hold, we can simply calculate the hip abduction moment demand by writing the static equilibrium moment around the stance hip joint center.

$$T_{Abd} = M_{HAT}g \times a + M_{Leg}g \times 2a = (M_{HAT} + 2M_{Leg})g \times a = \text{Weight} \times a$$

where ‘ M_{HAT} ’ is the mass of the head, arms, trunk and the pelvis, ‘ M_{Leg} ’ is the mass of each leg, and ‘ a ’ is half the inter-acetabular distance. This formula for the hip abduction moment demand during OLB was first presented by Inman in 1947 [24]. Charnley and McLeish experimentally showed that this formula is correct, however it was found to be very sensitive to the lateral bending of the trunk, pelvis inclination angle, and the contralateral hip

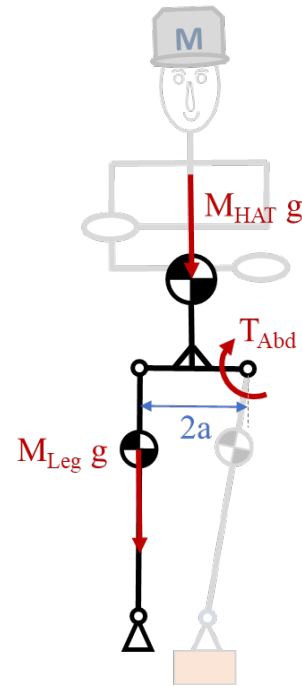


Figure 21- Assuming the body mass to be distributed symmetrically around the sagittal plane, the non-stance ankle is in the same vertical plane as the hip on the same side, and the pelvis is kept at a level inclination angle, the hip abduction moment demand (T_{Abd}) during quasistatic OLB can be estimated as the total body weight times half the inter-acetabular distance. Please see text for the calculations.

abduction angle [25]. We will use this value to normalize the mean hip abduction moment demand calculated by using the inverse dynamics equations of the double inverted pendulum model of each subject.

3.2.3.4 Calculating the Ankle and Hip Abduction Moments during the OLB Experiment

Inverse Dynamics Equation 1 to Inverse Dynamics Equation 6 in Appendix I fully describe the dynamics of the double inverted pendulum model with the assumption that the movements of the stance foot are negligible. Since we calculated the mean values for the inertial and anthropometric parameters of the model in 3.2.3.1 and calculating the derivatives of the states in 3.2.3.2, we can replace them in the Inverse Dynamics Equations to calculate ankle and hip abduction moments. We used a weighted least squares method for the inverse dynamic analysis described in [70].

3.2.3.5 Calculating the Intensity of Hip Abduction Moment at any Instant during the OLB Experiment

In the previous section we showed how we used inverse dynamics equations for the double inverted pendulum model to calculate the hip abduction moment demand during OLB experiments. The intensity of the hip abduction moment demand is defined as the hip moment demand divided by the maximum available isometric hip abduction strength. But force-length characteristics of the muscles surrounding the hip joint makes the maximum isometric strength a function of the hip abduction angle [41]. So we used the same method as A4 in 2.2.1.1 to account for the change in maximum isometric hip abduction strength with the hip abduction angle. To then calculate the intensity of the hip abduction moment demand, we divided the hip abduction moment demand by the maximum isometric strength at any time point and therefore derived a time-series for the intensity of the hip abduction moment demand. We repeated this process for the adjusted maximum hip abduction moment calculated using the endurance time test. For more details please refer to 3.2.2.1.

3.2.4 Feature Extraction from Time-Series Data for Each Subject during OLB Experiment

After processing the force plate and motion capture data recordings into meaningful variables described in 3.2.3, we obtain a time-series for each of them. For example, for three minutes of OLB, we have a time-series for the hip abduction moment consisting of 3 min x 60 s/min x 90 Hz = 16,200 data points. Since OLB is a mostly quasistatic experiment, we can

extract most of the meaningful information out of each time-series by just a few parameters. In order to do so we first ensured that we are extracting the correct information from each time-series by making a few considerations described in the next two sections.

3.2.4.1 Dealing with Missing Motion Capture Marker Data

In some instances, a glitch in the wire connections to the motion capture markers, or a temporary occlusion of the path of the motion capture cameras to the markers causes the system to purposely classify them as “missing”. So we used a shape-preserving piecewise cubic interpolation (“*resample*” command in MATLAB © with “*pchip*” method) to fill in the missing data, while keeping track of the time points where one of the critical markers (*i.e.*, pelvis, stance leg, or chest markers) were missing. This method works efficiently when only a few consecutive time points are missing, but big gaps in the data may result in erroneous calculations. So we created a tag for any time slot where any of the critical markers were missing for more than 15 consecutive time points (160 ms). To maintain rigor, the time slots with the “*Missing*” tag were removed from the analyses.

3.2.4.2 Alignment of the Participant’s Frontal Plane with the Lab xz-Plane

In all our analyses we assumed the OLB to be mostly contained in the frontal plane. We also assumed that the frontal plane of the participant and the xz-plane in the lab are aligned. We can make these assumption because all participants performed the OLB experiment facing the same direction, and they mostly stayed in the same orientation throughout the experiment. However, certain events like shuffling of the stance foot or rotation of the upper body by internal / external rotation around the stance hip could render our estimation of different states incorrect. This would then bias the ankle and especially hip moment calculations as well. To account for this uncommon event, we passed a vertical plane through the left and right hip joint centers along with the stance leg’s ankle and knee using the least squares method. By keeping track of the change of angle between this vertical plane and the xz-plane, we identified time slots where the assumptions at the beginning of this paragraph did not hold anymore (more than 5 degree deviation from the baseline) and tagged them as ‘misalignments’. To maintain rigor, the time slots with the “*Misalignment*” tag were removed from the analyses.

3.2.4.3 Trimmed Mean and Slope of Variables during OLB Experiments

Once we remove the time points with “Missing” and “Misalignment” tags, we can see that most of the time-series of the different calculated variables consists of a main linear trend with a small slope with variations around the linear trend (Figure 24). This is because OLB for healthy people is mostly a quasistatic balancing task which does not involve sudden changes in body posture. For the variables that are important for calculating the hip abduction moment, we extracted the linear trend (trimmed mean and slope) along with the root mean square error for the deviation from the linear trend. We did so because one of our main hypotheses for this chapter concerns the hip abduction moment during OLB. These variables included: hip abduction moment and intensity, pelvis inclination angle, hip abduction angle (θ_2), γ , lateral bending of the trunk, and the contralateral hip abduction angle.

Trimmed Mean (“*trimmean*” function in MATLAB © with 20% cut): The mean of the time-series excluding the ten percent of the highest and lowest data values. The trimmed mean has the advantage of being more robust to transitory outlier values than regular mean.

3.2.5 Plotting Subject Specific Feasible Balance Region and Trajectory of the OLB States

In Chapter 2, we introduced the concept of FBR and showed how its boundaries are defined by the anthropometry and the capacities of the lower extremities. In this chapter, we have extracted the anthropometric parameters (M_1 , M_2 , r , l , and h) in addition to measuring the left leg ankle and hip isometric strengths for each subject. We also ensured that all subjects had normal range of motion in their hip and ankle in all direction. Therefore, we can draw the FBR for each subject and calculate the Length, Width, and Area of the FBR for them. Besides, since we have the time-series of the states describing the orientation of the double inverted pendulum model (θ_1 , θ_2), we can now draw the trajectories of the states on the same plot as the FBR. While FBR assumes the states are quasistatic, we will relax this restriction in our demonstrations and calculate the percentage of time the states stayed within the boundaries of the calculated FBR during the eyes open OLB experiment. This will not introduce a substantial error because OLB with eyes open is mostly a quasistatic task.

3.2.6 Statistical Analyses

All statistical analyses were performed with R version 3.6.0. The kinematic and inverse dynamic calculations were performed with MATLAB © version R2018b. Plots were made with

MATLAB and the ggplot2 package in R. All between-group comparisons between age group and sex were performed using two-way ANOVA in R. Regression lines were fitted to the time-series data for each participant using MATLAB. Linear regressions analyses were performed in R to explore the relationship between UST as the dependent variable, and normalized strength data, weight, height, and FBR area as the predictors. AIC and improvements to R^2 were used to pick the best single or multiple variables for predicting UST.

3.3 Results

All the results presented here are from the maximum unipedal stance time experiment, which was performed with crossed arms and open eyes.

3.3.1 Maximum Measured Unipedal Stance Times (UST)

Nine out of 10 women and 6 out of 10 men in the young group, 0 out of 10 women and 1 out of 8 men in the old group stood on one leg with eyes open for four minutes, *i.e.* max length of the trial. Figure 22 shows the boxplot of the UST for men and women in our young and older groups. UST was significantly different between the young and older groups ($p < 0.0001$). Age Category, as the predictor of the linear regression model, accounted for 57% of the variations in UST ($R^2 = 0.57$). Amongst the measured normalized lower extremity strengths (please see Table 9 for a full list), weight, height, and FBR Area, we explored single variable or multiple variables as the predictors for the linear model with UST as the dependent variable. None performed better than age category or age (numeric) based on both improvements in R^2 and AIC. Also, none significantly improved the predictions of the linear model with age category or age variable. Even when we only considered the UST for older participants, so that we do not have so many outcome variables that are censored from the top, age category and age still outperformed all the other aforementioned predictors in terms of adjusted R^2 value and Akaike Information Criterion.

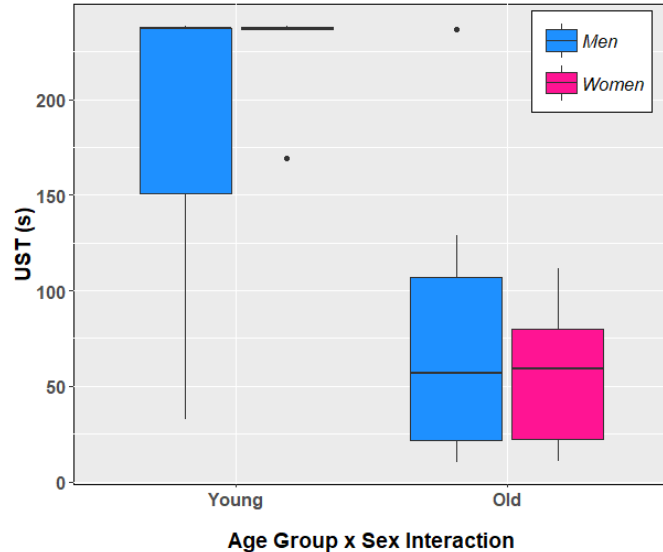


Figure 22- Unipedal Stance Time (UST) boxplot for men and women in the young and older groups. 9 out of 10 women and 6 out of 10 men in the young group stood on one leg for four minutes (maximum length of the trial). Only one subject in the old category reached 4 minutes. The black line in the middle of each box is the group median. In this and any following boxplots, the lower and upper hinges correspond to the first and third quartiles (the 25th and 75th percentiles). The whisker extends from the hinge to the largest and smallest value no further than 1.5 times the interquartile range. The data beyond the end of the whiskers are plotted individually.

3.3.2 Predicted Feasible Balance Region based on Subject-Specific Parameters

Figure 23 shows the FBR and the trajectory of OLB states for four different participants. It should be noted that FBR was only derived for quasistatic states (please see 2.2.1), and the full states of the OLB include $(\dot{\theta}_1, \dot{\theta}_2)$ in addition to (θ_1, θ_2) . However, since our participants spent most of their OLB time in a quasistatic posture, we can see that the boundaries of the FBR are still successfully containing the OLB states in these four subjects.

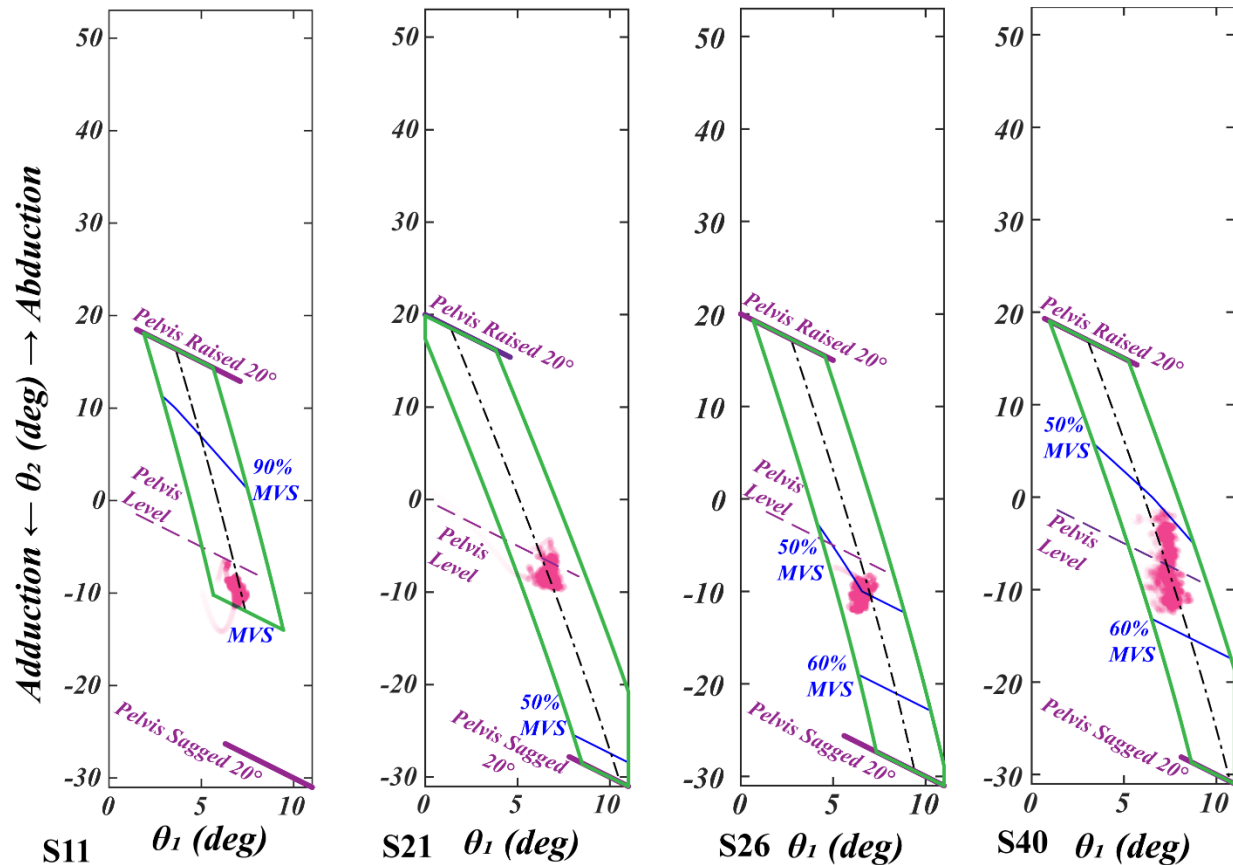


Figure 23- FBR (regions within the green border) and trajectory of the states of the double inverted pendulum model (cloud of pink points) for four different subjects during their OLB trial with eyes open. Opacity of the pink cloud points are related to the frequency of the states where the more transparent points indicate less frequency of occurrence. The blue lines indicate locus of states where the required abduction moment is equal to a constant percentage of the maximum adjusted hip abduction moments for each participant (3.2.2.1). For more details on how FBR is drawn and how each capacity constrains the length and width of the FBR, please refer to Figure 9. S11, S21, S26, and S40 are an older woman, young man, young woman, and an older man respectively.

Table 10 quantifies the FBR dimensions for our cohort of subjects and shows the efficiency of the FBR in predicting a boundary for the OLB states of the subjects. We can see that while the functional base of support boundaries are mostly successful in containing OLB

states (both quasistatic and dynamic), the maximum hip abduction strength boundary does not seem to perform as well. In the Discussion we will explore the reasons why this can happen.

*Table 10- Predicted Feasible Balance Region (FBR) dimensions and success of its boundaries in containing the OLB states for healthy young and healthy older adults in our OLB experiment. The FBR Length, Width, and Area from our cohort of subjects can be compared with those from Chapter 2 which were derived for the anthropometry of a 50th percentile man with strengths extracted from the literature (please see 2.2.1.1 for more details). **The entries inside the parentheses in this Table and all the following indicate the group standard deviation.** The three right columns indicate what percentage of the OLB trial each subject spent within different boundaries of the his/her own FBR: “States inside FBR” includes all the boundaries, “States inside FBOS” includes the bounds set by the functional base of support (i.e. the two long parallel FBR boundary lines in Figure 23), and “States inside Hip Strength” includes the boundary set by the maximum hip abduction strength. OLB states for 4 out of 10 women in the older group and 1 out of 8 men in the young group were completely below the maximum hip abduction strength line in the FBR. In the Discussion we will explore the possible reasons for this observation.*

Group		Predicted FBR based on subject-specific parameters					
		Area (deg ²)	Length (deg)	Width (deg)	States inside FBR (%)	States inside FBOS (%)	States inside Hip Strength (%)
HY	Men	168 (25)	46 (5)	3.6 (0.4)	80 (37)	86 (25)	88 (34)
	Women	162 (32)	45 (5)	3.6 (0.5)	100 (1)	100 (1)	100 (0)
HO	Men	128 (33)	39 (9)	3.2 (0.2)	97 (3)	98 (2)	99 (2)
	Women	90 (52)	26 (15)	3.5 (0.6)	56 (49)	94 (9)	60 (51)
Group		Predicted FBR based on literature values (Chapter 2)					
HY	Men	122	44	3			
	Women	121	44	3			
HO	Men	110	44	3			
	Women	82	34	2			

3.3.3 Primary Outcome Measure: Estimated Hip Abduction Moment Demand and Intensity during OLB Experiment

Figure 24 shows the estimated hip abduction moment demand and its intensity during the eyes open OLB trial for one of our participants. This was elected as a good representation of all subjects who stood for more than 20 seconds. We can see that while there are small variations in both the moment and intensity values, the general trend can be captured by a single line (please see 3.2.4.3 for more information on our feature extraction method for time-series). The trimmed mean value without 20% of the outliers, the slope of the trend line, and the root mean square of error between the trend line and the data were extracted from both time-series for each subject. Table 11 shows the descriptive statistics for the above extracted variables for all our subjects divided by age and sex categories. We can see that both the intensity of the hip abduction moment demand and RMSE of the data with the trend line was significantly higher in the older group. This difference is mostly driven by the difference in maximum voluntary hip abduction strength between young and older adults. We can also see that the slope of the changes in intensity was not significantly different from zero. *This indicates that even for the long OLB trials, our participants were not doing anything to alleviate the high hip abduction moment intensity.*

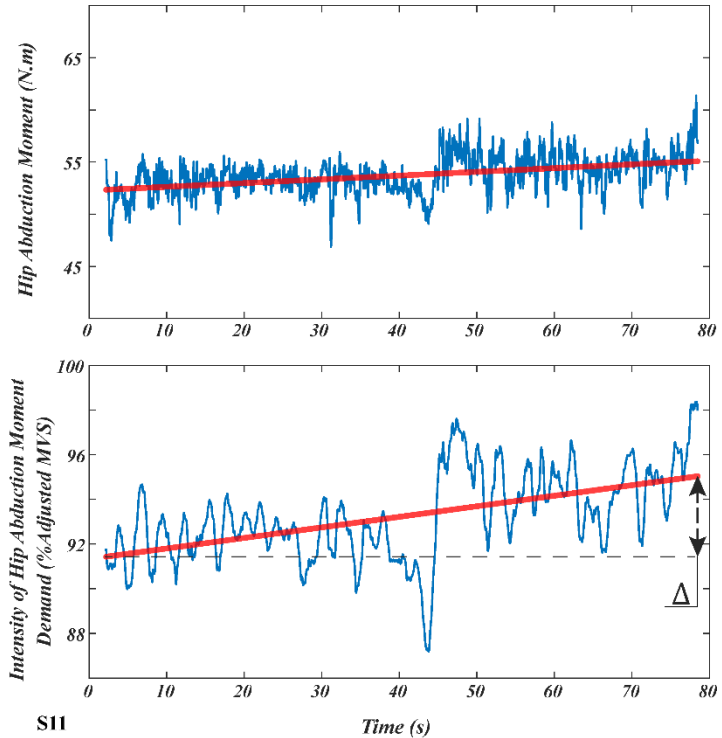


Figure 24- Sample time-series for hip abduction moment (top) and intensity of hip abduction moment demand (bottom) during OLB trial for subject S11. The red line in both plots is the linear model fitted to the time-series to capture the general trend of change over time. The trimmed mean value without 20% of the outliers, the slope of the trend line, and the root mean square of error between the trend line and the data were extracted from both time-series for each subject (please see 3.2.4.3 for more information on our feature extraction method for time-series).

Table 11- Descriptive statistics for the time-series of calculated hip abduction moment demand (normalized by weight and half the inter-acetabular distance), and intensity of the hip abduction moment demand (% of adjusted maximum voluntary hip abduction strength) during the eyes open trial for all subjects. The bolded entries are the mean values for the main outcome measure. For detailed description of Mean, Slope and RMSE please refer to Figure 24 and 3.2.4.3. The inter-acetabular distance was measured here by calculating the horizontal distance between the two hip joint centers (which were found functionally from motion capture data, please see 3.2.2.3) while the subject was quietly standing on both legs. Mean intensity of the hip abduction moment demand during OLB is defined as the mean ratio of the hip abduction moment and the maximum available voluntary hip abduction strength. The difference in maximum voluntary hip abduction strength drives the highly significant age group difference in the calculated Mean and RMSE for Intensity. For a review of the adjustment to the maximum voluntary hip abduction strength please refer to 3.2.2.1. We can also see that the slopes of the hip abduction demand and its intensity are not significantly different from zero. This indicates that even for the long OLB trials, our participants were not alleviating the high hip abduction moment intensity.

		Young (20-30 yrs)		Older (65-80 yrs)		p-value
		Men (n = 8)	Women (n = 10)	Men (n = 7)	Women (n = 10)	
Calculated Hip Abduction Moment Demand	Mean (N.m/N.m)	0.87 (0.1)	0.94 (0.05)	0.96 (0.11)	1.06 (0.11)	0.001 ¹ 0.01 ²
	Slope (1/min)	0.016 (0.053)	-0.002 (0.016)	0.001 (0.173)	-0.015 (0.233)	N.S.
	RMSE (N.m/N.m)	0.04 (0.02)	0.03 (0.01)	0.05 (0.01)	0.04 (0.01)	N.S.
Calculated Intensity of Hip Abduction Moment Demand (% Adjusted Voluntary Hip Abduction Strength)	Mean (%)	53 (19.7)	55 (15.8)	72 (16.9)	94 (22.7)	< 0.001¹
	Slope (%/min)	-0.36 (1.7)	-0.56 (0.7)	-1.6 (9.3)	-2.1 (9.1)	N.S.
	RMSE (%)	2.5 (1.5)	1.9 (0.9)	3.6 (1.6)	3.7 (1.1)	0.001 ¹

¹Age main group effect

²Sex main group effect

³Age:Sex group interaction

3.3.4 Measured Kinematic Changes: Pelvic Inclination Angle and Lateral Bending of the Lumbar Trunk

Both pelvic inclination angle and lateral bending of the trunk are related to how each participant chose to stand on one leg. This in turn affects the mean hip abduction moment demand during OLB. Lateral bending of the trunk is particularly important to track during the trial since the effect of changes to it during the OLB trial cannot be fully captured by our inverse dynamics calculations. This is due to the rigid body assumption for the head, arms and trunk. In Table 12 we can confirm that the changes in these two kinematic parameters in the course of the OLB trial are not substantial.

Table 12- Descriptive statistics for the trend line passing through the time-series of “Pelvic Inclination Angle” and “Lateral Bending of the Trunk” during the eyes open trial for all subjects with UST > 20 s. UST > 20 s was chosen to include only the participant who stood on one leg long enough to feel the effects of muscle fatigue. “Initial Angle” refers to the intercept, Δ is the total change in the trend line value over the full OLB trial (please refer to Figure 24 for demonstration), and RMSE is the root mean square error between the time-series and the trend line. While we see that men in our cohort of participant started the trial at a slightly more raised pelvic inclination angle, the mean initial pelvis inclination angle is not different than level in a meaningful way ([1.5, 5.4 deg] Men and [-1.2, 2.2 deg] Women, 95% Mean Confidence Interval). Also, all four groups slightly dropped their pelvis inclination angle on average for the duration of the OLB trial ([-3.4, -1.5 deg], 95% Mean Confidence Interval). Mean lateral bending of the trunk at the start of the OLB trial was slightly bigger than zero for the Young subjects ([2.0, 4.9 deg] Young and [-0.8, 2.7 deg] Older Subjects, 95% Mean Confidence Interval). In addition, on average all groups laterally bent their trunk further in the duration of the OLB trial ([1.5, 3.5 deg], 95% Mean Confidence Interval).

		Young (20-30 yrs)		Older (65-80 yrs)		p-value
		Men (n = 8)	Women (n = 10)	Men (n = 5)	Women (n = 7)	
Measured Pelvis Inclination Angle (deg)	Initial Angle	2.8 (3.9)	-0.6 (3.4)	4.4 (2.1)	2.2 (3.2)	0.03 ²
	Δ	-1.9 (1.9)	-2.9 (2.5)	-2.4 (4.5)	-2.4 (1.6)	N.S.
	RMSE	0.9 (0.4)	0.8 (0.6)	0.6 (0.2)	0.6 (0.2)	-
Measured Lateral Bending of the Trunk (deg)	Initial Angle	2.6 (3.8)	4.1 (2.5)	0.7 (2.2)	1.1 (3.0)	0.03 ¹
	Δ	2.2 (2.2)	3.2 (2.3)	3.2 (4.4)	1.4 (2.2)	N.S.
	RMSE	0.9 (0.5)	0.7 (0.4)	0.5 (0.2)	0.5 (0.1)	-

¹Age main group effect

²Sex main group effect

³Age:Sex group interaction

3.3.5 Relationship between Hip Abductor Muscle Endurance Times and UST

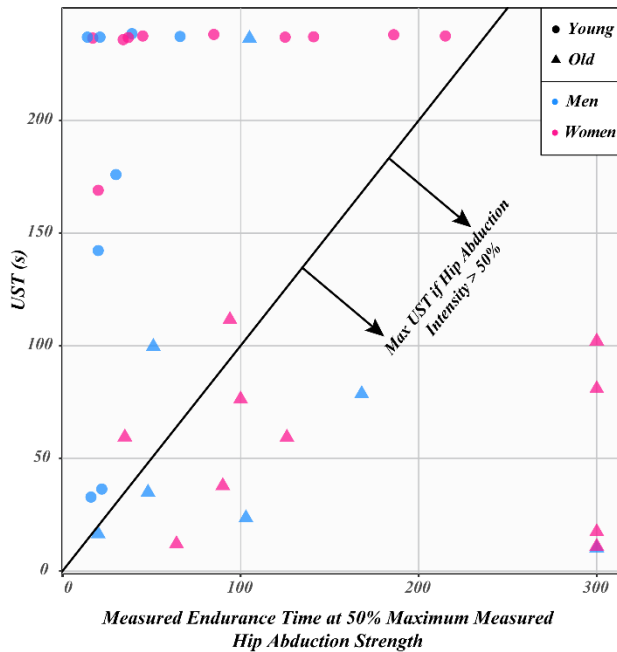


Figure 25- Measured Unipedal Stance Time (UST) vs. measured endurance time at half of each subject's measured maximum voluntary hip abduction strength. If subjects were using more than 50% of their maximum hip abduction muscle strength during OLB trial, then we would expect all the points to fall below the diagonal line with zero intercept and slope equal to one.

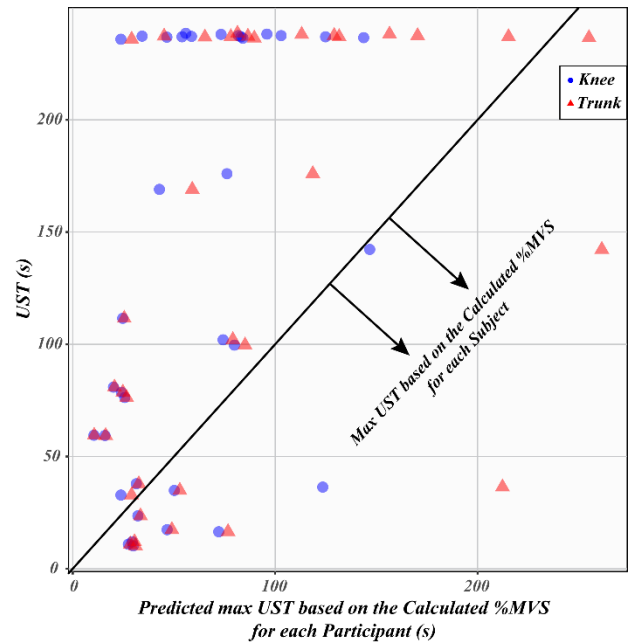


Figure 26- Measured UST vs. anticipated max UST based on the calculated intensity of the hip abduction moment demand for each subject and the isometric exertion endurance time model parameters for knee and trunk [15, 17]. Knee and trunk fatigue models were used because there are not enough endurance time studies for the hip abductor muscles in the literature. If all the hip abduction moment demand was coming from the hip abductor muscles, then the fatiguing of these muscles would have to keep the points below the diagonal line with zero intercept and slope equal to one.

Figure 25 compares the UST with the measured fatigue time at 50% of the maximum voluntary hip abduction strength. We can clearly see that all of the young participants and four of the older participants had a longer UST that their own fatigue time. This means they were using less than 50% of their maximum voluntary strength to stand on one leg. In Figure 26, we used the published endurance time curves for knee and trunk and the estimated subject specific intensity of the hip abduction moment demand during their OLB to estimate the maximum UST that was possible before fatiguing their abductor muscles [15, 17]. Again we can see that most of the subjects stood on one leg for much longer than either of the predicted fatigue times using the knee and trunk fatigue parameters.

3.4 Discussion

One-legged balance (OLB) is one of the most commonly used clinical tests of balance. Maximum unipedal stance time (UST) is the primary outcome measure for this clinical test. Given the large hip abduction moment demand of OLB, we hypothesized that quasistatic OLB states have to be contained in a feasible balance region whose boundaries are defined by the maximum hip abduction strength and ankle inversion/eversion strengths. Also we hypothesized that the UST is limited from above by the fatiguing in the hip abductor muscles most importantly the gluteus medius, gluteus minimus, and the tensor fasciae latae.

To our knowledge this is the first study of OLB where the intensity of the hip abduction moment demand as a percentage of maximum voluntary hip strength has been quantified experimentally. We confirmed that on average, the calculated abduction intensity was over 50% for both young and older adults. We therefore reject the hypothesis (H_1 in the Introduction) that all quasistatic OLB states stay contained within the boundaries of the FBR defined by maximum hip abduction strength and ankle inversion and eversion strengths. This result was surprising because we assumed during OLB subjects hip adduction angle was not close to the end of range of motion and therefore only the abductor muscles could counter the OLB hip abduction moment demand due to gravity.

Our second hypothesis (H_2 Introduction) was also rejected. Neither the measured endurance time of the hip abductor muscles at half of the measured maximum hip abduction strength nor the predicted hip abduction endurance time from the intensity of the hip abduction moment demand predicted an upper limit for the UST. How could the subjects (especially the young adults) stand for four minutes when both measures of endurance suggest they should have UST less than 2 minutes? This result could be explained by an underappreciated load sharing mechanism involving the iliotibial band, namely the iliotibial mechanism. In the remainder of the discussion we will first examine all the evidence pointing to the substantial role of the iliotibial mechanism that helps the abductor muscles in resisting the hip abduction moment demand of OLB. Then we try to estimate its contribution to resisting the OLB hip abduction moment demand. Subsequently, we will examine how accepting the role of such load sharing mechanism changes our description of the FBR and its utility in explaining the OLB posture of patients with severe hip abduction weakness. Finally, we will examine a possible reason why maximum

voluntary hip abduction strength is important in avoiding a lateral fall during OLB despite the existence of the load sharing mechanism.

3.4.1 Evidence for the Existence of a Load Sharing Mechanism between Hip Abductor Muscles and an Iliotibial Band during Quasistatic OLB

In this chapter, we have shown two distinct pieces of evidence that point to the existence of a load sharing mechanism between the hip abductor muscles (mainly gluteus medius, gluteus minimus and tensor fasciae latae), the iliotibial band (namely the iliotibial mechanism or ITM), and other passive tissues around the hip during OLB. In what follows, we will discuss the evidence and then briefly go over other examples from the literature. Examining all the evidence, we can conclude that even during OLB with a level pelvis, the hip abduction moment demand is being shared between the abductor muscles and most probably the ITM. Dropping the pelvic inclination angle will increase the ITM share of the load, whereas raising it will decrease it and put more load on the abductor muscles.

3.4.1.1 Ineffectiveness of the Maximum Hip Abduction Strength Boundary of FBR in Containing the OLB States

In Table 10 we showed that the maximum hip abduction strength constraint was violated for some of the OLB states of our participants, especially the women in the older group. In fact four out of ten women in the older group spent the entirety of their OLB time ($UST > 59$ s for three of them) well outside the maximum hip strength boundary. This implies that the hip abduction moment demand for their OLB was more than their maximum hip abduction strength. In other words the intensity of the hip abduction moment demand was more than 100%! Of course, this could be due to an underestimation of their maximum hip abduction strength, or errors in the calculation of the hip abduction moment demand. In terms of an underestimation of the hip abduction strength, it should be noted that we have already adjusted the measured maximum hip abduction strengths to an equal or higher value by using the endurance time model predictions found in the literature for young and older adults [15, 17] (please see 3.2.2.1 for details of this adjustment). In Appendix III we quantified the sensitivity of our estimation for intensity to different potential sources of bias in our measurements, including an underestimation of the maximum hip abduction strength. Still, even the most conservative estimations of an upward bias for our estimates of intensity will barely place the OLB states for the

aforementioned subjects inside the maximum hip abduction strength boundary of their FBR (similar to subject S11 in Figure 23).

3.4.1.2 Measured Unipedal Stance Times (UST) are longer than Measured and Predicted Endurance Times for Most Participants

In Chapter 2 we predicted the intensity of the hip abduction moment demand during OLB based on a double inverted pendulum model with anthropometry and lower extremity capacity data from literature. We showed that even for the younger adults, the mean intensity of the demand for standing with a level pelvic inclination angle was on average over 50% of the reported maximum hip abduction strengths (please see 2.3.5 for more details). We used this information in designing our OLB experiment procedures; after measuring the maximum hip abduction strength for each subject, we also measured their endurance time (ET) at close to half of their maximum voluntary strength (ET at 50% MVS). If our subjects were indeed using over 50% of their maximum strength to stand on one leg, then a plot of UST vs. ET at 50% MVS should have all the points below a diagonal line with slope equal to one and intercept equal to zero. This was not the case at all (Figure 25). All the young subjects and four of the older subjects stayed above the line. So we can safely conclude that those participants were using less than 50% of their real abduction MVS to stand on one leg. Indeed, our estimations showed that some of participants were at or below 50% MVS during their OLB trial. But the mean calculated intensity for the young subjects was over 50% (please see Table 11). In addition, using the estimated %MVS for each subject, we calculated the endurance time for them using the knee and trunk fatigue parameters in the literature [15, 17]. Figure 26 shows the UST vs. the predicted endurance time using both knee and trunk fatigue parameters. We can still see that most of the subjects' UST exceed their predicted endurance time based on their estimated %MVS. This could be due to four reasons that we will address in the remainder of this section.

1) Could there be a systematic bias in measurements of the parameters that leads to an overestimation of the intensity of hip abduction moment?

We think not. In Appendix III we compared our measurements of maximum voluntary hip abduction strength (MVS) and the mass of the body balancing over the stance leg as a percent of total body weight (m_2) with those from the literature and showed that our estimates are not biased compared to them. We also quantified the errors that we could have in determining the moment arm of m_2 and considered all the error to act as a bias contributing to an exaggerated

estimation of the intensity. We then showed that with even the most conservative (and unrealistic) way of accounting for these hypothetical biases, the mean calculated intensity for the young men and women would reduce from 53 and 55% to 38 and 45% respectively. Even at 38% of “allegedly unbiased” intensity the endurance time model for the knee and trunk would anticipate a maximum UST no longer than 120 s and 204 s respectively. Given that the subjects who were stopped at the four minute trial could still continue standing on one leg, this clearly shows that all the discrepancy between the anticipated endurance time and UST cannot be attributed to errors in estimation of the intensity of the hip abduction moment demand.

2) Could large variations in intensity of hip abduction moment demand during the OLB trial allow time for recovery from the effects of fatigue?

We think not. In Table 11 we showed that the mean slope of the trend line passing through the time-series for intensity during the OLB trial was not different than zero for any of our considered groups. We also showed that the average root mean square of error (RMSE) between the trend line and the time-series was less than 4%. Therefore such general slopes and variations cannot allow recovery from fatiguing of the hip abductor muscles.

3) Could the lateral bending of the trunk relieve the demand on the hip abductor muscles?

We think not. In 2.3.4 we showed that a lateral bending of the trunk at half of the maximum range of motion could reduce the intensity of the hip abduction moment demand during OLB by 37%. This is a substantial reduction! Should the participants keep bending their trunk in the medial and lateral directions, the effect would not be captured by the inverse dynamic algorithm calculating the hip abduction moments. That is because the model assumes the upper body and the non-stance leg as one rigid body (M_2). To account for this source of error, we calculated the time-series of the parameters describing the rigid body M_2 , namely α and r in Figure 6, and observed that they do not have large sudden changes, then chose the trimmed mean for r and γ instead of α (please see Figure 7) as the state of double inverted pendulum in the inverse dynamics equations. Besides, in Table 12 we then examined the time-series data for the lateral bending of the trunk for each subject. We noticed that on average our participants slightly bent their trunk laterally as the OLB trial continued ([1.5, 3.5 deg], 95% Mean Confidence Interval). But given the small additional bending of the trunk, our choice of r as the trimmed mean of all the time-series for r during the OLB trial, and our choice of γ instead of α in the inverse dynamic equations, this overestimation of intensity should be inconsequential.

4) Could out of plane rotation of the upper body towards the stance limb increase the moment arms of the hip abductor muscles and therefore reduce the hip abduction moment demand of OLB?

We think not. There are published modeling data that show that internal / external rotation of the hip can change the moment arms for the hip abductor muscles [71]. So if a participant keeps wobbling around the vertical axis, technically they could be changing their hip abductor muscles' moment arms and perhaps relieve some of the fatigue. Firstly the subjects were instructed and monitored to face forwards at all times during their OLB and not twist around the vertical axis. Secondly, we used least square method to pass a vertical plane through the two hip joints centers and the stance leg's knee and ankle. We then examined the time-series of the angle between the defined plane and the lab's xz-plane as a proxy for the hip internal / external rotation angle. We noticed that the slope of the trend line passing through the time-series was not significant and its RMSE were under 2 degrees. Therefore, we can conclude that this could not be a substantial contributor to relieving the abduction moment intensity for our subjects during the OLB trial.

5) Could the hip abductor muscle fiber composition be more fatigue resistant than neighboring knee and trunk muscles?

We think not. It is possible but unlikely that the hip abductor muscles have a higher type I composition than the knee and trunk muscles that we used to estimate endurance times [72, 73]. However, our measurements of each subject's own endurance at 50% of their maximum hip abduction strength pointed to the same conclusion that their UST was significantly longer than their measured hip abduction muscle endurance time. So we do not believe that the hip muscles had a higher Type I muscle fiber composition than the muscles in the knee and the trunk.

3.4.1.3 Additional Evidence from the Literature for the Existence of Load Sharing Mechanism between the Abductor Muscles and the Iliotibial Mechanism during OLB

Further evidence for the existence of a load sharing mechanism in providing the hip abduction moment demand during OLB comes from EMG studies. In 1947, Inman performed a series of tests to calculate the hip abduction moment demand during OLB [24]. He calculated a theoretical value for the demand of weight times half the inter-acetabular distance in the same way we described in 3.2.3.3. He measured the inter-acetabular distance from x-rays of the pelvis of his 35 subjects. Then he measured the maximum hip abduction strength in each of them while the subject was standing and needle and surface EMG data were being recorded from the major abductor muscles (Figure 27). He created a calibration curve for each subject with EMG action potentials on the y-axis and hip abductor muscle moment on the x-axis. Next he had subjects stand on one leg with a level pelvis. He noticed that the estimated hip abduction moment from his recorded EMG activity was substantially smaller than his theoretically calculated hip abduction moment. He repeated the test with the same subjects, this time recording EMG while each subject stood with a dropped pelvic inclination angle, level pelvis, and a raised pelvic inclination angle. He found that although the hip abductor moment demand decreased with raising the pelvic inclination angle on the non-stance hip side, the EMG activity increased, and vice versa; letting the pelvic inclination angle drop about 15 to 20 degrees, decreased the EMG activity to insignificant. He concluded that there has to be a “ligamentous pull” from the iliotibial band. He estimated that while subject stood on one leg with a level pelvis, on average the abductor muscles were providing 54.9 ± 17.9 % of the hip abduction moment demand in men and 57.7 ± 18.2 % in women.

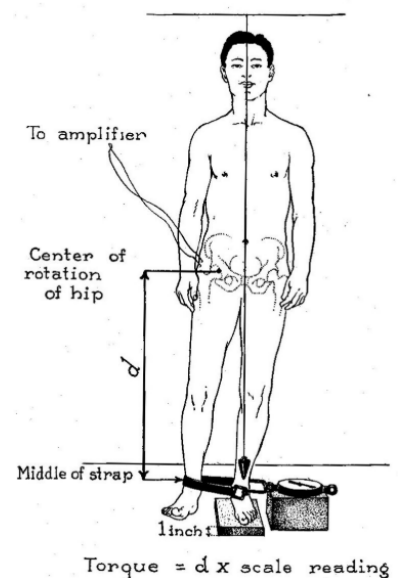


Figure 27- Inman's setup for measuring maximum hip abduction strength with the subject standing and needle and surface EMG data being recorded from the tensor fascia femoris, and gluteus medius and gluteus minimus muscles (Copied from [24]).

In 1970 Charnley and McLeish refuted Inman's theory of a ligamentus pull citing two reasons [25]: 1) Inman's EMG recording system and its amplifier were outdated, and 2) not being close to the end of hip adduction range of motion would make a ligamentus pull insignificant. Both reasons can be shown to be flawed. First, accepting that the exact numbers of the recorded EMG activity can be inaccurate, the trend in increasing or decreasing of the EMG activity however would still hold.

Additionally, in 2014, Prior *et al.* showed the same trend with a new surface EMG system [26]. They measured EMG activity of abductor

and adductor muscles in subjects standing on one leg between dropped and raised pelvic inclination angles and reported the same trend as Inman: Pelvic drop reduced the EMG activity in major abductor muscles, namely gluteus medius and tensor fascia latae, while a pelvic raise increased it. Charnley's second argument can also be disputed. An examination of [Ober's test](#) for evaluating a tightness in iliotibial band reveals that a tight IT band can reduce the hip adduction range of motion down close to zero degrees while in a normal case the hip can adduct 21 ± 5.5 degrees during the Ober's test [74, 75]. One can argue that during Ober's test, the only adduction moment that is being resisted by the IT band is due to the weight of the leg, which is smaller than the hip abduction moment demand of OLB. However, this still proves that the contribution of the IT band to providing some of the hip abduction moment demand during OLB cannot be neglected.

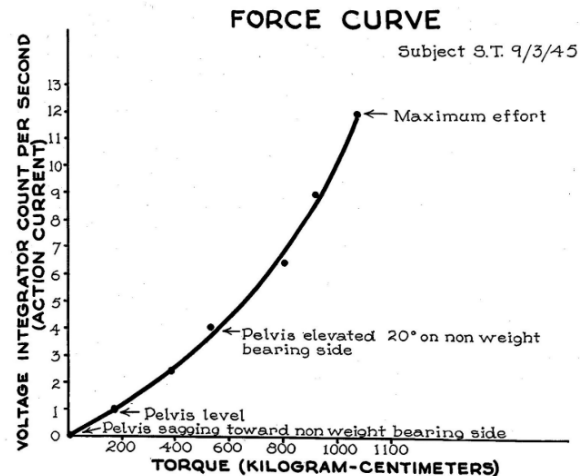


Figure 28- EMG Action Potential vs. Hip Abduction Torque in Inman's experiment. He noticed that raising the pelvic inclination angle on the non-stance hip side increased EMG activity while letting it drop reduced it to virtually zero activity at about 15-20 degrees. (Copied from [24])

3.4.2 Description of the Load Sharing Mechanism between the Hip Abductor Muscles and Iliotibial Band during OLB

In Figure 29 we can see that the Iliotibial (IT) band starts as one bundle at the knee (IT tract) and splits to a Y-shape at about the same level as the gluteal muscles; one bundle goes directly to the iliac crest while the other connects to the tensor fasciae latae (TFL) which in turn originates from the ASIS. It is likely that both bundles of the Y are sharing the hip abduction moment load during OLB.

We can divide the IT band to two parts: the lower part which inserts onto the tibia and connects proximally to the gluteal muscles, and the upper part which shares the load with the TFL and other abductor muscles. Activation of the TFL, gluteal muscles and vastus lateralis can change the pretension in the IT band (both axial and transverse direction) [77], and thereby changing its stiffness.

Figure 30 (A) shows the equilibrium for the major elements that can create a moment around the stance hip. We can write:

$$M_{OLB} + M_{aDd.} = M_{ITM} + M_{aBd.}$$

Equation 4- Equilibrium of the moments around the stance hip

M_{ITM} can be calculated as the force in the IT band times its moment arm around the hip joint center and the force in the IT band is a function of hip abduction angle (Figure 30) and activation of the muscles inserting into the IT band. On the other hand, both the moments from the hip abductor and adductor muscles depend on the activation in the muscles which is voluntary. If we assume that during OLB the hip adductor muscles are not activated, then $M_{aDd.} = 0$. Then the moments from the IT band and the abductor muscles have to counteract the OLB demand moment. Figure 31 shows the OLB hip abduction moment demand for the double inverted

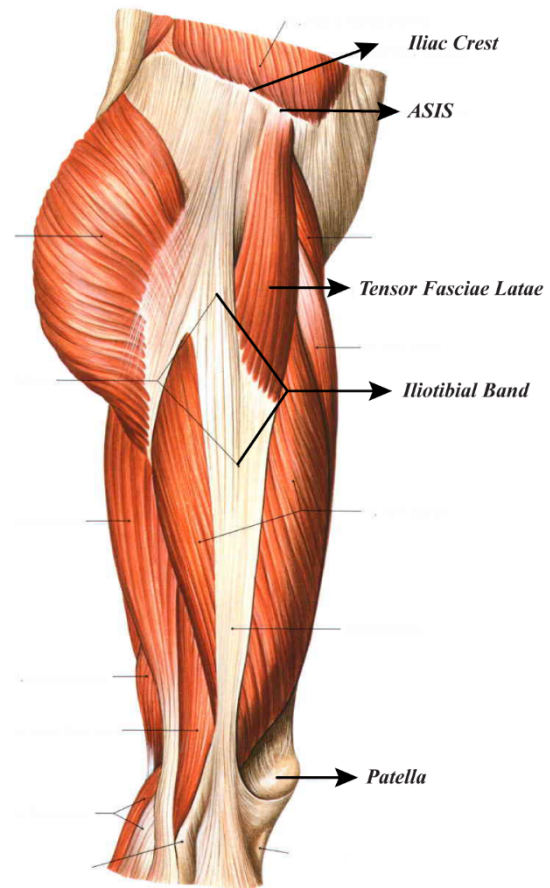


Figure 29- Muscles of the thigh and hip. Picture copied from Sobotta Atlas of Human Anatomy [76].

pendulum model of Chapter 2 and a hypothetical exponential curve representing the contribution of the IT band to resisting the OLB demand.

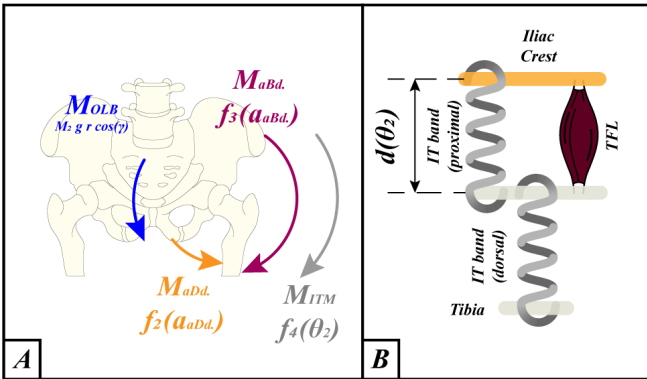


Figure 30- Demonstrations of load sharing between muscles of the hip and the IT band in bearing the OLB moment demand (A) Equilibrium of moments in the frontal plane due to OLB demand (M_{OLB}), muscles of the hip ($M_{aBd.}$ for abductor muscles and $M_{aDd.}$ for adductor muscles), and the IT mechanism (M_{ITM}) determines the pelvic inclination angle. M_{OLB} and M_{ITM} are mostly functions of γ and θ_2 respectively (please see Figure 7 for their demonstration). On the other hand the muscular abduction and adduction moments are mostly determined by activations of the muscles which are voluntary ($a_{aBd.}$ and $a_{aDd.}$ respectively). For simplicity, we assumed the effect of muscles' length changes on their force generating capacity is negligible in the range of lengths experienced during clinical OLB. (B) IT band can be modeled as a spring [78]; assuming no change in pretension from muscles inserting onto the IT band, the force in the IT band can change depending on its length (d) which in turn is determined as a function of hip abduction angle (θ_2).

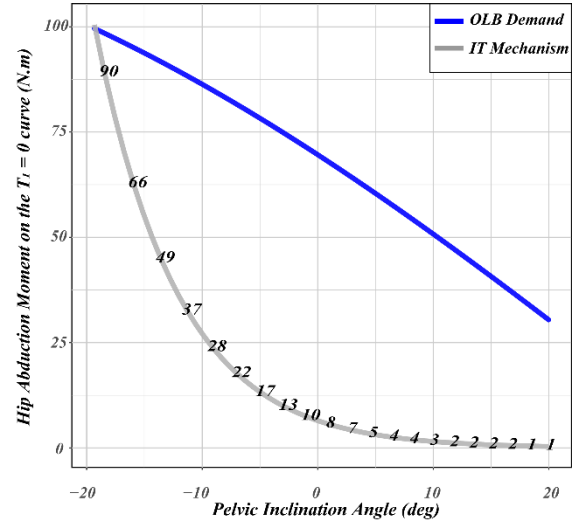


Figure 31- Hip abduction moment demand of OLB for the double inverted pendulum model of OLB from Chapter 2 (blue line) and a hypothetical exponential curve representing the contribution of IT band in resisting the OLB demand moment (grey line). The exponential curve is not based on experimental data and was fitted mathematically based on Inman's observation that the abductor muscles' activity was close to nothing at -20 degree pelvic inclination sag and equal to the OLB demand moment at about 20 degrees pelvic inclination raise (Figure 28 [24]). The numbers on the grey curve show the hypothetical percentage of the OLB demand provided by the IT band.

3.4.2.1 Towards Calculation of the Iliotibial Mechanism Contribution to Resisting the Hip Abduction Moment Demand during OLB

To get a realistic estimate of the contribution of the ITM to resisting the hip abduction moment demand during OLB we propose one of two different approaches.

Estimation of the Moment from ITM by Measuring EMG Activity of Hip Muscles (After Inman)

This is Inman's approach described in 3.4.1.3. Surface EMG markers should be applied to all the major abductor and adductor muscles. A calibration test should be performed to measure the maximum hip abduction and adduction moments on the stance leg while the subject

is standing on the opposite leg and EMG activity is being recorded. Motion capture markers should record pelvic inclination angle and lateral bending of the lumbar spine. Then each participant stands on one leg with a variety of different pelvic inclination angles, with enough rest between them, while EMG activity is being recorded. Hip abduction moment demand can be calculated from the motion capture data the same way we described here in this chapter. Using the calibration of the EMG activity with the maximum voluntary hip abduction and adduction strength, we can estimate the contribution of abductor and adductor muscles to the moments around the stance hip and use Equation 4 to calculate the moment from ITM as a function of pelvic inclination angle.

Amongst the limitations of this method, we can refer to the sources of error that we brought up in Appendix III for calculating the hip abduction moment demand. Additionally, some of the muscles of the hip, *e.g.* gluteus minimus, are not accessible for surface EMG recordings, which makes accounting for their contribution to hip abduction moment inaccurate.

Estimation of the Moments from the ITM during OLB from the Published in vitro Material Properties

If we could estimate the strain in the IT band at different hip abduction angles, we could then use the material properties of the IT band, *e.g.* stress-strain curve and cross-sectional area [77–81], to estimate its internal force. Then estimating the moment arm, also a function of abduction angle [82], we could estimate the moment from the IT band.

The most important limitation of this approach is that there is not one study that reports all the required parameters for this calculation. For example we could find stress-strain curves in a study but no information on the cross-sectional area or the strain at different hip abduction angles [78]. In fact there are no published data that estimate the strain in the IT band as a function of hip abduction angle during OLB. The closest we could find is a paper by Wang *et al.* where they

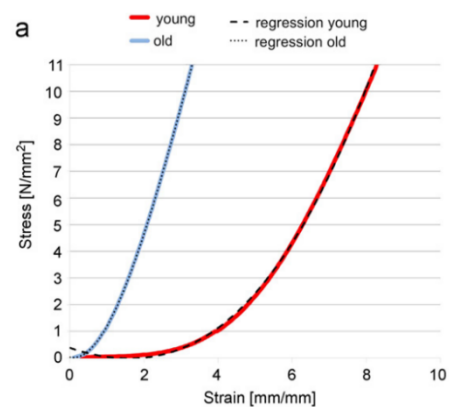


Figure 32- Comparison of the stress–strain curves of young and old specimens and the related regression curves (dotted lines). Copied from [78]

measured the changes in the width of the iliotibial tract during Ober's test⁵ using ultrasonography [74, 75]. This is further complicated by differences in stiffness of the IT band due to aging and conditioning [78]. For example, in a person with IT band contracture, the affected leg will stay close to zero hip adduction angle when, while the subject is lying on the side, and the tester stabilizes the pelvis. Finally, the activity of tensor fasciae latae, gluteus maximum and vastus lateralis muscles can tighten the IT band and also change its moment arm [77].

3.4.3 Effect of Load Sharing between Abductor Muscles and ITM on FBR

In Chapter 2 we defined FBR as the set of all states where maintaining OLB stance is possible. We then showed that for people with weak hip abduction strength, the bottom boundary was set by the maximum voluntary hip abduction strength 2.3.1. However, in our calculations of the FBR, we had not considered that the ITM and passive tissues surrounding the hip could have a notable contribution to resisting the hip abduction moment demand of OLB, especially around level pelvis inclination angles. Considering both abductor muscles and the ITM countering the OLB moment demand, for all our subjects, the lower boundary will no longer be set by the maximum strength and will extend down to the 20 degrees pelvis inclination sag. So the width of the FBR, which is set by the ankle inversion and eversion strengths, becomes the only factor that decides the area of the FBR for them.

In cases of severe loss of hip abduction strength, the FBR divides into two regions (Figure 33B), which show the two cases of the Trendelenburg signs during OLB [42]. In case of a positive Trendelenburg sign, the patient lets their pelvis noticeably sag which then allows them to balance relying on the passive tissue to avoid any further collapsing of their posture (bottom region in the FBR). For the negative Trendelenburg sign, patients use extreme lateral banding of their spine to reduce the OLB demand and then might even lift their pelvis to reduce the demand further (the top portion of the FBR).

⁵ Ober's test is commonly used by physiatrists to identify tightness of the IT band. For a demonstrative video, please click [here](#).

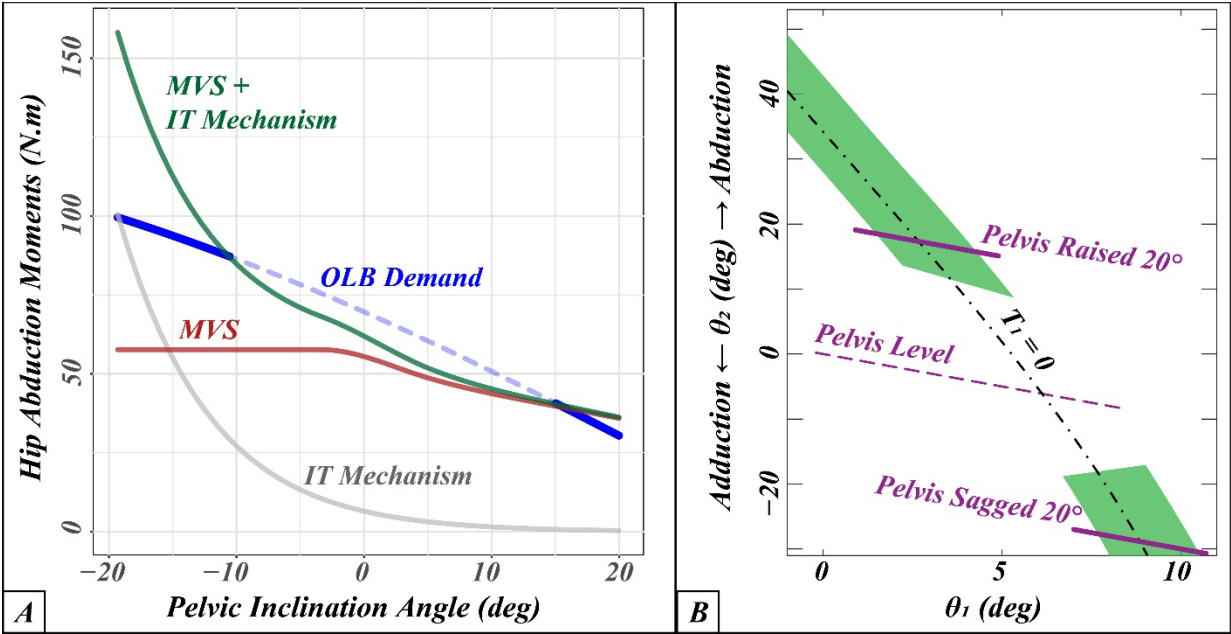


Figure 33- Predicted effect of 60% loss of maximum voluntary hip abduction strength (MVS) on the FBR of the 50th percentile man used in Chapter 2. (A) Variation of different hip abduction moments during OLB as a function of pelvic inclination angles. All moments were calculated assuming zero ankle torque ($T_1 = 0$ curve in B). The hypothetical contribution of iliotibial mechanism (ITM) to hip abduction moment is the same as Figure 31. We can see that between -10 to 15 degrees of pelvic inclination angle, the sum of ITM and muscle strength moment are not enough to resist the OLB demand. (B) The FBR shows two distinctive regions where OLB is possible (green areas). The top portion is for the higher pelvic inclinations angles where the OLB demand is smaller (right side of the thick blue line in (A)), while the bottom portion is for the angles where the passive tissues resist most of the hip abduction moment demand.

To sum up, the contribution of IT mechanism to providing resistance to some of the hip abduction moment demand of OLB makes maximum hip abduction strength inconsequential in determining the boundaries of FBR in most cases except for extreme weakness of the abductor muscles. So maximum hip abduction strength does not play a role in the possible quasistatic OLB states, during which only torques at the ankle are used to control balance (‘ankle strategy’). But what about dynamic states where ‘hip strategy’ is being used? In the next section we will address this question.

3.4.4 How Does Load Sharing between the Hip Abductor Muscles and Iliotibial Mechanism Affect OLB?

In 2.4.2 we showed how exerting maximum hip abduction / adduction moments (using the ‘hip strategy’) could create a substantial change in the angular momentum of the body and therefore create corrective shear forces under the stance foot to help recover OLB. So the hip strategy substantially extended the width of the FBR in calculating the recoverable quasistatic states. In 2.4.3.1 we also showed that accounting for the limited rate of torque development in the hip and ankle moments would shrink the said area. Here we will examine how load sharing between abductor muscles and the ITM would affect the rate of torque development.

Let us assume we want to use the hip strategy to create the highest medial acceleration of the COM to avoid a lateral fall during OLB. In 2.3.6 we showed that we then have to use the maximum hip abduction strength to raise the pelvic inclination angle rapidly. If most of the hip abduction moment was being provided by the passive tissue at the initial point which would result in a longer time for the abductor muscles to reach their maximum strength. In other words, sharing the OLB demand load between the hip abductor muscles and ITM would decrease the rate of hip abduction moment development and therefore shrink the area of recoverable OLB states. This is especially important when responding to an external perturbation and trying to avoid a lateral fall on the hip. If the person’s hip abductor muscles are weak, they would then have to rely more on the ITM during their daily tasks. In case of a perturbation then, they have a longer time to reach their maximum strength as well as a lower maximum strength. Both of these would make the use of hip strategy to recover balance in the frontal plane less effective and could thereby increase the chance of injury.

3.5 Conclusions

- Our experimental results corroborate the OLB hip abduction moment demand that was calculated in Chapter 2.
- On average, the hip abduction moment demand of OLB is more than half the maximum hip abduction strength for all adults.
- Our analyses show that the hip abduction moment demand is not resisted completely by the abductor muscles alone. Therefore one can deduce that there has to be an abduction moment contribution from the iliotibial mechanism (ITM) and other passive tissues surrounding the hip, even in pelvic inclination angles close to level.
- The contribution of ITM to resisting hip abduction moment demand of OLB leads to the rejection of our two initial hypotheses
 - Load sharing between ITM and abductor muscles, makes calculating the intensity of hip abductor muscles hard which makes it difficult to predict a maximum unipedal stance time. That is because the subject can potentially let most of the demand be carried by the ITM and rest their abductor muscles.
 - All the quasistatic OLB states may not fall inside the boundaries of the FBR. That is because our original derivation of FBR did not consider the contribution of ITM to resisting the hip abduction moment demand of OLB.
- Having to rely on the ITM for maintaining OLB, makes the hip strategy less effective in avoiding lateral falls by decreasing the rate of torque development available from the abductor muscles in response to a potential perturbation.

CHAPTER 4

Effect of Age, Gender, and Lower Extremity Strengths on Maximum Voluntary Frontal Plane Acceleration of the Stance Foot during Volitional Unipedal Shuffle Stepping

4.1 Introduction

In the previous two chapters, we modeled OLB as a 3-link double inverted pendulum: the top link represented the body supported by the hip joint, the middle link represented the lower limb between the hip and ankle joint, and the lowest link represented the foot. We assumed the foot was stationary. Similarly, all other studies of OLB assume the stance foot is either completely stationary or could only rock back and forth between the medial and lateral edges of the stance foot [28, 29, 32, 83]. This assumption stems from our definition for standing balance:

Standing Balance:** A person's current stance state is 'balanced' if they can reach a quasistatic state in any direction **without taking a step.

Since an individual can take a step (or steps) to avoid falling, a loss of standing balance does not necessarily lead to a fall. In the case of OLB, if (s)he does not want to fail the test, the individual cannot put the contralateral foot down to take a step, but (s)he can move the stance foot in the direction of the impending fall by moving either the stance foot heel or the stance foot toes in that direction to maintain their OLB, and even alternate between the two strategies, if they want to move the foot further in that direction. This “shuffle” step of the stance foot is achieved by either (a) engaging the plantarflexor muscles to shift the COP anteriorly towards the toes, followed by an internal or external rotation of the stance leg to move the heel laterally or medially, or (b) vice versa, in which the dorsiflexors shift the COP posteriorly followed by an external or internal rotation of the stance leg to move the toe laterally or medially. These movements can be concatenated by alternating them to move further medially or laterally. Whether a single or multiple movements are made in quick succession, we have called this the stance limb “Heel-Toe-Shuffle” (HTS) strategy.

‘Heel-Toe-Shuffle’ (HTS) Strategy for OLB: Using one or more shuffle steps of the stance foot during OLB to control the movements of the whole body center of mass.

The HTS strategy is similar to balancing an inverted pendulum on the tip of your finger [84] during which the finger is moved faster than the COM of the stick to create corrective angular acceleration of the stick to counteract the gravity pull, and keep it from falling. Based on our initial observations with subjects performing OLB, the HTS strategy has the potential to help recover OLB balance or at least postpone an impending fall in the same way. The effectiveness of the HTS strategy in recovering OLB depends on how fast a person can shuffle his/her foot in the direction of the impending fall in order to create medio-lateral accelerations of the ankle. To our knowledge there are no published articles in the literature that describe the HTS, the characteristics of the stance foot shuffle step(s), or its capacity to create the requisite corrective accelerations of the COM.

We therefore designed an experiment to measure the maximum volitional HTS speeds that healthy young and older subjects can achieve starting from a quasistatic one-legged stance. Our goal was to measure and quantify the maximum HTS capacity that could be used as an OLB strategy and determine which physiological or biomechanical factors affect it. We also wanted to compare the effectiveness of the HTS capacity with that of using maximum ankle inversion/eversion moments, better known as an ‘Ankle Strategy’ [28] for the recovery of OLB (please see 1.2.5.2 for more details). Our hypotheses were as follows:

H₁: Unipedal stance time (UST) and lower extremity strengths predict the effectiveness of HTS in creating corrective movements of the COM in both young and older adults.

H₂: HTS capacity is at least as effective as maximum ankle inversion/eversion torques in creating corrective movements of the COM during a single HTS step in both young and older adults.

In the Methods section we first describe our HTS experiment. In short each subject was asked to stand on one leg. After gaining quasistatic OLB, they were asked to shuffle their stance foot a prescribed distance (~ 45 cm) either medially or laterally as fast as they can. To analyze

the experimental data, we derived the equation of motion for a single inverted pendulum with a moving base in the frontal plane to model the OLB while shuffling the stance foot. Deploying the equation of motion, we quantify the *contribution of maximum ankle inversion/eversion torques ('DTA')* and *medio-lateral movements of the stance ankle ('DTH')* to the change in angular velocity of the COM during a single HTS step. We then showed how we can extract DTH and DTA, as the primary and secondary outcome measures of the experiment, for each HTS step in the recorded trials from our subjects. We posit that DTH can be used as a measure of HTS capacity.

In the Results section we review our findings. We will first show that all twenty of our young subjects and 13 out of 18 older subjects were successful in travelling more than half of the prescribed distance using the HTS strategy without losing their balance. Of all the independent covariates that we examined, UST was the only variable that came close to predicting if an older group participant was going to be successful in the HTS experiment (H_1). Deploying a linear regression analysis we then showed that hip internal-external rotation strength is the only lower extremity strength that has a significant, although weak, positive correlation with maximum measured DTH in the lateral HTS (H_1). Finally we used a linear mixed-effect analysis to compare DTH and DTA values during lateral HTS experiments. We showed that for both young and older subjects, mean DTH are significantly higher than DTA values (H_2). However the between-subject and within-subject variations of DTH are also much higher than DTA which suggest HTS is a riskier strategy for OLB compared to the ankle torque strategy. In the Discussion we consider the use of HTS strategy by our subjects during the OLB experiments (Chapter 3), especially during the eyes closed trials, in light of the HTS capacities measured in this chapter.

4.2 Methods

4.2.1 Heel-Toe Shuffle Experiment

The heel-toe shuffle (HTS) experiment in the medial and lateral directions was performed as part of the series of one-legged balance experiments described in Chapter 3. For details on the participants and the inclusion / exclusion criteria, lower extremity strength measurements, and the setup for the motion capture cameras and force plates, please refer to the Methods in Chapter 3. Below, we will describe the details of the medial and lateral HTS experiment.

Medial HTS: Each subject stood on the Optima force plate (blue surface in Figure 34) with arms crossed and their left foot at the far left side of the force plate (from subject's view point). They wore New Balance 411 shoes supplied by the laboratory, unless contraindicated. The test started with the subject lifting their right leg. After a successful transition to one leg and gaining quasistatic balance, the subject was asked to get to the far right edge of the force plate (approximately an 18" = 45 cm distance) using HTS strategy as fast as possible. Each subject was tested 3 times with enough time to practice and get comfortable with the test. In the first recording, the subject was instructed to just use the HTS strategy to get to the other side of the force plate at their own comfortable pace. On the second and third try, we asked them to do it as fast as they could. During the medial HTS experiment, the tester was standing on the right side of the subject ready to catch him/her at the arm level, in case they could not maintain their balance. A subject's HTS trial was considered successful if they could travel more than half the length of the force plate (25 cm) without losing their balance. If they lost their balance after the 25 cm distance, the trial



Figure 34- Heel-Toe Shuffle experiment setup during a lateral HTS trial. Subject starts on both feet with their left foot on the right edge of the force plate (from subject's view point). He first gains his balance on the left leg and then travels the width of the force plate to the other edge (~45 cm). The tester stands on the left side of the subject, prepared to catch him in case he loses his balance.

was still considered successful especially since we wanted to capture their fastest HTS without concern about their ability to stop their HTS.

Lateral HTS: This was the same as the Medial HTS, with the difference that this time the subject started with their left leg at the far right side of the force plate, and they were asked to get to the far left side of the force plate as fast as possible. The tester stood on the left side this time to catch the subject in case of a loss of balance during the experiment.

People with weak HTS were identified as those who failed in two or more of their total six medial and lateral HTS trials. A failed HTS trial was recorded if the subject lost their balance before traveling at least 25 cm, a little more than half of the appointed path.

4.2.2 Modeling HTS during OLB with a Single Inverted Pendulum with a Moving Base of Support

To quantify the effectiveness of the HTS strategy on controlling the OLB, we will first model the frontal plane movements of a person standing on one leg as a single inverted pendulum with a moving base. The lower joint in the model represents the ankle of the stance leg and the mass at the top is the mass of the whole body concentrated at the COM. Two variables and their derivatives are required to describe the *states* of this inverted pendulum, the angle of the pendulum (θ) and the position of the base of support (x_s). Equation 5 was derived in Appendix IV and shows the equation of motion for the model. We can see that both moments at the ankle (T_1), and accelerations of the base of support (\ddot{x}_s) can create accelerations of the COM and therefore can be used to control it.

$$\ddot{\theta} \approx \frac{MgL}{I + ML^2} \theta + \frac{T_1}{I + ML^2} - \frac{ML}{I + ML^2} \ddot{x}_s$$

Equation 5- Equation of motion for a single inverted pendulum with a moving base of support. In this equation, θ is the angle that the pendulum makes with the vertical line, M is the mass of the whole body, L is the length of the pendulum, I is the mass moment of inertia around the COM, T_1 is the inversion / eversion torque at the ankle, and \ddot{x}_s is the lateral acceleration of the stance ankle.

4.2.3 Effectiveness of a Single HTS Step in Changing the Angular Velocity of Body (Identifying the Outcome Measures from Theory)

Equation 5 shows that acceleration of the base of support can induce a momentary angular acceleration of the body. However, such an acceleration cannot be maintained at a constant value (like ankle torque for example) because HTS strategy is by nature made up of steps. However, if we integrate Equation 5 for the duration of a single shuffle step, then we have

a better estimate of the effectiveness of HTS in changing the angular momentum of the body and therefore controlling OLB.

Duration of a Heel-Toe Shuffle Step: *The time between movement of the center of pressure (COP) under the stance foot from heel to toe (HT) or toe to heel (TH) during HTS strategy.*

If t_i and t_{i+1} are the time points when the COP is closest to the heel and toes during a single step, then

$$\begin{aligned}\Delta\dot{\theta} &= \frac{MgL}{I + ML^2} \left(\int_{t_i}^{t_{i+1}} \theta dt \right) + \frac{1}{I + ML^2} \left(\int_{t_i}^{t_{i+1}} T_1 dt \right) - \frac{ML}{I + ML^2} \Delta\dot{x}_s \\ &= \Delta\dot{\theta}_{Gravity} + \Delta\dot{\theta}_{AT} + \Delta\dot{\theta}_{HTS}\end{aligned}$$

Equation 6- Change in angular velocity of the center of mass during a single HTS due to gravity (in blue), inversion / eversion torque at the ankle (in purple), and movements of the base of support (in red). The time at beginning and end of the step are t_i and t_{i+1} respectively. $\Delta\dot{x}_s$ is the velocity of the base of support at the end of the step minus the velocity in the beginning.

The term ($\Delta\dot{\theta}_{HTS} = -\frac{ML}{I+ML^2} \Delta\dot{x}_s$) in Equation 6 is the contribution of a single HTS step to changes in the angular velocity of the whole body. We will also refer to $\Delta\dot{\theta}_{HTS}$ as *DTH* (short for Delta Thetadot due to HTS). This term is the **primary outcome measure of the HTS experiment**. On the other hand $\Delta\dot{\theta}_{AT}$ ($= \frac{1}{I+ML^2} \left(\int_{t_i}^{t_{i+1}} T_1 dt \right)$) is the contribution of inversion / eversion moment in the ankle in the same duration as a single step. We will also refer to $\Delta\dot{\theta}_{AT}$ as *DTA* (Delta Thetadot due to Ankle Moment). If we assume the subject was using their maximum available ankle inversion / eversion moment during the step, then this term simplifies to $\frac{T_1(t_{i+1}-t_i)}{I+ML^2}$. This is the **secondary outcome measure of the HTS experiment**. Finally, the term $\frac{MgL}{I+ML^2} \left(\int_{t_i}^{t_{i+1}} \theta dt \right)$ is the contribution of gravity to changes in the angular velocity of the body. If the subject is successful in maintaining their upright stance, θ remains close to zero which makes its contribution to changes in angular velocity of the body minimal. Since in this study we are mostly concerned with the first two HTS steps, this assumption is not unrealistic.

Note: *In all the presented results, we will only consider the first two HTS steps. This choice was made because of two reasons:*

1) *To make sure the contribution of gravity terms to change in angular velocity of the body is minimal. Since all subjects started their HTS from a quasistatic OLB this assumption is realistic.*

2) At the end of HTS path, the tester was standing guard to stop the subject from falling (Figure 34). So subjects could potentially have changed their HTS strategy in the later steps to account for reaching the end of the HTS path and/or falling onto the tester. Using only the first two HTS steps ensures this was not the case.

4.2.4 Extracting the Outcome Measures from each HTS Trial

To find $\Delta\dot{\theta}_{HTS}$ and $\Delta\dot{\theta}_{AT}$ (please see the previous section for details) we have first to identify the time points marking the beginning and end of each HTS step (t_i). We do so by examining the center of pressure (COP) trajectory during each trial (red line in Figure 35). The extrema of the COP trajectory in the lab xy-plane show when the subject has moved all his/her weight to the toes and the heel (green and purple dots on the red line in Figure 35). These are the beginnings and ends of all the heel-to-toe (HT) and toe-to-heel (TH) steps. The corresponding times for the COP extrema were then extracted for each subject. The maximum contribution of ankle torque strategy ($\Delta\dot{\theta}_{AT}$) was then calculated for each HTS step (please see the previous section for more details). The estimated maximum $\Delta\dot{\theta}_{AT}$ for four subjects during all their HTS steps in their second and third HTS trials can be seen in Figure 36.

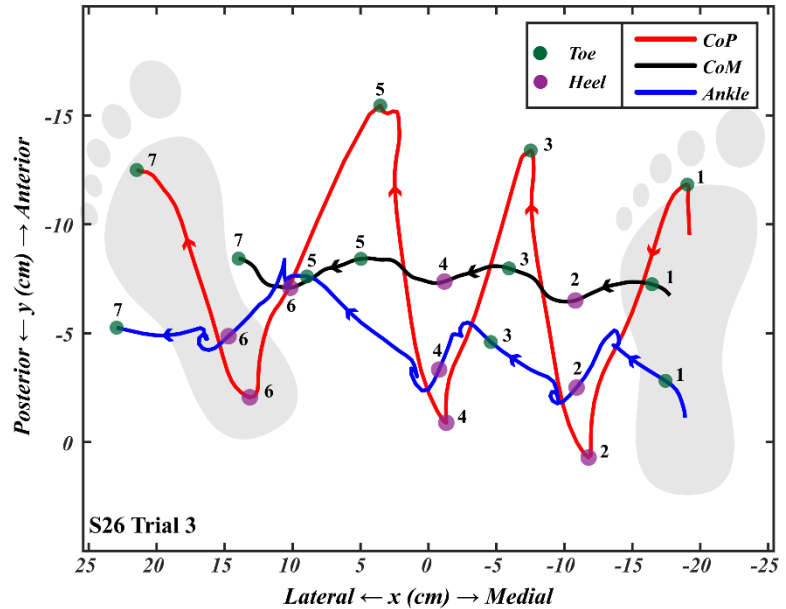


Figure 35- An example of a lateral heel-toe shuffle trial in shoes. The trajectory of the center of pressure (COP) of the stance foot (the red line) has the characteristic zig-zag shape travelling to the left. The local extrema of the COP trajectory were identified to find the times when the COP was closest to the toes (green dots) and the heel (purple dots). Same time points are identified on the ankle position and center of mass projections onto the floor. The range of x values seen here is the same as the width of the force plate.

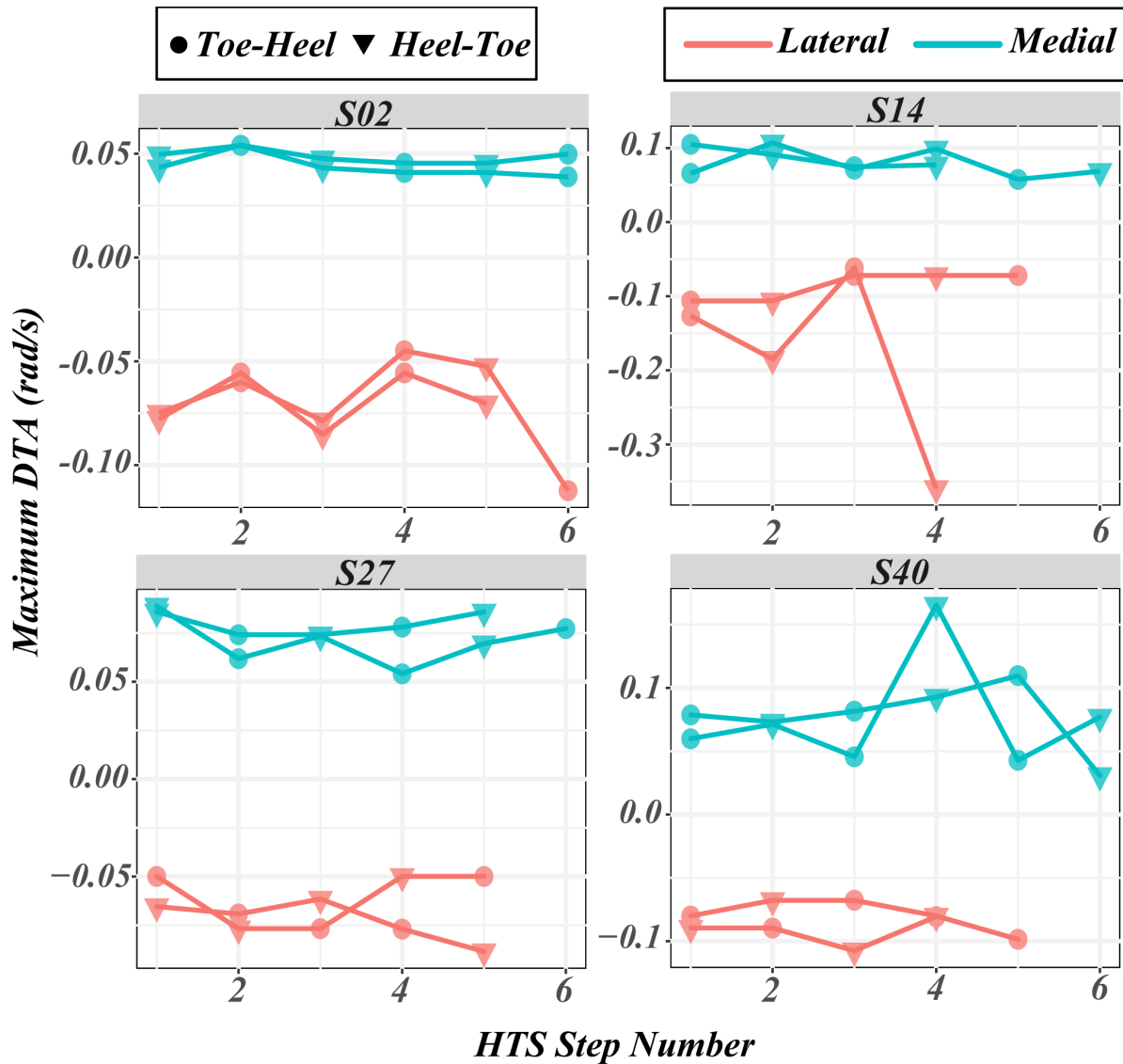


Figure 36- Maximum estimated DTA (or $\Delta\dot{\theta}_{AT}$, secondary outcome measure of the experiment) for four subjects during their second and third HTS trials in the medial and lateral directions. DTA is the change in COM angular velocity due to torque at the ankle during a single HTS step. During a lateral (medial) HTS, a negative (positive) DTA is needed to arrest a lateral (medial) angular momentum of the body. Since we used maximum measured ankle inversion and eversion strengths as T_1 in the formula for $\Delta\dot{\theta}_{AT}(= \frac{T_1(t_{i+1}-t_i)}{I+ML^2})$ the variations within each subject represents the variations in step times ($t_{i+1} - t_i$). For more details on the calculation of DTA from recorded trials, please refer to 4.2.3. The circle symbols are for the HTS steps where the COP was moving from toe to heel; the triangles are for the heel to toe. S02 and S27 are in the young group (man and woman respectively); S40 and S14 are in the older group (man and woman respectively).

Calculating $\Delta\dot{\theta}_{HTS}(= -\frac{ML}{I+ML^2}\Delta\dot{x}_S)$ presents another challenge. If we use the measured medio-lateral velocity of the ankle (\dot{x}_S) at the identified times (t_i) for the beginning and end of

HTS steps to calculate $\Delta\dot{\theta}_{HTS}$ the results would be highly sensitive to the choice of t_i . This is because unlike COP trajectories, the ankle position trajectory will not necessarily be at an extremum. Also, to calculate \dot{x}_S we need to numerically differentiate x_S which is also sensitive to the choice of method for differentiation. Next we introduce our method which was less sensitive to the choice of t_i and also uses all the recorded ankle positions to calculate the average change in ankle velocity during a HTS step.

4.2.4.1 Fitting a semi-periodic function to the ankle position trajectories in the medio-lateral direction

HTS strategy involves a heel-to-toe step followed by a toe-to-heel step, or vice versa, followed by another series of steps until the last step. If one assumes that each consecutive pair of steps are repeated, there is a periodicity in the acceleration of the ankle with a full period lasting a heel-toe-heel or alternatively toe-heel-toe combination. But there is no reason why a single HTS step should have the same period as the previous one or the next. Indeed a subject might choose to take their heel-to-toe step faster than their previous toe-to-heel step or vice versa. So we considered each HTS step as half of the period of a periodic function.

Therefore:

$$\omega = 2\pi f = \frac{2\pi}{2(t_{i+1} - t_i)} = \frac{\pi}{(t_{i+1} - t_i)}$$

Equation 7- Calculating the angular frequency of the fitted semi-periodic function for each HTS step.

With the value of ω set for each HTS step, we can fit a function of the form seen below to the ankle position trajectory in the medio-lateral direction (x_S) for each HTS step.

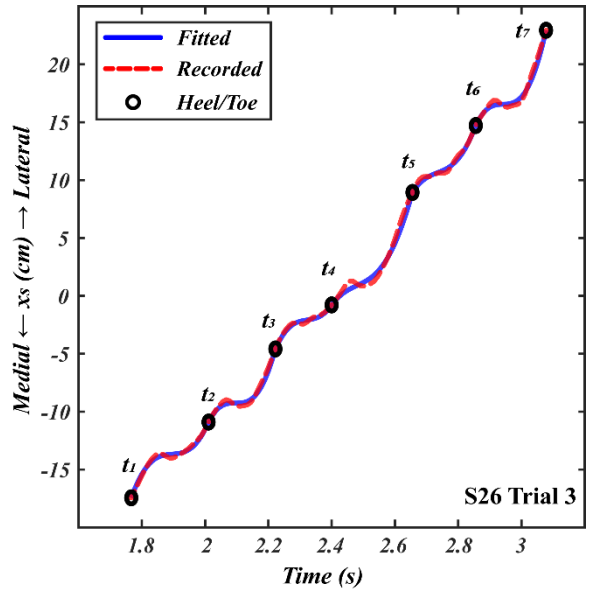


Figure 37- Using a semi-periodic function between each consecutive pair of heel/toe time points to fit the trajectory of ankle positions in the medio-lateral position (x_S) for each HTS step. The period of the semi-periodic function for each step was set at $2(t_{i+1} - t_i)$. For more details on the shape of the fitted function and the boundary conditions please refer to the text in 4.2.4.1.

$$x_{fitted} = A \sin(\omega(t - t_i) + \varphi) + C(t - t_i) + D, \text{ for } t \in [t_i, t_{i+1}]$$

Equation 8- General function shape fitted to the ankle position trajectory in the medio-lateral direction (x_S) for each HTS step. A , C , D , and φ are the constants that uniquely define the fitted function for each HTS step.

The only boundary condition was that $x_{fitted}(t_i) = x_S(t_i)$. This ensured continuity of the fitted functions positions while leaving two of the constants to be fitted to all recorded x_S values using a least squares algorithm. The root mean square error between x_{fitted} and x_S for the duration of the HTS trial for all subjects was under 0.1 mm.

Having x_{fitted} as a function for each HTS step, we can then easily differentiate it and calculate $\Delta\dot{x}_S$.

$$\begin{aligned} \Delta\dot{x}_S &= \dot{x}_S(t_{i+1}) - \dot{x}_S(t_i) = A\omega \cos(\omega(t_{i+1} - t_i) + \varphi) - A\omega \cos(\omega(t_i - t_i) + \varphi) \\ &= -2A\omega \cos(\varphi) \end{aligned}$$

Equation 9- Calculating $\Delta\dot{x}_S$ from the parameters of x_{fitted} for each HTS step.

Using the calculated $\Delta\dot{x}_S$ for each HTS step, mean values for the length of the inverted pendulum (L) from the kinematic recordings (please see Methods in Chapter 3), Mass of each subject, and the mass moment of inertia from the anthropometric measurements, we can then calculate $\Delta\dot{\theta}_{HTS}$ ($= -\frac{ML}{I+ML^2} \Delta\dot{x}_S$) for each HTS step. This method is more robust than using the measured velocities of the ankle in the medio-lateral direction because it incorporates all the measured x_S values into the calculations.

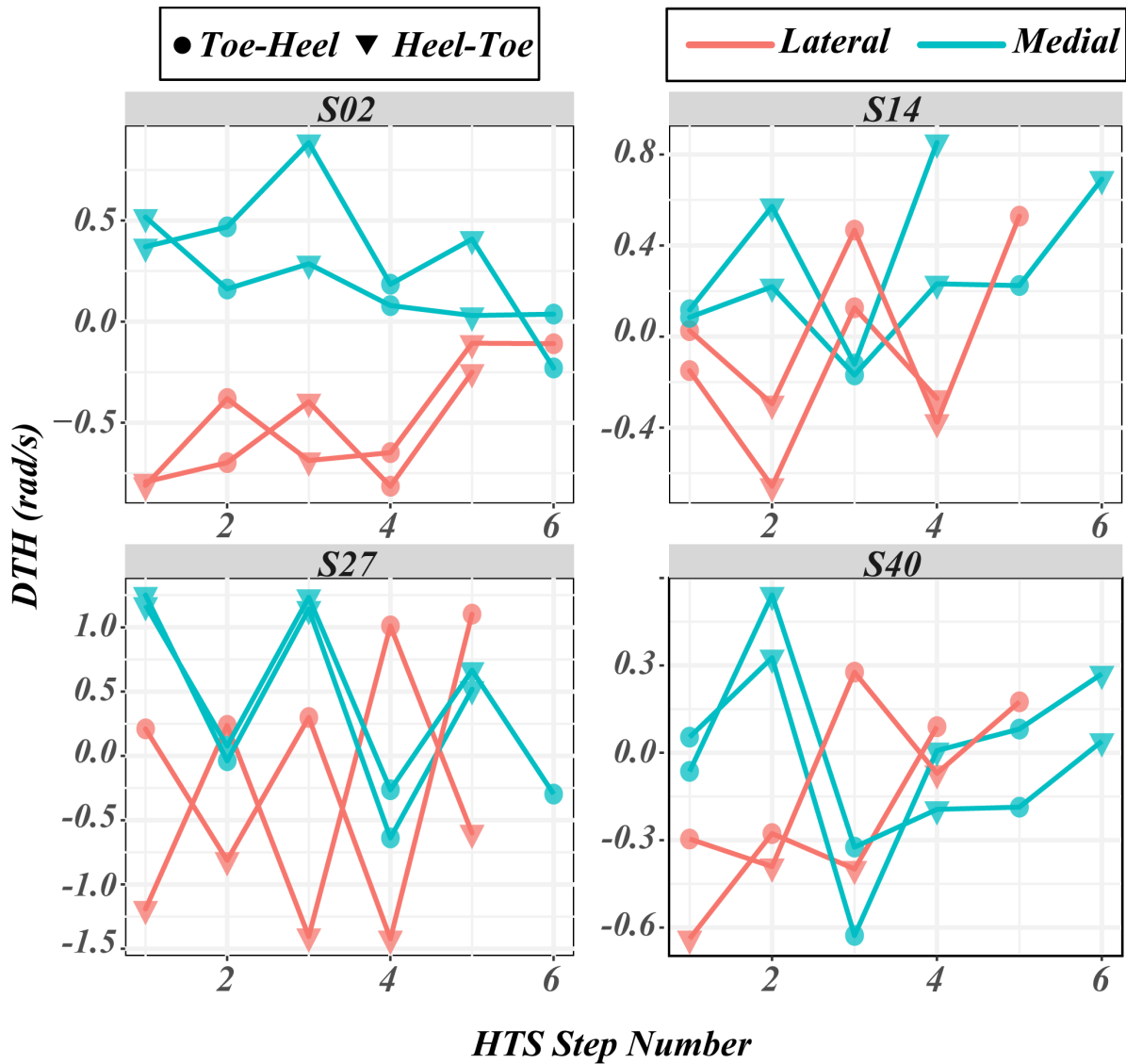


Figure 38- Estimated DTH (or $\Delta\dot{\theta}_{HTS}$, primary outcome measure of the experiment) for four subjects during their second and third HTS trials in the medial and lateral directions. DTH is change in COM angular velocity due to averaged change in velocity measured during a single HTS. During a lateral (medial) HTS, a negative (positive) DTA is needed to arrest a lateral (medial) angular momentum of the body. For more details on the calculation of DTH from recorded trials, please refer to text body in this section. The circle symbols are for the HTS steps where the COP was moving from toe to heel; the triangles are for the heel to toe. S02 and S27 are in the young group (man and woman respectively); S40 and S14 are in the older group (man and woman respectively).

4.2.5 Statistical Analyses

All statistical analyses were performed with R (a language and environment for statistical computing) version 3.6.0. In 4.3.2 Linear mixed-effect models (LMM) with a random intercept for each subject were fit to the data using the ‘nlme’ version 3.1-139 package. We allowed for different residual variations for young and old subjects. Likelihood Ratio and t-tests were used

to examine the roles of age group, sex, HTS direction, step type (heel-toe vs. toe-heel) and their interactions on an individual's DTH and DTA for their first two steps of the second and third HTS trials in each direction. For details of the LMM fit in 4.3.4 please refer to Appendix VI.

4.3 Results

4.3.1 Heel-Toe Shuffle Success Rate

All 20 subjects in the young group and the majority, 13 out of 18 subjects, in the older group, succeeded in locomoting more than half of the appointed distance using the heel-toe shuffle (HTS) strategy in at least five of their six recorded HTS attempts. To find common characteristics between subjects with unsuccessful HTS attempts, we defined a new variable (*'Bad HTS'*) to each subject with a '1' value assigned to the five subjects with two or more unsuccessful HTS attempt and '0' for all other subjects. We only used the data for old subjects because none of the young subjects had difficulty with the HTS trial, so including them in the analysis would only introduce bias in the results. We then fit a linear regression model to 'Bad HTS' as the outcome measure and normalized lower extremity strengths (by weight), age (numerical variable), weight, height, and unipedal stance time (UST measured in the experiment discussed in Chapter 3) as predictors. The single best variable for predicting 'Bad HTS' was UST ($R^2 = 20\%$, $p = 0.06$). Adding another predictor from the aforementioned list did not improve the predictions of regression model (using the AIC method). Also, none of the measured normalized strengths were successful at predicting 'Bad HTS' in a linear regression model.

Note: All the results in the following sections, except for 4.3.5, pertain to successful HTS trials.

4.3.2 Primary Outcome Capacity Measure: Estimated DTH during Medial and Lateral HTS Locomotion Trials

Figure 39 shows the boxplot of estimated DTH for the first two steps in the medial and lateral HTS locomotion trials. For the justification of only using the first two steps please refer to 4.2.3. To find the possible effect of age category, sex, direction, and step type on DTH, we used the above variables and their interactions as the predictors for a linear mixed-effect model (LMM) with DTH as the outcome variable and a random intercept for each subject. Using the Likelihood Ratio test we simplified the fixed effects and the most parsimonious LMM that we could find had age category, direction, and step type as main effects. The coefficients for the resulting fixed effects can be seen in Table 13. When considered with Figure 39, they suggest that DTH was significantly higher for young subjects, in the lateral direction, and during heel-to-toe steps. Also, the variation of DTH in the young group was significantly higher than the old ($p < 0.001$). The diagnostic plots for the LMM in Table 13 can be seen in Appendix V.

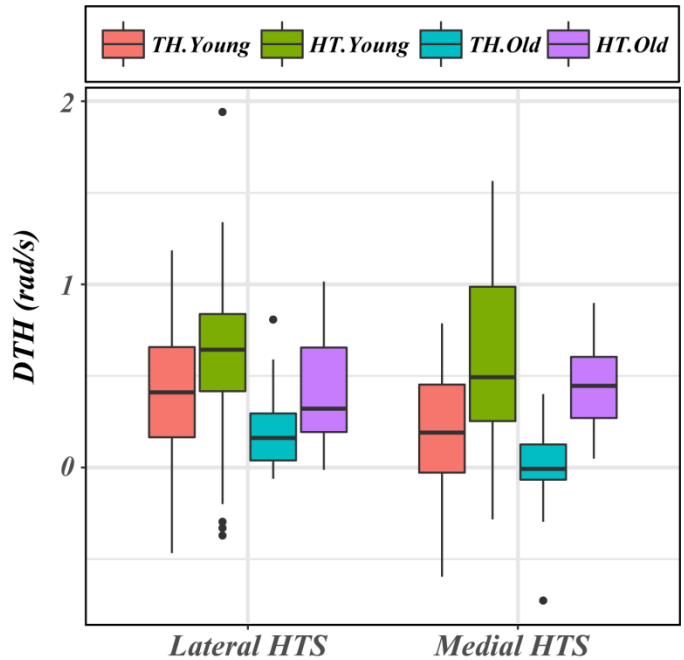


Figure 39- Estimated DTH during the first two steps in the medial and lateral HTS experiments categorized by Age Group and Step Type (HT for heel-to-toe and TH for toe-to-heel). Lateral DTH values were multiplied by a negative so their value can be compared with the medial. No significant interaction between Step Type, Age Category, Sex, or Direction was observed. For the results of the linear mixed-effect model fitted to DTH values please refer to Table 13. The black line in the middle of each box is the group median. In this and any following boxplots, the lower and upper hinges correspond to the first and third quartiles (the 25th and 75th percentiles). The whisker extends from the hinge to the largest and smallest value no further than 1.5 times the interquartile range. The data beyond the end of the whiskers are plotted individually.

Table 13- Linear mixed-effect model for DTH

Fixed effect	Parameter estimate (rad/s)	SE	p
<i>Heel-to-Toe</i>	0.35	0.049	<0.001
<i>Toe-to-Heel</i>	0.67	0.049	<0.001
<i>Medial Direction</i>	-0.11	0.036	0.002
<i>Old Category</i>	-0.19	0.055	0.001

4.3.3 Secondary Outcome Capacity Measure: Estimated maximum DTA during Medial and Lateral HTS Experiments

Figure 40 shows DTA for the first two steps of the medial and lateral HTS trials for all subjects categorized by Age Group and Step Type. In a way DTA shows how much change in angular velocity of the COM we could expect if instead of a HTS step, the subject would just use their maximum ankle inversion / eversion torques. Since DTA in this format is only valuable as a reference point for comparison with DTH, we did not run a mixed-effect modeling analysis to find the effects of Age, Sex, Step Type, and Direction.

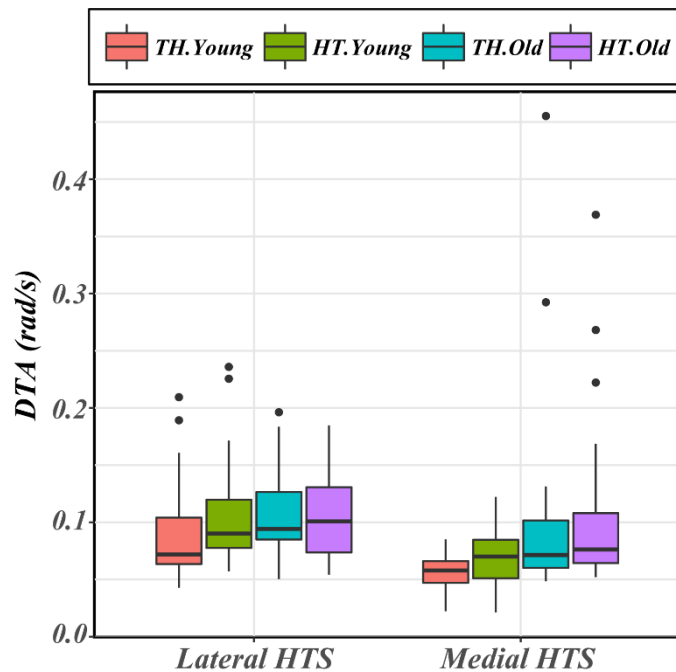


Figure 40- Estimated DTA for the first two steps in the medial and lateral HTS experiments categorized by Age Group and Step Type (HT for heel-to-toe and TH for toe-to-heel). Lateral DTA values were multiplied by a negative so their value can be compared with the medial.

4.3.4 Comparison of HTS and Ankle Torque Strategies in Avoiding a Lateral Fall (DTH vs. DTA)

Figure 41 shows the DTH and DTA values for the first two steps during the lateral HTS experiments. We divided the measurements for each outcome measure by Age Group and Step Type.

Based on the fitted LMM (please see Appendix VI), we can see that HTS strategy was clearly capable of creating higher changes in the angular velocity of the body in both young and older subjects, except for the Toe-to-Heel step type in the elderly where the difference was not significant. Considering the fitted random effect positive definite variance-covariance matrix, the within-subject variations was higher in the DTH values compared to the DTA (SD = 0.109 vs 0.029, $p = 0.005$). Also the residual variations in the DTH group (which could be used as the between-subject variations) was significantly higher in the DTH group compared to the DTA (SD = 0.36 vs. 0.025, $p < 0.001$). For the fixed effects and the difference in the estimated group means, please see Table 14.

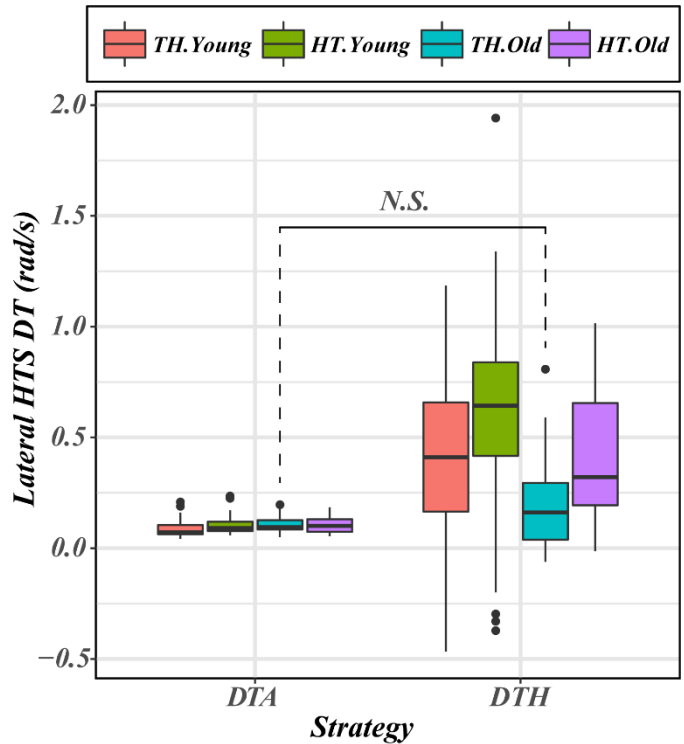


Figure 41- Comparison of DTA and DTH during the first two steps in lateral HTS experiments categorized by Age Group and Step Type (HT for heel-to-toe and TH for toe-to-heel). A negative DTH shows that the subjects decelerated during the medial HTS step instead of accelerating. DTH mean is significantly higher than DTA mean across all groups except in the TH Old. For details of the comparisons using contrasts in the fitted LMM, please refer to Appendix VI. Both within-subject and between-subjects variations were significantly higher in the DTH measurements compared to the DTA ($p = 0.005$ and $p < 0.001$ respectively).

Table 14- Linear mixed-effect model for the comparison of the DTH and DTA. Last four rows show the difference between DTH and DTA for each of the considered group (Age Category by Step Type interaction).

Fixed effect	Parameter estimate (rad/s)	SE	p
<i>DTA.Young.TH</i>	0.087	0.008	<0.001
<i>DTA.Young.HT</i>	0.104	0.008	<0.001
<i>DTA.Old.TH</i>	0.105	0.009	<0.001
<i>DTA.Old.HT</i>	0.104	0.009	<0.001
<i>DTA.Young.TH : DTH</i>	0.317	0.065	<0.001
<i>DTA.Young.HT : DTH</i>	0.531	0.065	<0.001
<i>DTA.Old.TH : DTH</i>	0.109	0.080	0.18
<i>DTA.Old.HT : DTH</i>	0.318	0.080	<0.001

4.3.5 Lower Extremity Capacities Affecting Maximum DTH Capacity during Lateral HTS

To examine the relationship between maximum subject capacities and the ability to create larger DTH values, we selected the maximum DTH value within the first two steps of all lateral HTS trials for each subject. Then we used exploratory plots and linear regression to look for the maximum capacity that predicted maximum DTH.

Amongst all the lower extremity capacities that were measured, normalized by subject's weight (please see 3.2.2.1 for a list and method of measurement), only hip internal-external rotation strength was significantly correlated with maximum DTH (Figure 42).

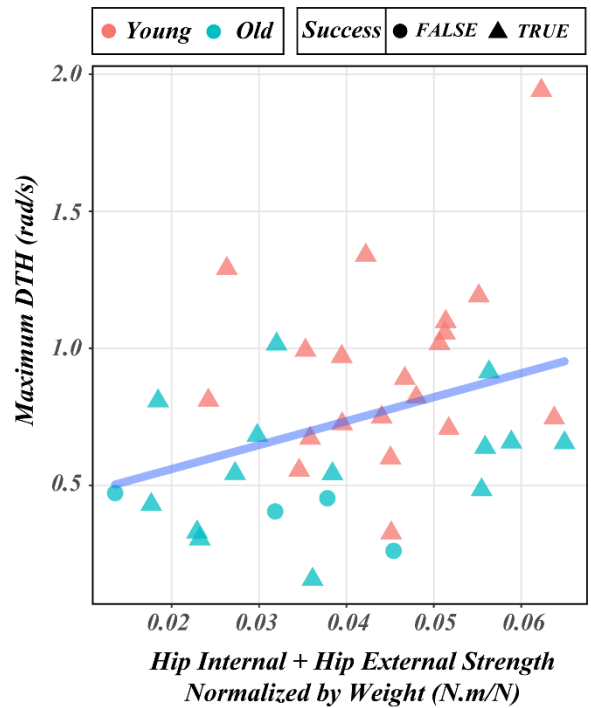


Figure 42- Maximum DTH value vs. Normalized Hip Internal - External Strength for all the subjects. Hip internal-external rotation strength was the only lower extremity capacity which showed significant correlation with maximum DTH ($p = 0.037$, $R^2 = 12\%$).

4.4 Discussion

Shuffling of the stance foot often occurs in some of our daily activities which require standing on one leg. For example, consider the task of standing on one leg in order to pull one trouser leg over the other leg, when all of a sudden its foot gets stuck in a hem. The natural response after a few seconds is to start fidgeting the stance foot medio-laterally back and forth to maintain balance while bending down to get the foot unstuck. One might use HTS or even hopping to locomote over to a nearby wall or heavy piece of furniture to hold on to while one frees the foot stuck in the pant leg. Despite its commonality, there is dearth of experimental or modeling studies that consider heel-toe-shuffle (HTS) as a strategy that could be used for recovering one-legged balance (OLB). To our knowledge, this is the first study that uses both modeling techniques and experimental data to quantify HTS as a locomotion capacity that can be used to restore OLB.

Perhaps a reason why HTS has not received much attention in the OLB literature is that it sits right outside the boundary of our definition for standing OLB: if someone has to take a step, even if it is just a shuffling step, to stop themselves from falling then they have already lost their standing balance. However, when we think of OLB as a clinical test of balance for predicting injurious falls in the elderly [85], then HTS becomes every bit as relevant as the other oft-studied OLB strategies, namely the ‘ankle strategy’ and the ‘hip strategy’. Chapters 2 and 3, and the entire literature on OLB, focus on these two strategies. So, by studying HTS, we are extending the current knowledge in a new direction.

In this chapter we first examined if all our subjects could actually reliably and intentionally use HTS to locomote either medially or laterally. Predictably, all twenty of the subjects in the young group were successful in traveling a 45 cm distance using the HTS strategy while standing on one leg. Amongst the subjects in the old group, almost everyone was ambivalent at first. After all, this is not a locomotion task that we ever perform intentionally, even though many of us are actually skilled at it. So for the elderly the learning curve was steep. However, once they were assured that even if they fell, I would catch them safely, they were willing to try the task. Some 13 out of the 18 subjects in the older group succeeded in reliably traveling more than half of the prescribed distance (~25 cm) without losing their balance. In 4.3.1 we showed that only variable that came close to predicting success in HTS experiments in the older adults was the unipedal stance time ($R^2 = 20\%$, $p = 0.06$). We excluded the younger

subjects from this analysis because all of them succeeded and exhibited a ceiling effect on the task. Later in 4.3.5 we used the maximum recorded DTH in the lateral direction for each subject to examine the effect of UST and lower extremity strengths on the effectiveness of HTS in creating corrective changes in the angular velocity of the body (Introduction H₁). We showed that hip internal-external rotation strength was the only predictor that was significantly correlated with DTH ($p = 0.037$, $R^2 = 12\%$). Figure 43 is also aligned consistent with our earlier result that longer UST, and therefore good OLB, is a necessary but not sufficient condition for performing well in the HTS experiment.

In 4.3.4 we showed that a single HTS step can create a corrective change in angular velocity of the body that is two to six times higher than the maximum ankle inversion moment in the same amount of time (Introduction H₂). But we also showed that both within-subject and between-subject variations in DTH were significantly and substantially higher than the DTA. We believe that this finding suggests why HTS is always used as an alternative strategy when all other strategies fail. While the changes in angular velocity of the body due to ankle torque are not substantial, they are reliable and continuous. One can adjust their ankle torque finely to get precise control

over the COM. However, a HTS step is a somewhat drastic, yet an unreliable strategy due to two reasons: 1) it is discontinuous in the sense that one cannot adjust the accelerations of the ankle continuously; a step is initiated which creates the required acceleration in the correct direction, but inevitably a counter acceleration has to be created if the person is to regain their balance since their foot should not be moving by then. 2) Having planned to take a HTS step, one cannot be sure that it was the right amount for regaining OLB balance with just that one step. Within-subject variations in random intercepts for DTH provide evidence for this claim. However, if there is room on the floor to take more HTS steps, and if there isn't too much fatigue in the

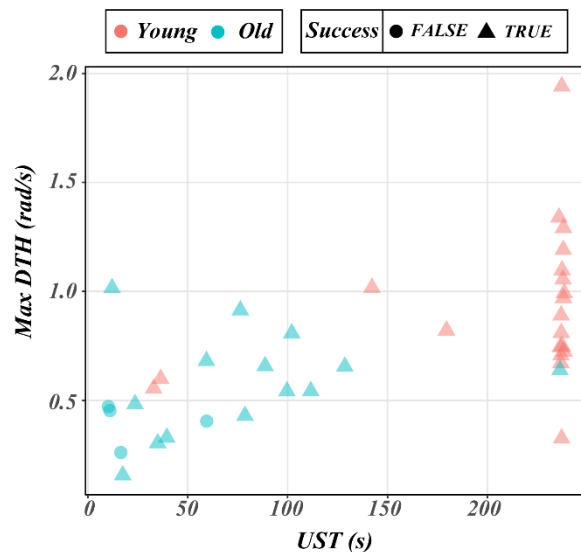


Figure 43- Maximum DTH measured during the first two steps in the lateral HTS trials vs Unipedal Stance Time (UST) for all subjects. The plot suggests that a long UST is a necessary but not sufficient condition for being capable of producing large DTH values.

muscles required to perform the HTS, then one can always concatenate extra steps in order to slow and arrest COM motion in that direction as long as one or more HTS steps brings the COP ahead of the COM to arrest its momentum.

It is important to make a distinction between DTH and HTS strategy during OLB. By asking the subjects to use the shuffling of their stance foot to locomote the appointed distance as fast as they can, we are measuring each person's *capacity* for creating the maximum velocity of their stance foot starting from a stationary one-legged stance. So DTH is a measure for that HTS capacity. This is similar to measuring a subject's maximum ankle inversion-eversion moments while standing on one leg which then could be used by the subject during their OLB (width of the FBR in Chapter 3). But the question remains: *if given the choice, would subjects actually use HTS strategy to extend their UST?*

The answer is 'Yes'. In the Chapter 3 OLB experiment we measured each subject's maximum UST with eyes open and eyes closed. During the eyes open trials, one young subject (S15) used a medial HT step to extend his UST before falling. Similarly, another young subject (S36) used a medial HT step followed by a lateral HT step to successfully regain her balance. The eyes closed trials forced more subjects into using the HTS strategy. Ten different subjects in the young group and three subjects in the old group used HTS during their eyes closed OLB trial on multiple occasions. So overall there were 14 of 38 subjects used a HTS strategy to prolong their UST. The observed HTS occurrences could be categorized into three groups: 1) the subject took a single HTS step and successfully recovered his/her balance, 2) the subject took one or two HTS steps which extended their UST before eventually ending OLB by placing their raised foot on the ground, and 3) once the subject started using the HTS strategy they took several HTS steps in both medial and lateral directions extending their UST by several seconds. All three groups of HTS responses have the advantage of postponing the need for putting the contralateral foot down. In 2.4.3.2 we showed that even introducing a 250 ms latency in initiating a maximal corrective response would reduce the recoverable OLB states by more than half. Conversely, if one can postpone an impending fall, one has more chance to organize a recovery of balance, or at least more time to prepare for the impact of the fall and reduce it.

In this chapter, we chose to only use the lateral HTS experiments for the comparison of DTH with DTA. Other than simplifying the statistical analyses, this choice was based on the relative risk of injury associated with a lateral vs. a medial loss of OLB. In the case of a medial

loss of OLB, the subject can simply put their contralateral foot down and arrest the accelerations of their body due to gravity. On the other hand, a lateral loss of OLB requires a cross-over step [86] to avoid falling onto the greater trochanter. So, a lateral HTS is more crucial to master than a medial one if one is to avoid a fall directly onto the greater trochanter which is known to have a high risk of injury [87, 88].

There are two important limitations to this study. First, HTS locomotion is not a task that we practice daily. While we do have to stand on one leg during some of the transitions of our daily lives, only a small portion of them require the HTS strategy to recover balance. So our HTS locomotion experiment was essentially a new task for our subjects, so there would have been a learning effect. In this case it should be rapid because most are using a HTS strategy that is already learned and that they have used, without thinking, for decades. We tried to minimize the learning effect by giving our subjects plenty of HTS locomotion tries for them to feel comfortable with the task before we started recording the trial. Also, we had the subjects practice only HTS locomotion trials in the same direction that they were going to perform for the recordings. So, for example, each subject started practicing lateral HTS trials only before the three lateral HTS trials were recorded. Then we switched to the medial trial practices and recorded them afterwards. The other limitation is that for five out of 38 subjects, we did not have the right size New Balance walking shoe for them in the lab on the day of the testing. So they had to wear their own sport shoes during the test. This could have affected the coefficient of friction between the shoe sole and the metal force under their stance foot and this could have then changed the person's ability to perform. A high coefficient of friction would make it more difficult, a low coefficient of friction would make it easier. If the coefficient of friction is too high, then it take much more strength to be able to turn the stance foot in order to shuffle.

4.5 Conclusions

- All twenty young subjects and the majority, 13 out of 18, of older subjects succeeded in performing the HTS locomotion task.
- A single HTS step in the lateral direction was on average two to six times more effective in changing the angular velocity of the body than exerting maximum ankle inversion moment in the same amount of time.
- DTH showed substantially more within-subject and between-subject variability than DTA
- The results suggests that longer unipedal stance times are a necessary but not sufficient condition for success in our HTS locomotion task.
- Hip internal-external rotation strength was the only lower extremity strength that showed a significant correlation with the primary outcome capacity measure (DTH).
- Measured DTH values were significantly higher in the lateral direction during heel-toe transitions of the center of pressure, and in younger subjects.
- We found no evidence for a sex difference in the measured DTH values.

CHAPTER 5

General Discussion

In Chapter 1 we reviewed the literature on OLB and discovered two knowledge gaps.

KG1: Can strength and range of motion affect OLB time?

KG2: Are there any as yet unrecognized strategies for extending OLB time?

5.1 Dissertation Part I: How do Chapters 2 & 3 Address KG1?

Our literature review in Section 1.2 revealed two important points in regard to KG1:

1. *To study the strength requirements of OLB, in addition to the stance limb ankle joint strength status, we have to also include the ipsilateral hip muscle strength capacities.*

This is because of two reasons: first, to include the effect of a ‘Shear Force Strategy’. Otten clearly showed that the most effective joint in the body in creating shear force under the stance foot is the ipsilateral hip [33]. So the ‘Hip Strategy’ has to be considered in the analyses. Second, in terms of the hip muscle strength, even if we are only considering the ‘Ankle Strategy’ and quasistatic OLB, the majority of the body weight stays medial to the stance limb hip during OLB, which should create a large hip abduction moment requirement. Not including the ipsilateral hip strength in the analyses carries an important and often overlooked assumption that the muscle-equivalent hip abduction moment demand of OLB is negligible compared to the available hip abduction strength. It is possible that this assumption is a result of an attempt to directly translate what has been learned in the literature on bipedal standing to OLB. During bipedal standing, the mass of the head, arms and trunk stays mostly above the hip joints in the sagittal plane, which makes the required hip extension moment for neutral bipedal stance virtually zero. We saw that for both published average parameters (Section 2.3.5) and individuals in our OLB experiment (Section 3.3.3) that this was indeed a substantial

value and on average more than 50% of the maximum voluntary hip abduction strength even in our strongest population, the healthy young men.

2. ***The capacity requirements of OLB most commonly addressed in the literature are the ankle inversion-eversion strength and proprioception.*** The published literature, reviewed in Chapter 1, shows that given a large enough BOS and having sufficient ankle inversion-eversion strength ensures that the COP under the stance foot can travel in a large enough area (functional BOS) to create a sufficient moment arm for controlling the center of mass. In addition, having good proprioception in the ankle and under the stance foot allows the person to accurately assess the current position of the COP under his/her foot in order to better control the position of the COM. From these two capacity requirements, we could infer that people with weak ankles and bad proprioception will have lower UST on average compared to the healthy controls [21, 89]. In this dissertation we did not focus on proprioception since it is not a modifiable risk factor; a reduction in proprioception acuity is often a result of irreversible nerve degeneration, e.g. diabetic peripheral neuropathy. However, it can be shown that even with severe loss of ankle muscle strength and poor ankle proprioception, patients with diabetic peripheral neuropathy should be able to use their vision in lieu of the poor sensation and solely use their ‘Shear Force Strategy’ (in this particular case, the ‘Hip Strategy’) to compensate for the lack of ankle muscle strength in order to maintain their balance, even if that entails larger than normal movements. So when considering the capacity requirements of OLB hip muscle strength should also be included in addition to ankle inversion-eversion strength [21].

The concept of quasistatic feasible balance region (FBR), introduced theoretically in Chapter 2 (Section 2.3.1), is a direct result of combining the above two points and therefore extends the current literature. More specifically, by creating a model of OLB that includes the range of motion and strength of both the ankle and hip joint of the ipsilateral leg, it takes into account the requirement of having enough muscle-equivalent hip abduction moment for quasistatic OLB (point 1) to the currently known capacity requirement for OLB (point 2). Indeed we showed (in Section 2.3.2) that the width of the FBR is in direct proportion to the functional BOS and the length depends on the maximum hip abduction strength. To draw the FBR for a person, we need to measure his/her functional BOS, anthropometry, mass distribution, and

maximum hip abduction strength. Examining the FBR driven from both published population parameters (Section 2.3.2) and individuals participating in our OLB experiment (Chapter 3, Section 3.3.2) confirmed that maximum muscle-equivalent hip abduction moment can indeed be a limiting factor in determining the FBR cross-sectional area and therefore the anticipated quasistatic OLB postures of even healthy individuals, especially older women.

Having shown that the muscle-equivalent maximum hip abduction moment could affect the OLB quasistatic states, as explained by the FBR, the next question came naturally: what proportion of maximum muscle-equivalent hip abduction moment are people using to stand on one leg? Due to the well-established inverse relationship between intensity of an isometric load and the time one could endure such a load (endurance time, Section 2.4.1) we then hypothesized that the fatiguing of the hip abductor muscles due to the OLB hip abduction moment demand could be a contributing factor to the mechanistic link between lower extremity weakness and short UST. This would be especially true since unlike the use of ankle moments in the ‘Ankle Strategy’, the hip abduction moment demand never decreases to zero or changes signs during regular clinical OLB trials. So if the hip abductor muscles are fatigued beyond the hip abduction moment demand of OLB, none of the strategies could be effective in controlling balance and therefore the participant OLB trial would have to place their raised foot back on the ground, thereby ending the trial.

We set out two main goals for our OLB experiment described in Chapter 3: 1) to validate the FBR to be an extension of the already established functional BOS as a capacity requirement of OLB, and 2) test our hypothesis that the endurance time in the hip abductor muscles during OLB act as an upper limit for the measured UST. Both of these goals were based on an important assumption that all the hip abduction moment demand was being provided by the abductor muscles, namely the gluteus medius and minimus, and tensor fasciae latae. This assumption stemmed from the belief that at least with healthy individuals, we do not see marked ‘sagging’ of the pelvis during OLB; so the ipsilateral hip adduction angle would not be close enough to the end of its range of motion (reported to occur at 20°-25° ‘pelvic sag’) where the ligaments surrounding the joint would be involved in providing some of the OLB moment to protect the hip. Indeed in Section 3.3.4 we checked this assumption for our cohort of subjects and showed that, on average, the subjects had less than 5° of ‘pelvic sag’ during their OLB trials. However, examination of the trajectory of OLB states inside the subject-specific drawn FBR (Section

3.3.2), revealed that the maximum hip abduction strength constraint was violated for some of the OLB states of our participants, especially the women in the older group. Additionally, both measured endurance times at 50% intensity and anticipated endurance times, based on the calculated intensity of the isometric hip abduction moment demand, were shorter than the UST in a large portion of our subjects, even in the older group (Section 3.3.5). These two pieces of evidence pointed to the conclusion that hip abductor muscles have to share the OLB load with another mechanism. Based on the anatomy of the human body and the evidence that was found in the literature, we posited that the load sharing mechanism probably involves the iliotibial band (Section 3.4.2). In Sections 3.4.3 and 3.4.4 then we reviewed how we expect the existence of the ‘iliotibial mechanism’ to affect the FBR and OLB. Particularly, regarding the FBR, only a severe hip abductor muscle strength loss would cause the FBR length to be affected. In these cases, we anticipate that the change in FBR length will be in the form of a splitting in the middle showing that maintaining OLB with a level pelvis is not possible. This finding is corroborated by the Trendelenburg’s test of function in the clinic in which patients with severe abductor muscle atrophy are asked to stand on one leg; they would either exhibit one or both classic signs: a marked ‘sagging of their pelvis’ or maximal lateral flexion of their torso in order to reduce the hip abduction moment demand.

5.2 Dissertation Part II: How does Chapter 4 Address KG2?

Our theoretical calculations for the effectiveness of the proposed ‘Heel-Toe-Shuffle’ (HTS) strategy for OLB (Section 4.2.3) depended heavily on the acceleration profile of the ipsilateral ankle during the HTS maneuver. Also, unlike the ‘Ankle Strategy’ and the ‘Hip Strategy’ where we can measure ankle and hip strength to derive the corresponding strategy capacity, we could not directly derive the HTS strategy capacity based on other measured capacities. This is because the success of someone in using the HTS strategy depends on multiple factors. We speculate that these factors include 1) being able to stand on one leg to begin with (Section 4.3.1), having enough plantarflexion strength to lift the heel, enough dorsiflexion strength to lift the toes, and enough hip internal-external rotation strengths to overcome the friction under the shoe to turn the ipsilateral leg around its vertical axis (Section 4.3.5). Finally, developing the coordination of muscle activity to achieve intentional HTS locomotion requires training and a learning curve. So our main goal in Chapter 4 was to quantify the HTS capacity for each of the subjects based on the fastest volitional HTS locomotion task. We successfully

achieved this goal (Section 4.3.2) in the form of contributions of a single HTS step to changes in the angular velocity of the whole body which we called ‘DTH’. Then, for the lateral HTS steps, we showed that in the time it takes to take a single HTS step, DTH was two to six times higher than the maximum possible contribution of the ‘Ankle Strategy’ (DTA) to changes in the angular velocity of the whole body (Section 4.3.4). So, in summary, HTS can be considered as a third effective strategy to maintain OLB, particularly in avoiding an impending loss of balance.

In daily life, many factors will affect whether or not HTS is a viable recovery strategy. Foremost among them being the coefficient of friction between the shoe (foot) and the floor. Clearly, wearing soccer cleats on a thick pile carpet would make HTS close to impossible even for the healthy young. In that case he/she might actually invoke hopping to move their BOS instead of the HTS. On the other hand wearing socks on a hardwood surface would make HTS very easy to use and render the hopping response unneeded.

5.3 Comparison of the Effectiveness of Ankle, Hip, and HTS Strategies in Recovering OLB

A proper comparison of these strategies in controlling OLB is not possible without making assumptions on the control strategy that the central nervous system (CNS) uses for coordinating between them. Characterizing that control strategy is a large challenge that lies well beyond the scope of this dissertation. Of more interest here however, is the effectiveness of these strategies in avoiding a fall in a given direction. After all the reason why we are studying OLB here is its utility in predicting injurious falls [8]. So the question we are addressing here is how can we compare the three OLB strategies in their effectiveness in recovering OLB to avoid a lateral fall? The reason for choosing the lateral direction was that in case of a medial loss of OLB, the person can simply place their contralateral foot down to arrest the angular momentum of their body. But in case of a lateral fall, a failure to react properly could result in falling onto the ipsilateral greater trochanter which can result in serious injury like a fracture of that hip [88].

Changing the question to that of recovering OLB, makes the coordination of the strategies unique. For example, to avoid a lateral fall, we need to use all the strategies in a direction that would create the maximum medial acceleration of the COM. Combining Sections 2.3.6 and 4.3.2 we know that for avoiding a lateral fall, the COP should be brought to the lateral edge of the functional BOS, maximum hip abduction moment should be exerted resulting in a lifting of the pelvic inclination angle, and quick lateral HTS steps should be used to get the ankle at least under and preferably ahead of the COM. To compare the three strategies, one might

consider to just examine the maximum angular acceleration of the COM induced by a maximum ankle inversion moment, maximum hip abduction, or a maximum ankle acceleration during HTS (Appendix I). However this comparison is not meaningful. For example, in healthy young subjects, the maximum hip abduction moment can create an initial acceleration of the COM that is more than ten times higher than that of the maximum ankle inversion moment. However, the resulting angular velocity of the stance hip will cause the ipsilateral hip to reach its end of ROM rapidly which would then create an opposing and larger hip adduction moment to stop injury to the hip joint. This is why it is important to consider both the magnitude and duration of the effectiveness of each strategy when comparing them.

Another complication of comparing the three OLB strategies is that using one might interact with the possibility of deploying the other. For example, the ‘Hip Strategy’ is part of a larger synergy of joint moments that induce a net corrective shear force under the stance foot. Otten showed that his subjects used their hip moment in the direction to create corrective accelerations of the COM, while moving their non-stance limbs in the opposite direction, allowing the hip moment to last for a longer time [33]. Hence, although ‘Hip Strategy’ is always accompanied by an ‘Ankle Strategy’ [30, 33], it probably will not allow deployment of HTS strategy due to the necessary coordination involved. Then to make the comparison of OLB strategies possible, we used the ‘Ankle Strategy’ as the medium between the three strategies. This is because we suspect using the ‘Ankle Strategy’ alone does not cause a large dynamic movements of the body and the limbs allowing the initiation of the other strategies.

In Section 2.4.2 (Table 7) we showed that using the maximum hip abduction moment allowed extending the functional BOS laterally by more than two-fold. This calculation had accounted for reaching the end of ROM by the ipsilateral hip and the time that the hip strategy could remain effective (Appendix II). So we could claim that the ‘Hip Strategy’ is as effective as the ‘Ankle Strategy’ in recovering OLB. On the other hand, in Section 4.3.4 we showed that in the time it takes to take one lateral HTS step, the contribution of HTS step to changes in the angular velocity of the whole body (DTH) was two to six times higher than the maximum contribution of the ‘Ankle Strategy’ (DTA).

Although this comparison lacks a common test ground between the effectiveness of the three OLB strategies in recovering OLB from a lateral fall, we posit that it does show that HTS is at least as important as the other two strategies, if not more important. In Chapter 4 we found that

there is a learning curve for people to intentionally locomote medially or laterally using HTS steps, but in Chapter 3 for some individuals this was already an automatically invoked response, especially with the eyes closed OLB trials (Section 4.4). For those subjects, the learning curve to perform an intentional HTS locomotion would be rapid.

5.4 How May the Lower Extremity Weakness, Shorter UST, and Falls be Related?

In thinking about the findings of Vellas *et al.* that $UST < 5$ s increased the relative risk for injurious falls in a nursing home population, our original approach was to use the endurance time in the hip abductor muscles to predict a maximum UST for each subject. This was warranted given the high demand that we believed is being placed on the hip abductor muscles during OLB. However, the evidence that we encountered for the existence of a load sharing mechanism between the hip abductor muscles and possibly an iliotibial mechanism (Section 3.4.1) makes this approach non-effective. If we knew the muscles' share of the OLB hip abduction moment demand, we could still use their endurance time as an upper limit for UST. However, the load sharing mechanism makes the OLB demand on the abductor muscles much smaller and therefore the endurance time for the hip abductor muscles much longer. Many other factors could cut the UST short in the meantime making the estimation of the endurance time with considerations for the load sharing mechanism inconsequential.

A possible relationship between good performance in the OLB test (having long UST) and an ability to avoid falls is that the capacity of the same strategies that allow one to have good OLB help one to recover from perturbations to one's balance during one-legged transitions of the daily life. For example, a perturbation to one's OLB could be due to delays in sensing the need for corrective strategies, as is the case for patients with diabetic peripheral neuropathy. In our hypothetical case in Section 2.4.3.2 we showed how a 250 ms latency in initiating a maximum corrective strategy by both ankle and hip strategies reduced the area of recoverable quasistatic OLB states by more than half. Limited rate of torque development in ankle and hip muscles was another source of delay that we considered in 2.4.3.1. We showed that introduction of a 90 ms rise time for the moments from zero to half of the maximum [44], considerably reduced the area of recoverable quasistatic OLB states. Those calculations assumed that the hip abduction moment demand was being provided fully by the abductor muscles. Now consider the effectiveness of the 'Hip Strategy' in OLB recovery, if someone had to rely on the iliotibial mechanism during their OLB because their hip abductor muscles were weak. On one hand, the

person will experience a latency in raising his/her pelvis, since the muscles are starting from a lower activation level and therefore take a longer time to reach their maximum. On the other hand, the maximum muscular hip abduction moment is not going to be as large deeming the ‘Hip Strategy’ ineffective. So in this case the ‘Hip Strategy’ is not even a viable option.

Another example, regarding the effectiveness of an OLB strategy capacity in recovering balance was presented in Section 4.3.4, where we showed that a single HTS step could create a large net change of angular velocity of the whole body. In Section 5.3 we argued how the HTS is at least as effective as the other two strategies in avoiding lateral falls. We also noticed in our OLB experiment with closed eyes, that some people used the HTS strategy. Even if their use of HTS strategy did not help them fully recover their OLB, it extended their UST by the time of a one or two HTS steps (~ 250 ms per step, from the HTS experiment in Chapter 3). This extra time could provide the person with enough opportunity to recover or at least prepare for the fall.

To summarize, one can speculate that the link between lower extremity weakness, shorter UST, and falls could be that lower extremity weakness diminishes the capacities of ankle, hip, and HTS strategies, thereby diminishing the ability of the person to recover from perturbations to their balance using said strategies. We saw this clearly in the form of reductions in FBR and recoverable quasistatic OLB states in Chapter 2 & Chapter 3. On the other hand, having better UST and stronger hip internal-external rotation strengths allowed our subjects to be more effective during their HTS trials in creating corrective changes to the angular velocity of their body (Chapter 4) and extending their UST even by a few milliseconds, which could be the difference between recovery of balance or not.

5.5 Can We Predict Use of the HTS Strategy during an OLB Trial Based on the Methods Used in this Dissertation?

The short answer is yes, if we modify to the OLB experiment to exclude lateral bending of the neck and trunk, and movements of the non-stance leg. To elaborate on this answer, we need to review the quasistatic FBR and show how it can be extended to include dynamic states as well.

The FBR (2.3.1) shows all the states where the subject has enough ankle and hip abduction strength to maintain a quasistatic stance. In 2.4.2 we showed that if the OLB state travels outside the FBR, the subject could still recover their balance using the ‘Hip Strategy’. We then went on to present the recoverable quasistatic OLB states on the same θ_1 - θ_2 plane as the

FBR. Choosing initial quasistatic states was a matter of choice to show a comparison between the recoverable OLB states and the maintainable ones. However, deploying the same approach, we can consider any initial state in the full four-dimensional states-space $(\theta_1, \dot{\theta}_1, \theta_2, \dot{\theta}_2)$ and calculate whether recovering OLB is possible, given the effectiveness of ankle and hip strategy (Appendix II). This would entail a ‘Feasible Balance Volume’ (FBV) instead of the FBR. Although demonstration of the FBV is not easily possible due to its 4-D nature, mathematically determining if it contains an initial OLB state can easily be done in MATLAB.

We can use the FBV to predict if a subject has to use the HTS strategy to recover OLB. If the OLB state travels outside the FBV then one has to use a strategy other than the ankle or hip to recover OLB. If we modify the OLB experiment to preclude the subject from laterally bending their neck or trunk, or moving their non-stance leg (please see section 2.3.4 for the significant effect of these movements on the FBR and the hip abduction moment demand of OLB), then the only option remaining is the HTS strategy. It is important to note however, that crossing the boundary of the FBV is a sufficient, but not necessary condition for eliciting the HTS strategy. Depending on the general strategy and comfort of the subject, a HTS step could be initiated well before crossing the boundaries of the FBV. Indeed in our experiment for measuring the HTS capacity in Chapter 4, all subjects first gained their quasistatic balance first (initial state inside the FBV) and then initiated the HTS locomotion task as instructed. It should also be noted, that the motivation of the subject for continuing the OLB trial determines whether they are going to even try a hip strategy or a HTS strategy in the first place. So the methods of this dissertation can be used to predict when an HTS strategy will be used, if body movements other than those of the stance limb hip and ankle are experimentally eliminated.

5.6 Recommendations for Physiatrists and Physical Therapists

In the following three sections, we will present three recommendations for clinicians that are the result of insights gained from this dissertation.

5.6.1 Using OLB for Measuring Hip Abduction Strength

In Section 3.4.1 we provided evidence for the existence of a load sharing mechanism between the hip abductor muscles and possibly an iliotibial mechanism. Using population means from the literature (Section 2.3.5) and subject-specific measurements (Section 3.3.3) we showed that the hip abduction moment demand of OLB is a substantial portion compared to the

maximum voluntary hip abduction strength (mean value more than 50% in both healthy and older adults). Finally, we also found evidence in the literature that despite decreasing the hip abduction moment demand, raising the pelvic inclination angle increases the share of the abductor muscles from the load [24, 26]. This can be readily confirmed with any healthy subject: ask the subject to stand on one leg with a more or less level pelvic inclination angle for as long as they can and measure their UST. Next ask them to repeat the trial raising their pelvic inclination angle by at least 15 degrees (no need for any accurate sensors, just place visible markers on their ASIS and visually assess). Two things will happen: 1) the UST in the second trial is substantially shorter than the first, and 2) their hip abductor muscles will be fatigued.

On the one hand, reliably measuring maximum voluntary hip abduction strength (i.e. including only the active elements) in the clinic is difficult, due to the possibility of patients cheating by engaging their extensor muscles and the coordination involved in exerting a maximum effort. On the other hand, there is a link between lower extremity weakness, shorter UST, and injurious falls [8, 34]. So using an OLB test to assess a patients 'maximum voluntary hip abduction strength' seems like a natural choice. The criterion that we suggest is that if you expect a patient to be able to balance on one leg for 30 s to consider them healthy, you can also expect them to stand on one leg for the same time using only their voluntary hip abduction strength, without substantial contribution from the posited iliotibial mechanism. Then to test if the patient has enough maximum voluntary hip abduction strength, you can ask them to stand on one leg with a pelvic inclination angle that is raised at least 15 degrees. The patient can medially bend their lumbar spine to keep their head vertical if that is their preference. This will actually increase the demand on their hip abductor muscles (i.e. gluteus medius and minimum and tensor fasciae latae) and keep the OLB hip abduction moment demand closer to the theoretically calculated value of weight times half the distance between hip joint centers (Section 3.2.3.3). The patient can use small touches of their fingers on supports around them to help them not lose their balance. If they can maintain their elevated pelvic inclination angle for the duration of the OLB test, 30 s for example, you can be sure that they have more than enough maximum voluntary hip abduction strength for their OLB test. Also, this ensures that if the need arises, the patient has enough maximum voluntary hip abduction strength to use their 'Hip Strategy'. Of course 30 s is a long time, but we suggest that this value can be adjusted experimentally by comparing it to the current best methods.

5.6.2 Training Elderly to Practice the HTS Strategy

Our results in Chapter 4 showed that even in healthy elderly, HTS can be at least as effective as the maximum ankle torque in creating a corrective change in the angular velocity of the body, *i.e.* arresting a fall. Despite the initial complexity of the task, after only a few practice trials, 13 out of 18 of our healthy older subjects succeeded in traveling more than 25 cm by using the HTS steps. Two of them actually used the HTS strategy during their eyes closed OLB trial to extend their UST. We suggest that strengthening the hip internal/external rotator muscles and practicing the HTS with non-frail subjects can improve their ability to invoke the strategy when needed. Increasing the foot-floor friction is a way to challenge them, but then a spotter needs to be vigilant in catching them should they lose their balance, unless they were to practice at a kitchen counter which they could use for support should they lose their balance.

5.6.3 Modifying the Clinical OLB Trial to Include Hip and HTS Strategies

Based on the results of this dissertation one-legged balance could be tested in two ways: first, the prescribed method in which no arm or foot movements are permitted versus a second, ‘freestyle’, method in which any recovery motions are permissible. A good ‘freestyle’ performance provides confidence in the ability of the patient to recover their balance outside the clinic.

5.7 Limitations

In what follows, I consider the main limitations of this dissertation in order of importance, with the most important limitation stated first.

1. ***Inaccuracies in determining body segment inertial properties (BSIP):*** Currently the gold standard for calculating the BSIP is considered to be the DXA scan images [90, 91]. The logistics involved in getting access to the equipment, the cost, and the added testing time per subject convinced us to seek an alternative method. Our approach was to use an optimization algorithm to minimize the error between center of gravity (COG) estimations to two different methods (described in the Methods in Chapter 3). Both of these methods have their inaccuracies and therefore our method will also be inaccurate. However, ensuring root mean square error of COG measurements between them was not higher than 15 mm during the OLB experiment helped us find the three subjects whose motion capture markers had slipped permanently on their skin after the digitization

process. This method is tested and validated in the literature as an appropriate one for a motion capture lab setting [92, 93] and improves the regression model method based on cadaveric data which are mostly based on a Caucasian population [66, 68, 94].

2. ***Inaccuracies in the functional determination of the hip joint centers (HJC):*** The location of HJC is important in the estimation of the hip abduction moment demand during OLB, because it directly affects the moment arm of the large mass over the stance hip that constitutes the head, arms, trunk and the contralateral leg (Appendix III). The only way to accurately determine the exact location of the hip joint centers is by X-Ray. This method was common in older studies [24, 25], it is however abandoned due to the X-Ray exposure risk to the subjects. We used the movements of the motion capture markers mounted on the pelvis and the leg of the subjects to functionally estimate the location of the HJC on either sides. Our algorithm was based on the SCORE method published and validated in the literature [62]. Our choice of SCORE as our algorithm of choice was due to the fact that it allowed an estimation of the error of the method as well [63].
3. ***Inaccuracies due to simplifying OLB to a double inverted pendulum model:*** A double inverted pendulum model cannot capture the movements of the trunk and other limbs in the inverse dynamic calculations. In Sections 2.2.3 and 2.2.4 we showed that the FBR and hip abduction moment demand could change considerably by the medio-lateral movements of the non-stance leg and bending of the trunk. To minimize this inaccuracy, we asked our subjects to keep their torso straight and the hip abduction angle of their contralateral leg constant during all the experiments. We also kept track of both kinematic parameters (Section 3.3.4) during our analyses. If a subject had a noticeable change in either of the kinematic parameters, we tagged the times this happened and excluded it in the final analyses.
4. ***Inaccuracies introduced by considering the stance foot as one solid link:*** The stance foot is the interaction site between the person balancing on one leg and the environment. Therefore it is an influential factor on OLB. Accounting for the multi-segment nature of the foot however required more detailed motion capture marker placement and more complicated dynamical equations. Our choice of considering foot as one solid link was a compromise to keep the frequency of the motion capture recordings high and keeping the

dynamic equations simple. For the OLB experiment with eyes open (Chapter 3) we believe this choice is valid since for most of the experiment, subjects are quasistatic, and the foot stays stationary with small movements of the ipsilateral ankle. But during the OLB with eyes closed and the HTS experiment (Chapter 4) the dynamic of the foot becomes more important. Since we did not present a dynamic analysis of the eyes closed OLB experiment and constrained our HTS experiment analyses to kinematics of the COP and that of the ankle, we believe this limitation does not affect the results presented.

5. ***Inaccuracies introduced by considering the subtalar joint as a hinge joint:*** In our analyses in Chapters 2&3 we considered the ankle joint at the subtalar level to act as a hinge joint with its axis of rotation perpendicular to the frontal plane. In reality the axis of rotation of the subtalar joint is oblique relative to the frontal plane [95]. But considering this would require a 3D analysis. Besides, this assumption is only consequential in more dynamic cases where the ankle inversion/eversion angles vary a larger amount within the range of motion. Our calculations of the trajectory of the OLB states in Chapter 3 showed that the ankle angle only changed within a few degrees. So this assumption would not have a substantial effect on the outcome of the Chapters.
6. ***Inaccuracies due to constraining the analyses to the frontal plane:*** The theoretical derivations of Chapter 2 and the analyses of Chapters 3 & 4 were all 2D and constrained to the frontal plane. Although during quasistatic OLB and for validation/rejection of our hypotheses throughout the dissertation this assumption is valid, in more dynamic cases it can lead to oversimplification of the analyses. We consider two examples where a 3D dynamic analysis would have been more appropriate:
 - Dynamic analysis of the HTS strategy: Dynamic analysis of HTS by nature requires a 3D analysis. The rotation of the foot around the stance leg's longitudinal axis deems a 2D frontal plane analysis inadequate. A proper dynamic analysis would be able to reveal a more causal relationship between the lower extremity strengths and HTS ability. In Chapter 4 we did not perform a dynamic analysis for our experiment and instead just used the experimentally measured kinematics of the ankle to estimate the effectiveness of the HTS capacity in recovering OLB (DTH). A 3D analysis of the HTS is further complicated by the multi-segment nature of the stance foot (limitation 4).

- Accounting for OLB strategies that involve out of plane movements: In our OLB experiment in Chapter 3 especially with eyes closed, we noticed a strategy that some of the younger subjects tended to use when they were close to losing their OLB. They would redirect the frontal plane angular momentum of their body to the sagittal plane by rotating around their stance hip where their higher ankle plantarflexion strength could arrest the momentum. A 3D analysis of the observed kinematics with a proper experimental setup that involves better marker placement on the stance foot could shed light on this forth OLB strategy.

7. *Inaccuracies in hip abduction maximum strength measurement:* We measured the maximum isometric hip abduction strength by having the subject lie supine and push against a bracket. This helped ensure the measurements were made in a gravity-free plane. However, the coordination involved in exerting a maximum effort in this orientation might have caused some of our subjects not to give their best efforts. We tried to account for this by incorporating the fatigue test measurements which was performed in the same orientation and seemed easier for some (Section 3.2.2.1). Perhaps a modification of Inman's method for measuring the hip abduction strength would have been more appropriate for our test [24]. Briefly, he had the subjects stand on one leg. Meanwhile a non-flexible belt that was connected to a force measurement device wrapped around the ankle of the non-stance leg. The subject would push the belt out using their hip abduction strength. The recorded force times the distance between the HJC and the belt would then give the maximum isometric hip abduction strength.

8. *Inaccuracies in ankle strengths and hip internal/external rotation strength measurements:* We could have error in our strength measurements due to the coordination involved in our method. For ankle strengths, we had already designed a balance board based on an earlier experiment in the biomechanics research lab that would have measured the maximum ankle strengths more accurately [39]. However, due to time constraints for each subject in the lab (less than three hours) and the fact that the base of support limits the maximum exerted ankle inversion/eversion strength we think our method was the right choice. In terms of measuring maximum hip internal/external rotation strength, we would have ideally preferred to have a fixture that allowed us to isolate the hip internal/external rotator muscles. However using the friction on the bottom

of the shoe to measure the hip internal/external rotation strengths had the advantage of accounting for the maximum torque that the friction between the bottom of the shoe and the top of the force plate would allow.

- 9. *Inaccuracies in inverse dynamic calculations due to skin artefacts:*** Any inverse dynamic analysis of the human motion based on motion capture is confounded by the movements of the skin compared to the bone underneath. This is the reason one of our inclusion criteria was to have a BMI less than 35 kg/m². Also, during the OLB experiment (Chapter 3), the subjects were mostly quasistatic which should reduce this effect. We also used a Monte Carlo method to reduce the effect of skin artefact on the OLB inverse dynamic estimations [70]. During the HTS experiment (Chapter 4), we mostly just used the position of ankle which was based on markers placed on the left shank. Since those markers are placed on the anterior side of the shank close to the knee, there was not much fatty tissue under them and so the relative movements of the markers and the tibia should be minimal.
- 10. *No EMG measurements during the OLB experiment:*** Ideally, we would have liked to have EMG measurements of all the abductor and adductor muscles of the stance hip during the maximum hip strength measurements and the OLB experiments. This would allow us to have a subject-specific confirmation for the existence of load sharing of the OLB hip abduction moment demand between the abductor muscles and the posited iliotibial mechanism. However, since surface EMG would not be able to capture the activity of the deeper muscles, we would still have needed a more invasive method such as fine wire EMG measurements.
- 11. *Limited and unbalanced subject group sizes:*** We planned to have balanced groups with ten subject in each groups (young and older, men and women). After phone screening we had to disqualify six older men from participating due to the polypharmacy exclusion criterion. Three more were disqualified after the vibration fork test. So in the time table of the study we could only recruit eight older men. After data collection was concluded, in the analyses of Chapter 3, we had to drop the data for two young men and one old man due to technical issues with the motion capture markers and other equipment.
- 12. *Inaccuracies due to motion capture marker occlusion:*** We used two separate motion capture cameras in series to ensure visibility of markers during the experiments.

However, there were still some instances, especially during more dynamic maneuvers such as the HTS, when some of the key markers like those of pelvis and chest were invisible. For short times we used an interpolation of the same marker to fill in the missing marker data. However for missing time epochs longer than 150 ms we had no choice but to remove the outcome of the inverse dynamic algorithm in those times from the analysis. We also had three markers on the foot to better capture the initiation of the HTS step during the HTS and OLB trials. However, they proved to be unreliable and frequently went missing. So instead we had to rely on only the COP measurements from the force plate to capture the event.

13. ***Inaccuracies introduced by not including individual muscles in the analysis:*** The full analysis of the contribution of individual muscles in creating net torques around ankle and hip joint would have allowed a more detailed capture of the force-length and lengthening effect of the muscles. However, the current methods also involve assumptions on the moment arm of the muscles and their size which are based on a small sample size and would not account for the between-subject variations. Since subjects were mostly quasistatic during the OLB experiments (Chapter 3) and our HTS experiment analyses are only kinematic, we believed that this would not be an important limitation for our study.
14. ***Friction under the bottom of the shoes during HTS experiment:*** We used the same New Balance walking shoes for all subjects, except for five where the right fit was not available. This was to account for the differences in the coefficient of friction between the bottom of the shoe and the top of the force plate where they performed both HTS and OLB experiments. For those who had to wear their own shoes, we did not measure the relative coefficient of friction of the shoe compared to the lab shoes.
15. ***Subject Selection, Obesity and Neuropathy:*** We picked our subjects from a healthy pool of volunteers. This was due to two reasons: 1) our original hypothesis stating that endurance of the hip abductor muscles could dictate a ceiling for the UST, required the subjects to be free of other known deficits that could curtail their OLB trial. 2) The HTS experiment was the first of its kind in the literature and for the older subjects, we did not know at the beginning if the subjects could perform it. As a result we picked only healthy subjects to give the HTS strategy the best chance of succeeding. Proper assessment of the

utility of the HTS strategy for avoiding injury however, requires a feasibility of the strategy with subjects with different levels of mobility impairment. We suspect that obesity would be a limiting factor in HTS, since unless the person can shift his/her weight between the toes and the heel, the friction under the stance foot might be too large to overcome, hence making a lateral shuffle step impossible.

16. **Control of OLB:** Unfortunately, we do not have a direct line into the central nervous system that would allow us to know how the CNS coordinates between different OLB strategies. Our work tries to capture the capacity of some of the recovery strategies that are available for the CNS to use to control OLB and avoid falls after perturbations. A full understanding of the control of OLB however is the only way for a proper comparison between the OLB strategies.

CHAPTER 6

Conclusions

- The model based on published literature data for anthropometry and maximum hip abduction strengths, makes it clear that the hip abduction moment that is required to stand on one leg is substantial, ranging from 50% of maximum voluntary muscle strength in healthy young men to 82% of the maximum in healthy older women (Chapter 2).
- Our experimental results corroborate the OLB hip abduction moment demand that was calculated in Chapter 2. On average, the hip abduction moment demand of OLB is more than half the maximum hip abduction strength for all adults (Chapter 3)
- Our analyses show that the hip abduction moment demand cannot be resisted completely by the abductor muscles alone, for the observed duration of OLB trials. Therefore one can deduce that there has to be an abduction moment contribution from the iliotibial mechanism (ITM) and other passive tissues surrounding the hip, even in pelvic inclination angles close to level. (Chapter 3)
- Load sharing between ITM and abductor muscles, makes calculating the intensity of hip abductor muscles hard which makes it difficult to predict a maximum unipedal stance time. That is because the subject can potentially let most of the demand be carried by the ITM and rest their abductor muscles. (Chapter 3)
- All the quasistatic OLB states may not fall inside the boundaries of the FBR. That is because our original derivation of FBR did not consider the contribution of ITM to resisting the hip abduction moment demand of OLB. (Chapter 3)
- Having to rely on the ITM for maintaining OLB, makes the hip strategy less effective in avoiding lateral falls by decreasing the rate of torque development available from the abductor muscles in response to a potential perturbation. (Chapter 3)
- All twenty young subjects and the majority, 13 out of 18, of older subjects succeeded in performing the HTS locomotion task. (Chapter 4)

- DTH showed substantially more within-subject and between-subject variability than DTA. (Chapter 4)
- The results suggests that longer unipedal stance times are a necessary but not sufficient condition for success in our HTS locomotion task. (Chapter 4)
- Hip internal-external rotation strength was the only lower extremity strength that showed a significant correlation with the primary outcome capacity measure (DTH). (Chapter 4)
- Measured DTH values were significantly higher in the lateral direction during heel-toe transitions of the center of pressure, and in younger subjects. (Chapter 4)
- We found no evidence for a sex difference in the measured DTH values. (Chapter 4)
- A single HTS step in the lateral direction was on average two to six times more effective in changing the angular velocity of the body than exerting maximum ankle inversion moment in the same amount of time. (Chapter 4)
- HTS strategy is at least as effective as the ‘Ankle Strategy’ and the ‘Hip Strategy’ in recovering OLB. (Chapters 2, 3, and 4)
- To avoid a lateral OLB fall, one should bring the COP under the stance foot as far laterally as possible, use their maximum hip abduction strength the raise their pelvic inclination angle as rapidly as possible, and initiate rapid HTS steps to get the stance ankle ahead of the COM. (Chapters 2, 3, and 4)

CHAPTER 7

Suggestions for Future Research

- ***Investigating the iliotibial mechanism*** by measuring the material properties of the proximal region of the IT band, measuring myoelectric activity of the muscles that insert onto it as well as the other abductor muscles, and developing a model for the synergy between the IT band mechanism and the abductor and adductor muscles surrounding the hip joint. A better understanding of this mechanism (3.4.2.1) allows us to incorporate it with the equations of motion of the double inverted pendulum leading to better estimates for the FBR (2.3.1, 3.3.2, and 3.4.3), hip abduction moment demand of OLB on the abductor muscles (2.3.5 and 3.3.3), endurance times (3.3.5), and effectiveness of the hip strategy for recovering OLB (2.4.2).
- ***Three-dimensional dynamic analysis of one-legged balance*** for investigating the momentum plane change strategy (explained in limitation 6).
- ***Three-dimensional dynamic analysis of the heel-toe shuffle strategy*** for understanding the causal relationship between the strengths and the HTS capacity. This in turn allows the physical therapists to have a more focused HTS training regimen.
- ***Study of HTS strategy with patients with different levels of mobility deficits***. Some possible factors to consider include obesity, diabetic peripheral neuropathy, and osteoarthritis.

APPENDICES

Appendix I Deriving the Equations of Motion for the Double Inverted Pendulum Model

I. Kinematics of the 3-link double inverted pendulum model

$$\vec{r}_{M_1} = \vec{r}_S + l \hat{k}_1$$

$$\vec{r}_H = \vec{r}_S + h \hat{k}_1$$

$$\vec{r}_{M_2} = \vec{r}_H + r \hat{k}_2 = \vec{r}_S + h \hat{k}_1 + r \hat{k}_2$$

$$\vec{v}_{M_1} = \vec{v}_S + \vec{v}_{rel} + \dot{\theta}_1 \hat{j} \times l \hat{k}_1$$

$$\vec{v}_{M_1} = \vec{v}_S + (l\dot{\theta}_1) \hat{i}_1$$

$$\vec{v}_H = \vec{v}_S + (h\dot{\theta}_1) \hat{i}_1$$

$$\vec{v}_{M_2} = \vec{v}_H + (\dot{\theta}_1 + \dot{\theta}_2) \hat{j} \times r \hat{k}_2$$

$$\vec{v}_{M_2} = \vec{v}_S + (h\dot{\theta}_1) \hat{i}_1 + r(\dot{\theta}_1 + \dot{\theta}_2) \hat{i}_2$$

$$\vec{a}_{M_1} = \vec{a}_S + \vec{a}_{rel} + 2\vec{\omega}_B \times \vec{v}_{rel} + \ddot{\theta}_1 \hat{j} \times l \hat{k}_1 + \dot{\theta}_1 \hat{j} \times (\dot{\theta}_1 \hat{j} \times l \hat{k}_1)$$

$$\vec{a}_{M_1} = \vec{a}_S + l\ddot{\theta}_1 \hat{i}_1 - l\dot{\theta}_1^2 \hat{k}_1,$$

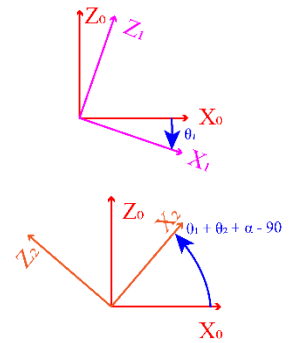
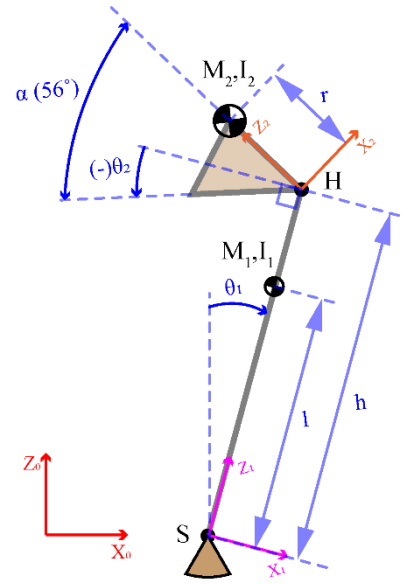
$$\vec{a}_{M_1} = \vec{a}_S + \begin{Bmatrix} l\ddot{\theta}_1 \\ 0 \\ -l\dot{\theta}_1^2 \end{Bmatrix}_{X_1Y_1} = \vec{a}_S +$$

$$\begin{Bmatrix} l\ddot{\theta}_1 \cos(\theta_1) - l\dot{\theta}_1^2 \sin(\theta_1) \\ 0 \\ -l\ddot{\theta}_1 \sin(\theta_1) - l\dot{\theta}_1^2 \cos(\theta_1) \end{Bmatrix}_{X_0Y_0},$$

$$\vec{a}_H = \vec{a}_S + (h\ddot{\theta}_1) \hat{i}_1 - h\dot{\theta}_1^2 \hat{k}_1$$

$$\vec{a}_{M_2} = \vec{a}_H + (\ddot{\theta}_1 + \ddot{\theta}_2) \hat{j} \times r \hat{k}_2 + (\dot{\theta}_1 + \dot{\theta}_2) \hat{j} \times ((\dot{\theta}_1 + \dot{\theta}_2) \hat{j} \times r \hat{k}_2)$$

$$\vec{a}_{M_2} = \vec{a}_H + r(\ddot{\theta}_1 + \ddot{\theta}_2) \hat{i}_2 - r(\dot{\theta}_1 + \dot{\theta}_2)^2 \hat{k}_2$$



$$\vec{a}_{M_2} = \vec{a}_S + \left\{ \begin{array}{c} h\ddot{\theta}_1 \cos(\theta_1) - h\dot{\theta}_1^2 \sin(\theta_1) \\ 0 \\ -h\ddot{\theta}_1 \sin(\theta_1) - h\dot{\theta}_1^2 \cos(\theta_1) \end{array} \right\}_{X_0Y_0} + \left\{ \begin{array}{c} r(\ddot{\theta}_1 + \ddot{\theta}_2) \\ 0 \\ -r(\dot{\theta}_1 + \dot{\theta}_2)^2 \end{array} \right\}_{X_2Y_2}$$

$$\vec{a}_{M_2} = \vec{a}_S + \left\{ \begin{array}{c} h\ddot{\theta}_1 \cos(\theta_1) - h\dot{\theta}_1^2 \sin(\theta_1) \\ 0 \\ -h\ddot{\theta}_1 \sin(\theta_1) - h\dot{\theta}_1^2 \cos(\theta_1) \end{array} \right\}_{X_0Y_0} + \left\{ \begin{array}{c} r(\ddot{\theta}_1 + \ddot{\theta}_2) \sin(\theta_1 + \theta_2 + \alpha) + r(\dot{\theta}_1 + \dot{\theta}_2)^2 \cos(\theta_1 + \theta_2 + \alpha) \\ 0 \\ r(\ddot{\theta}_1 + \ddot{\theta}_2) \cos(\theta_1 + \theta_2 + \alpha) - r(\dot{\theta}_1 + \dot{\theta}_2)^2 \sin(\theta_1 + \theta_2 + \alpha) \end{array} \right\}_{X_0Y_0}$$

II. Dynamics of the double inverted pendulum model

We are assuming planar dynamics assumptions.

$$\vec{g} = \begin{pmatrix} 0 \\ 0 \\ -g \end{pmatrix}_{x_0 y_0}$$

Stance Leg:

$$\sum \vec{F} = \vec{F}_S + M_1(\vec{g} - \vec{a}_{M_1}) - \vec{F}_H = 0 \leftrightarrow,$$

$$F_{Sx} = F_{Hx} + M_1 a_{M_1x} \rightarrow,$$

$$F_{Sx} = F_{Hx} + M_1 \left(\ddot{x}_S + l\ddot{\theta}_1 \cos(\theta_1) - l\dot{\theta}_1^2 \sin(\theta_1) \right) \rightarrow, F_{Sx} = F_{Hx} + M_1 \ddot{x}_S + M_1 l\ddot{\theta}_1 \cos(\theta_1) - M_1 l\dot{\theta}_1^2 \sin(\theta_1),$$

Inverse Dynamics Equation 1

$$F_{Sz} = F_{Hz} + M_1(a_{M_1z} + g) \rightarrow,$$

$$F_{Sz} = F_{Hz} + M_1 \left(-l\ddot{\theta}_1 \sin(\theta_1) - l\dot{\theta}_1^2 \cos(\theta_1) + g \right) \rightarrow,$$

$$F_{Sz} = M_1 g + F_{Hz} - M_1 l\ddot{\theta}_1 \sin(\theta_1) - M_1 l\dot{\theta}_1^2 \cos(\theta_1),$$

Inverse Dynamics Equation 2

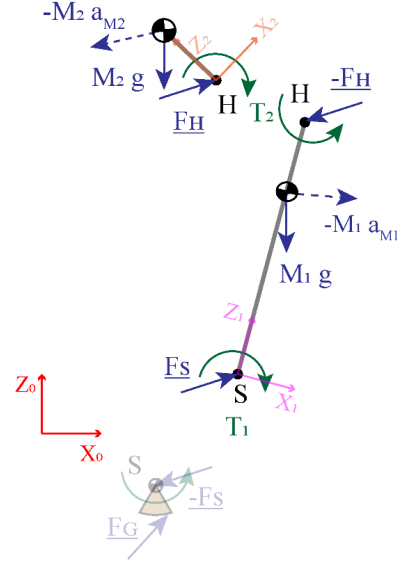
$$\sum \vec{M}_{M_1} = (T_1 - T_2) \hat{j} - l \hat{k}_1 \times \vec{F}_S - (h - l) \hat{k}_1 \times \vec{F}_H = I_1 \ddot{\theta}_1 \hat{j} \leftrightarrow,$$

$$(T_1 - T_2) - F_{Sx} l \cos(\theta_1) + F_{Sz} l \sin(\theta_1) - F_{Hx} (h - l) \cos(\theta_1) + F_{Hz} (h - l) \sin(\theta_1) = I_1 \ddot{\theta}_1,$$

Inverse Dynamics Equation 3

Rest of the Body:

$$\sum \vec{F} = \vec{F}_H + M_2(\vec{g} - \vec{a}_{M_2}) = 0 \leftrightarrow,$$



$$F_{Hx} = M_2 a_{M_2x} \rightarrow,$$

$$F_{Hx} = M_2 \ddot{x}_S + M_2 h \ddot{\theta}_1 \cos(\theta_1) - M_2 h \dot{\theta}_1^2 \sin(\theta_1) + M_2 r (\ddot{\theta}_1 + \ddot{\theta}_2) \sin(\theta_1 + \theta_2 + \alpha) + M_2 r (\dot{\theta}_1 + \dot{\theta}_2)^2 \cos(\theta_1 + \theta_2 + \alpha),$$

Inverse Dynamics Equation 4

$$F_{Hz} = M_2 g + M_2 a_{M_2z} \rightarrow,$$

$$F_{Hz} = M_2 g - M_2 h \ddot{\theta}_1 \sin(\theta_1) - M_2 h \dot{\theta}_1^2 \cos(\theta_1) + M_2 r (\ddot{\theta}_1 + \ddot{\theta}_2) \cos(\theta_1 + \theta_2 + \alpha) - M_2 r (\dot{\theta}_1 + \dot{\theta}_2)^2 \sin(\theta_1 + \theta_2 + \alpha),$$

Inverse Dynamics Equation 5

$$\sum \vec{M}_{M_2} = T_2 \hat{j} - r \hat{k}_2 \times \vec{F}_H = I_2 (\ddot{\theta}_1 + \ddot{\theta}_2) \hat{j} \rightarrow,$$

$$T_2 - F_{Hx} r \sin(\theta_1 + \theta_2 + \alpha) - F_{Hz} r \cos(\theta_1 + \theta_2 + \alpha) = I_2 (\ddot{\theta}_1 + \ddot{\theta}_2),$$

Inverse Dynamics Equation 6

Replace F_S values into Inverse Dynamics Equation 3:

$$(T_1 - T_2) - \left(F_{Hx} + M_1 \ddot{x}_S + M_1 l \ddot{\theta}_1 \cos(\theta_1) - M_1 l \dot{\theta}_1^2 \sin(\theta_1) \right) l \cos(\theta_1) + \left(M_1 g + F_{Hz} - M_1 l \ddot{\theta}_1 \sin(\theta_1) - M_1 l \dot{\theta}_1^2 \cos(\theta_1) \right) l \sin(\theta_1) - F_{Hx} (h - l) \cos(\theta_1) + F_{Hz} (h - l) \sin(\theta_1) = I_1 \ddot{\theta}_1,$$

And now replace F_H values in the above equation:

$$(T_1 - T_2) - \left(M_1 \ddot{x}_S + M_1 l \ddot{\theta}_1 \cos(\theta_1) - M_1 l \dot{\theta}_1^2 \sin(\theta_1) \right) l \cos(\theta_1) + \left(M_1 g - M_1 l \ddot{\theta}_1 \sin(\theta_1) - M_1 l \dot{\theta}_1^2 \cos(\theta_1) \right) l \sin(\theta_1) - \left(M_2 \ddot{x}_S + M_2 h \ddot{\theta}_1 \cos(\theta_1) - M_2 h \dot{\theta}_1^2 \sin(\theta_1) + M_2 r (\ddot{\theta}_1 + \ddot{\theta}_2) \sin(\theta_1 + \theta_2 + \alpha) + M_2 r (\dot{\theta}_1 + \dot{\theta}_2)^2 \cos(\theta_1 + \theta_2 + \alpha) \right) h \cos(\theta_1) + \left(M_2 g - M_2 h \ddot{\theta}_1 \sin(\theta_1) - M_2 h \dot{\theta}_1^2 \cos(\theta_1) + M_2 r (\ddot{\theta}_1 + \ddot{\theta}_2) \cos(\theta_1 + \theta_2 + \alpha) - M_2 r (\dot{\theta}_1 + \dot{\theta}_2)^2 \sin(\theta_1 + \theta_2 + \alpha) \right) h \sin(\theta_1) = I_1 \ddot{\theta}_1 \rightarrow,$$

$$\begin{aligned}
& (T_1 - T_2) - M_1 l \cos(\theta_1) \ddot{x}_S - M_1 l^2 \cos(\theta_1)^2 \ddot{\theta}_1 + M_1 l^2 \sin(\theta_1) \cos(\theta_1) \dot{\theta}_1^2 + M_1 g l \sin(\theta_1) - \\
& M_1 l^2 \sin(\theta_1)^2 \ddot{\theta}_1 - M_1 l^2 \sin(\theta_1) \cos(\theta_1) \dot{\theta}_1^2 - M_2 h \cos(\theta_1) \ddot{x}_S - M_2 h^2 \cos(\theta_1)^2 \ddot{\theta}_1 + \\
& M_2 h^2 \sin(\theta_1) \cos(\theta_1) \dot{\theta}_1^2 - M_2 r h \sin(\theta_1 + \theta_2 + \alpha) \cos(\theta_1) (\ddot{\theta}_1 + \ddot{\theta}_2) - M_2 r h \cos(\theta_1 + \theta_2 + \\
& \alpha) \cos(\theta_1) (\dot{\theta}_1 + \dot{\theta}_2)^2 + M_2 g h \sin(\theta_1) - M_2 h^2 \sin(\theta_1)^2 \ddot{\theta}_1 - M_2 h^2 \sin(\theta_1) \cos(\theta_1) \dot{\theta}_1^2 + \\
& M_2 r h \cos(\theta_1 + \theta_2 + \alpha) \sin(\theta_1) (\ddot{\theta}_1 + \ddot{\theta}_2) - M_2 r h \sin(\theta_1 + \theta_2 + \alpha) \sin(\theta_1) (\dot{\theta}_1 + \dot{\theta}_2)^2 = \\
& I_1 \ddot{\theta}_1 \rightarrow,
\end{aligned}$$

$$\begin{aligned}
& T_1 - T_2 + (M_1 l + M_2 h) g \sin(\theta_1) - (M_1 l + M_2 h) \cos(\theta_1) \ddot{x}_S - M_2 r h \sin(\theta_2 + \alpha) (\ddot{\theta}_1 + \ddot{\theta}_2) - \\
& M_2 r h \cos(\theta_2 + \alpha) (\dot{\theta}_1 + \dot{\theta}_2)^2 = (I_1 + M_1 l^2 + M_2 h^2) \ddot{\theta}_1,
\end{aligned}$$

Double Inverted Pendulum Equation 1

Similarly replace F_H values into Inverse Dynamics Equation 6:

$$\begin{aligned}
& T_2 - M_2 r \sin(\theta_1 + \theta_2 + \alpha) \ddot{x}_S - M_2 h r \sin(\theta_1 + \theta_2 + \alpha) \cos(\theta_1) \ddot{\theta}_1 + M_2 h r \sin(\theta_1 + \theta_2 + \\
& \alpha) \sin(\theta_1) \dot{\theta}_1^2 - M_2 r^2 \sin(\theta_1 + \theta_2 + \alpha)^2 (\ddot{\theta}_1 + \ddot{\theta}_2) - M_2 r^2 \sin(\theta_1 + \theta_2 + \alpha) \cos(\theta_1 + \theta_2 + \\
& \alpha) (\dot{\theta}_1 + \dot{\theta}_2)^2 - M_2 g r \cos(\theta_1 + \theta_2 + \alpha) + M_2 h r \sin(\theta_1) \cos(\theta_1 + \theta_2 + \alpha) \ddot{\theta}_1 + \\
& M_2 h r \cos(\theta_1 + \theta_2 + \alpha) \cos(\theta_1) \dot{\theta}_1^2 - M_2 r^2 \cos(\theta_1 + \theta_2 + \alpha)^2 (\ddot{\theta}_1 + \ddot{\theta}_2) + M_2 r^2 \sin(\theta_1 + \\
& \theta_2 + \alpha) \cos(\theta_1 + \theta_2 + \alpha) (\dot{\theta}_1 + \dot{\theta}_2)^2 = I_2 (\ddot{\theta}_1 + \ddot{\theta}_2) \rightarrow,
\end{aligned}$$

$$\begin{aligned}
& T_2 - M_2 g r \cos(\theta_1 + \theta_2 + \alpha) - M_2 r \sin(\theta_1 + \theta_2 + \alpha) \ddot{x}_S - M_2 h r \sin(\theta_2 + \alpha) \ddot{\theta}_1 + \\
& M_2 h r \cos(\theta_2 + \alpha) \dot{\theta}_1^2 = (I_2 + M_2 r^2) (\ddot{\theta}_1 + \ddot{\theta}_2),
\end{aligned}$$

Double Inverted Pendulum Equation 2

III. Equations of Motion for the 3-Link Double Inverted Pendulum Model with a Moving Base

Since in Chapter 2 we use (θ_1, θ_2) as our states, here we will arrange Double Inverted Pendulum Equation 1 and Double Inverted Pendulum Equation 2 to have them in matrix format:

$$\begin{bmatrix} I_1 + M_1 l^2 + M_2 h^2 + M_2 r h \sin(\theta_2 + \alpha) & M_2 r h \sin(\theta_2 + \alpha) \\ I_2 + M_2 r^2 + M_2 h r \sin(\theta_2 + \alpha) & (I_2 + M_2 r^2) \end{bmatrix} \begin{Bmatrix} \ddot{\theta}_1 \\ \ddot{\theta}_2 \end{Bmatrix} =$$

$$\begin{bmatrix} 1 & -1 & -(M_1 l + M_2 h) \cos(\theta_1) \\ 0 & 1 & -M_2 r \sin(\theta_1 + \theta_2 + \alpha) \end{bmatrix} \begin{Bmatrix} T_1 \\ T_2 \\ \ddot{x}_S \end{Bmatrix} +$$

$$\begin{Bmatrix} (M_1 l + M_2 h) g \sin(\theta_1) - M_2 r h \cos(\theta_2 + \alpha) (\dot{\theta}_1 + \dot{\theta}_2)^2 \\ -M_2 g r \cos(\theta_1 + \theta_2 + \alpha) + M_2 h r \cos(\theta_2 + \alpha) \dot{\theta}_1^2 \end{Bmatrix}, \text{ where:}$$

$$[MM] = \begin{bmatrix} I_1 + M_1 l^2 + M_2 h^2 + M_2 r h \sin(\theta_2 + \alpha) & M_2 r h \sin(\theta_2 + \alpha) \\ I_2 + M_2 r^2 + M_2 h r \sin(\theta_2 + \alpha) & (I_2 + M_2 r^2) \end{bmatrix},$$

$$[BB] = \begin{bmatrix} 1 & -1 & -(M_1 l + M_2 h) \cos(\theta_1) \\ 0 & 1 & -M_2 r \sin(\theta_1 + \theta_2 + \alpha) \end{bmatrix},$$

$$\{CC\} = \begin{Bmatrix} (M_1 l + M_2 h) g \sin(\theta_1) - M_2 r h \cos(\theta_2 + \alpha) (\dot{\theta}_1 + \dot{\theta}_2)^2 \\ -M_2 g r \cos(\theta_1 + \theta_2 + \alpha) + M_2 h r \cos(\theta_2 + \alpha) \dot{\theta}_1^2 \end{Bmatrix},$$

$$[MM] \begin{Bmatrix} \ddot{\theta}_1 \\ \ddot{\theta}_2 \end{Bmatrix} = [BB] \begin{Bmatrix} T_1 \\ T_2 \\ \ddot{x}_S \end{Bmatrix} + \{CC\}$$

$$\begin{Bmatrix} \ddot{\theta}_1 \\ \ddot{\theta}_2 \end{Bmatrix} = [MM]^{-1} [BB] \begin{Bmatrix} T_1 \\ T_2 \\ \ddot{x}_S \end{Bmatrix} + [MM]^{-1} \{CC\}$$

Double Inverted Pendulum Equation 3

IV. Angular Acceleration of the COM Relative to the Stance Ankle:

Given (θ_1, θ_2) , we can calculate the tangent of the angle that COM makes with the vertical line (θ).

$$\tan(\theta) = f(\theta_1, \theta_2) \rightarrow \frac{d^2(\tan(\theta))}{dt^2} = \frac{d^2(f(\theta_1, \theta_2))}{dt^2}$$

$$LHS\ 1: \frac{d(\tan(\theta))}{dt} = (1 + \tan(\theta)^2)\dot{\theta} = (1 + f^2)\dot{\theta}$$

$$LHS\ 2: \frac{d\left((1 + \tan(\theta)^2)\dot{\theta}\right)}{dt} = (1 + f^2)\ddot{\theta} + 2f(1 + f^2)\dot{\theta}^2$$

$$RHS\ 1: \frac{d(f(\theta_1, \theta_2))}{dt} = \begin{bmatrix} \frac{\partial f}{\partial \theta_1} & \frac{\partial f}{\partial \theta_2} \end{bmatrix} \begin{Bmatrix} \dot{\theta}_1 \\ \dot{\theta}_2 \end{Bmatrix}$$

$$RHS\ 2: \frac{d\left(\begin{bmatrix} \frac{\partial f}{\partial \theta_1} & \frac{\partial f}{\partial \theta_2} \end{bmatrix} \begin{Bmatrix} \dot{\theta}_1 \\ \dot{\theta}_2 \end{Bmatrix}\right)}{dt}$$

$$= \begin{bmatrix} \frac{\partial f}{\partial \theta_1} & \frac{\partial f}{\partial \theta_2} \end{bmatrix} \begin{Bmatrix} \ddot{\theta}_1 \\ \ddot{\theta}_2 \end{Bmatrix} + \begin{Bmatrix} \dot{\theta}_1 & \dot{\theta}_2 \end{Bmatrix} \begin{bmatrix} \frac{\partial^2 f}{\partial \theta_1^2} & \frac{\partial^2 f}{\partial \theta_1 \partial \theta_2} \\ \frac{\partial^2 f}{\partial \theta_1 \partial \theta_2} & \frac{\partial^2 f}{\partial \theta_2^2} \end{bmatrix} \begin{Bmatrix} \dot{\theta}_1 \\ \dot{\theta}_2 \end{Bmatrix}$$

Now we put LHS and RHS together again:

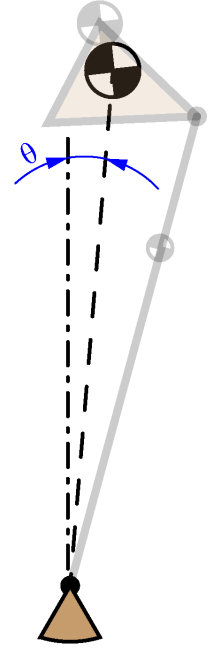
$$LHS\ 1 = RHS\ 1 \rightarrow (1 + f^2)\dot{\theta} = \begin{bmatrix} \frac{\partial f}{\partial \theta_1} & \frac{\partial f}{\partial \theta_2} \end{bmatrix} \begin{Bmatrix} \dot{\theta}_1 \\ \dot{\theta}_2 \end{Bmatrix} \rightarrow \dot{\theta} = \frac{1}{(1 + f^2)} \begin{bmatrix} \frac{\partial f}{\partial \theta_1} & \frac{\partial f}{\partial \theta_2} \end{bmatrix} \begin{Bmatrix} \dot{\theta}_1 \\ \dot{\theta}_2 \end{Bmatrix}$$

$$\rightarrow LHS\ 2: (1 + f^2)\ddot{\theta} + 2f(1 + f^2) \left(\frac{1}{(1 + f^2)} \begin{bmatrix} \frac{\partial f}{\partial \theta_1} & \frac{\partial f}{\partial \theta_2} \end{bmatrix} \begin{Bmatrix} \dot{\theta}_1 \\ \dot{\theta}_2 \end{Bmatrix} \right)^2$$

LHS 2 and RHS 2 are equal. Then:

$$(1 + f^2)\ddot{\theta} + \frac{2f}{(1 + f^2)} \left(\begin{bmatrix} \frac{\partial f}{\partial \theta_1} & \frac{\partial f}{\partial \theta_2} \end{bmatrix} \begin{Bmatrix} \dot{\theta}_1 \\ \dot{\theta}_2 \end{Bmatrix} \right)^2$$

$$= \begin{bmatrix} \frac{\partial f}{\partial \theta_1} & \frac{\partial f}{\partial \theta_2} \end{bmatrix} \begin{Bmatrix} \ddot{\theta}_1 \\ \ddot{\theta}_2 \end{Bmatrix} + \begin{Bmatrix} \dot{\theta}_1 & \dot{\theta}_2 \end{Bmatrix} \begin{bmatrix} \frac{\partial^2 f}{\partial \theta_1^2} & \frac{\partial^2 f}{\partial \theta_1 \partial \theta_2} \\ \frac{\partial^2 f}{\partial \theta_1 \partial \theta_2} & \frac{\partial^2 f}{\partial \theta_2^2} \end{bmatrix} \begin{Bmatrix} \dot{\theta}_1 \\ \dot{\theta}_2 \end{Bmatrix}$$



$$\ddot{\theta} = \frac{1}{(1+f^2)} \begin{bmatrix} \frac{\partial f}{\partial \theta_1} & \frac{\partial f}{\partial \theta_2} \end{bmatrix} \begin{Bmatrix} \ddot{\theta}_1 \\ \ddot{\theta}_2 \end{Bmatrix} + \frac{1}{(1+f^2)} \begin{pmatrix} \dot{\theta}_1 & \dot{\theta}_2 \end{pmatrix} \begin{bmatrix} \frac{\partial^2 f}{\partial \theta_1^2} & \frac{\partial^2 f}{\partial \theta_1 \partial \theta_2} \\ \frac{\partial^2 f}{\partial \theta_1 \partial \theta_2} & \frac{\partial^2 f}{\partial \theta_2^2} \end{bmatrix} \begin{Bmatrix} \dot{\theta}_1 \\ \dot{\theta}_2 \end{Bmatrix} \\ - \frac{2f}{(1+f^2)^3} \begin{pmatrix} \dot{\theta}_1 & \dot{\theta}_2 \end{pmatrix} \begin{bmatrix} \left(\frac{\partial f}{\partial \theta_1}\right)^2 & \frac{\partial f}{\partial \theta_1} \frac{\partial f}{\partial \theta_2} \\ \frac{\partial f}{\partial \theta_1} \frac{\partial f}{\partial \theta_2} & \left(\frac{\partial f}{\partial \theta_2}\right)^2 \end{bmatrix} \begin{Bmatrix} \dot{\theta}_1 \\ \dot{\theta}_2 \end{Bmatrix}$$

Equation 10

Now we need to calculate $f(\theta_1, \theta_2)$ from the kinematics of OLB:

$$(M_1 + M_2) \vec{r}_{COM} = m_1 \vec{r}_{M_1} + m_2 \vec{r}_{M_2}$$

$$(M_1 + M_2) (\vec{r}_S + \vec{r}_{S-COM}) \\ = M_1 (\vec{r}_S + l \hat{k}_1) + M_2 (\vec{r}_S + h \hat{k}_1 \\ + r \hat{k}_2)$$

$$(M_1 + M_2) \vec{r}_{S-COM} = (M_1 l + M_2 h) \hat{k}_1 + M_2 r \hat{k}_2$$

$$(M_1 + M_2) \vec{r}_{S-COM} \\ = (M_1 l + M_2 h) (\sin(\theta_1) \hat{i}_0 \\ + \cos(\theta_1) \hat{k}_0) \\ + M_2 r (-\cos(\theta_1 + \theta_2 + \alpha) \hat{i}_0 \\ + \sin(\theta_1 + \theta_2 + \alpha) \hat{k}_0)$$

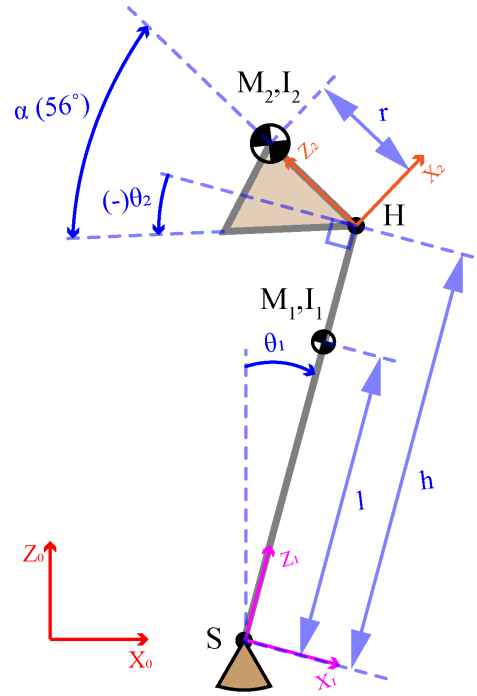
$$f(\theta_1, \theta_2) = \tan(\theta) = \frac{r_x}{r_z}$$

$$f(\theta_1, \theta_2) = \tan(\theta) = \frac{(M_1 l + M_2 h) \sin(\theta_1) - M_2 r \cos(\theta_1 + \theta_2 + \alpha)}{(M_1 l + M_2 h) \cos(\theta_1) + M_2 r \sin(\theta_1 + \theta_2 + \alpha)}$$

$$P = (M_1 l + M_2 h), Q = M_2 r, \text{ then}$$

$$f(\theta_1, \theta_2) = \tan(\theta) = \frac{P \sin(\theta_1) - Q \cos(\theta_1 + \theta_2 + \alpha)}{P \cos(\theta_1) + Q \sin(\theta_1 + \theta_2 + \alpha)}$$

$$1 + f^2 = \frac{P^2 + Q^2 + 2PQ \sin(\theta_2 + \alpha)}{(P \cos(\theta_1) + Q \sin(\theta_1 + \theta_2 + \alpha))^2}$$



Calculate the partial derivatives of $f(\theta_1, \theta_2)$:

$$\frac{\partial f}{\partial \theta_1} = \frac{[P \cos(\theta_1) + Q \sin(\theta_1 + \theta_2 + \alpha)]^2 + [P \sin(\theta_1) - Q \cos(\theta_1 + \theta_2 + \alpha)]^2}{[P \cos(\theta_1) + Q \sin(\theta_1 + \theta_2 + \alpha)]^2} = 1 + f^2$$

$$\frac{\partial^2 f}{\partial \theta_1^2} = 2f \frac{\partial f}{\partial \theta_1} = 2f (1 + f^2)$$

$$\frac{\partial f}{\partial \theta_2} = \frac{Q \sin(\theta_1 + \theta_2 + \alpha) \times [P \cos(\theta_1) + Q \sin(\theta_1 + \theta_2 + \alpha)] - Q \cos(\theta_1 + \theta_2 + \alpha) \times [P \sin(\theta_1) - Q \cos(\theta_1 + \theta_2 + \alpha)]}{[P \cos(\theta_1) + Q \sin(\theta_1 + \theta_2 + \alpha)]^2}$$

$$\frac{\partial f}{\partial \theta_2} = \frac{Q^2 + PQ \sin(\theta_2 + \alpha)}{[P \cos(\theta_1) + Q \sin(\theta_1 + \theta_2 + \alpha)]^2}$$

$$\frac{\partial^2 f}{\partial \theta_1 \partial \theta_2} = 2f \frac{\partial f}{\partial \theta_2}$$

$$\frac{\partial^2 y}{\partial \theta_2^2} = \frac{PQ \cos(\theta_2 + \alpha) [P \cos(\theta_1) + Q \sin(\theta_1 + \theta_2 + \alpha)]^2 - 2 [P \cos(\theta_1) + Q \sin(\theta_1 + \theta_2 + \alpha)] Q \cos(\theta_1 + \theta_2 + \alpha) [Q^2 + PQ \sin(\theta_2 + \alpha)]}{[P \cos(\theta_1) + Q \sin(\theta_1 + \theta_2 + \alpha)]^4}$$

$$\frac{\partial^2 f}{\partial \theta_2^2} = \frac{PQ \cos(\theta_2 + \alpha)}{[P \cos(\theta_1) + Q \sin(\theta_1 + \theta_2 + \alpha)]^2} - \frac{2 Q \cos(\theta_1 + \theta_2 + \alpha)}{[P \cos(\theta_1) + Q \sin(\theta_1 + \theta_2 + \alpha)]} \times \frac{\partial f}{\partial \theta_2}$$

If we are in a quasi-static OLB state, we can move the COM medially or laterally using any of our three control mechanisms, namely ankle torque, hip abduction moment, and HTS. To decide which direction to exert the control we have to combine Double Inverted Pendulum Equation 3 and Equation 10. First Equation 10:

$$\ddot{\theta} = \frac{1}{(1+f^2)} \begin{bmatrix} \frac{\partial f}{\partial \theta_1} & \frac{\partial f}{\partial \theta_2} \end{bmatrix} \begin{Bmatrix} \ddot{\theta}_1 \\ \ddot{\theta}_2 \end{Bmatrix} + \frac{1}{(1+f^2)} \left(\begin{Bmatrix} \dot{\theta}_1 & \dot{\theta}_2 \end{Bmatrix} \begin{bmatrix} \frac{\partial^2 f}{\partial \theta_1^2} & \frac{\partial^2 f}{\partial \theta_1 \partial \theta_2} \\ \frac{\partial^2 f}{\partial \theta_1 \partial \theta_2} & \frac{\partial^2 f}{\partial \theta_2^2} \end{bmatrix} \begin{Bmatrix} \dot{\theta}_1 \\ \dot{\theta}_2 \end{Bmatrix} \right) -$$

$$\frac{2f}{(1+f^2)^3} \left(\begin{Bmatrix} \dot{\theta}_1 & \dot{\theta}_2 \end{Bmatrix} \begin{bmatrix} \left(\frac{\partial f}{\partial \theta_1}\right)^2 & \frac{\partial f}{\partial \theta_1} \frac{\partial f}{\partial \theta_2} \\ \frac{\partial f}{\partial \theta_1} \frac{\partial f}{\partial \theta_2} & \left(\frac{\partial f}{\partial \theta_2}\right)^2 \end{bmatrix} \begin{Bmatrix} \dot{\theta}_1 \\ \dot{\theta}_2 \end{Bmatrix} \right) \rightarrow,$$

$$\ddot{\theta} = \frac{1}{(1+f^2)} \begin{bmatrix} \frac{\partial f}{\partial \theta_1} & \frac{\partial f}{\partial \theta_2} \end{bmatrix} \begin{Bmatrix} \ddot{\theta}_1 \\ \ddot{\theta}_2 \end{Bmatrix} + g(\theta_1, \theta_2, \dot{\theta}_1, \dot{\theta}_2, P, Q)$$

Now Double Inverted Pendulum Equation 3:

$$\begin{Bmatrix} \ddot{\theta}_1 \\ \ddot{\theta}_2 \end{Bmatrix} = [MM]^{-1} [BB] \begin{Bmatrix} T_1 \\ T_2 \\ \dot{x}_s \end{Bmatrix} + [MM]^{-1} \{CC\}$$

Then when combined we have:

$$\ddot{\theta} = \frac{1}{(1+f^2)} \begin{bmatrix} \frac{\partial f}{\partial \theta_1} & \frac{\partial f}{\partial \theta_2} \end{bmatrix} [MM]^{-1} [BB] \begin{Bmatrix} T_1 \\ T_2 \\ \dot{x}_s \end{Bmatrix} + \frac{1}{(1+f^2)} \begin{bmatrix} \frac{\partial f}{\partial \theta_1} & \frac{\partial f}{\partial \theta_2} \end{bmatrix} [MM]^{-1} \{CC\}$$

$$+ g(\theta_1, \theta_2, \dot{\theta}_1, \dot{\theta}_2, P, Q)$$

Equation 11- Angular Acceleration of the COM of a 3-Link Double Inverted Pendulum with Respect to the Stance Foot

$$[MM] = \begin{bmatrix} I_1 + M_1 l^2 + M_2 h^2 + M_2 r h \sin(\theta_2 + \alpha) & M_2 r h \sin(\theta_2 + \alpha) \\ I_2 + M_2 r^2 + M_2 h r \sin(\theta_2 + \alpha) & (I_2 + M_2 r^2) \end{bmatrix},$$

$$[BB] = \begin{bmatrix} 1 & -1 & -(M_1 l + M_2 h) \cos(\theta_1) \\ 0 & 1 & -M_2 r \sin(\theta_1 + \theta_2 + \alpha) \end{bmatrix},$$

$$\{CC\} = \begin{Bmatrix} (M_1 l + M_2 h) g \sin(\theta_1) - M_2 r h \cos(\theta_2 + \alpha) (\dot{\theta}_1 + \dot{\theta}_2)^2 \\ -M_2 g r \cos(\theta_1 + \theta_2 + \alpha) + M_2 h r \cos(\theta_2 + \alpha) \dot{\theta}_1^2 \end{Bmatrix},$$

V. Strategies for Creating Maximum COM Acceleration in the Medial and Lateral Directions during OLB:

Regardless of our initial state, our control over the dynamics of the OLB is limited to the first term in Equation 11. The other terms are all inertial terms related to the gravity and current velocities.

$$\ddot{\theta} = [GG][MM]^{-1}[BB] \begin{Bmatrix} T_1 \\ T_2 \\ \ddot{x}_S \end{Bmatrix} = [K_{Ankle} \quad K_{Hip} \quad K_{HTS}] \begin{Bmatrix} T_1 \\ T_2 \\ \ddot{x}_S \end{Bmatrix}, \text{ where}$$

$$P = (M_1 l + M_2 h) \text{ and } Q = (M_2 r)$$

$$f(\theta_1, \theta_2) = \tan(\theta) = \frac{P \sin(\theta_1) - Q \cos(\theta_1 + \theta_2 + \alpha)}{P \cos(\theta_1) + Q \sin(\theta_1 + \theta_2 + \alpha)}$$

$$[GG] = \frac{1}{(1+f^2)} \begin{bmatrix} \frac{\partial f}{\partial \theta_1} & \frac{\partial f}{\partial \theta_2} \end{bmatrix} = \frac{1}{(1+f^2)} \left[(1+f^2) \left(\frac{Q^2 + PQ \sin(\theta_2 + \alpha)}{[P \cos(\theta_1) + Q \sin(\theta_1 + \theta_2 + \alpha)]^2} \right) \right] \rightarrow$$

$$[GG] = \left[1 \quad \left(\frac{Q^2 + PQ \sin(\theta_2 + \alpha)}{P^2 + Q^2 + 2PQ \sin(\theta_2 + \alpha)} \right) \right]$$

$$[MM] = \begin{bmatrix} I_1 + M_1 l^2 + M_2 h^2 + M_2 r h \sin(\theta_2 + \alpha) & M_2 r h \sin(\theta_2 + \alpha) \\ I_2 + M_2 r^2 + M_2 h r \sin(\theta_2 + \alpha) & I_2 + M_2 r^2 \end{bmatrix},$$

$$[BB] = \begin{bmatrix} 1 & -1 & -(M_1 l + M_2 h) \cos(\theta_1) \\ 0 & 1 & -M_2 r \sin(\theta_1 + \theta_2 + \alpha) \end{bmatrix} = \begin{bmatrix} 1 & -1 & -P \cos(\theta_1) \\ 0 & 1 & -Q \sin(\theta_1 + \theta_2 + \alpha) \end{bmatrix}$$

We calculated $[K_{Ankle} \quad K_{Hip} \quad K_{HTS}]$ for all the states within the range of motion. The signs never change. Here is a summary:

$$\begin{aligned} & [K_{Ankle} \pm (SD) \quad K_{Hip} \pm (SD) \quad K_{HTS} \pm (SD)] \\ & = [0.015 \pm (2e - 4) \quad -0.0147 \pm (6e - 4) \quad -0.99 \pm (0.024)] \end{aligned}$$

So at any state of OLB, to move the COM laterally ($\ddot{\theta} > 0$), we should increase ankle torque (take the COP towards the medial margin of BOS), decrease hip abduction moment (drop the pelvis), and shuffle the stance foot medially. Reversely, if we want to move the COM medially ($\ddot{\theta} < 0$) e.g. to avoid a lateral fall on the hip, we should decrease the ankle torque (take the COP toward the lateral margin of BOS), increase hip abduction moment (raise the pelvis), and shuffle the stance foot laterally.

Having the same strategy for moving the COM medially and laterally does not imply that we will be successful in doing so. The magnitude of the initial momentum of the body and the gravitational pull have to be considered. Since in this dissertation, we are mostly concerned with quasi-static OLB, we can assume ($\dot{\theta}_1 \approx \dot{\theta}_0 \approx 0$). This will simplify Equation 11 to just have the effect of the gravitational forces.

$$\ddot{\theta} = [GG][MM]^{-1}[BB] \begin{Bmatrix} T_1 \\ T_2 \\ \ddot{x}_S \end{Bmatrix} + [GG][MM]^{-1}\{CC\}, \text{ where:}$$

$$\{CC\} = \begin{Bmatrix} (M_1l + M_2h)g \sin(\theta_1) \\ -M_2gr \cos(\theta_1 + \theta_2 + \alpha) \end{Bmatrix} = \begin{Bmatrix} Pg \sin(\theta_1) \\ -Qg \cos(\theta_1 + \theta_2 + \alpha) \end{Bmatrix}$$

Since there are no data available in the literature for the achievable accelerations of the stance foot using the HTS method, and also the periodic and discontinuous nature of the HTS strategy, we will assume ($\ddot{x}_S \approx 0$) in Chapter 2. We will revisit this assumption when we are considering the results of our HTS experiment with subjects in Chapter 4.

Appendix II

Simulation of the Planar Movements of a Double Inverted Pendulum Model with Range of Motion Constraints

Equations of motion for the double inverted pendulum model were derived in Appendix I. To simulate the movements of the model, we can set up our equations in the following manner:

$$X = (\theta_1, \dot{\theta}_1, \theta_2, \dot{\theta}_2)' \rightarrow \dot{X} = (\dot{\theta}_1, \ddot{\theta}_1, \dot{\theta}_2, \ddot{\theta}_2)',$$

Where we replace the values for $(\ddot{\theta}_1, \ddot{\theta}_2)$ from Double Inverted Pendulum Equation 3.

Numerically solving the above non-linear differential equation using MATLAB © is common in many fields. So we will not include it here. However, there are certain assumptions that needs further explanations. In the following sections the important assumptions that were used in solving the above differential equation in MALAB are discussed.

I. Enforcing the ROM Constraint for the Stance Hip and Ankle ROM

Enforcing the end of ROM for the stance hip is very important for the results of Sections 2.4.2 and 2.4.3 where we consider how using the hip strategy can expand the boundaries of the FBR to be able to recover from more quasi-static initial states. The large hip abduction / adduction moments can rapidly change the angular momentum of the upper body and therefore affect the angular acceleration of the COM relative to the BOS. However, this also means that using the hip strategy will cause the person to reach the end of ROM of the stance hip quickly. At the end of ROM, the ligaments surrounding the hip will exert a reverse moment in order to stop the joint from reaching the end of ROM with a high velocity, and therefore damaging the joint.

To enforce the end of ROM, we split the hip moment to two parts: T_{Active} and $T_{Passive}$. The first one is the muscle-equivalent hip abduction/adduction moment. Since in our simulations, we were looking for the maximum effect from the ‘Hip Strategy’, the T_{Active} value was set at the maximum hip abduction or adduction strength depending on whether we were trying to use the ‘Hip Strategy’ to create a maximum medial or lateral acceleration of the COM respectively. We also included the force-length characteristics of the muscular isometric hip abduction/adduction

the same way we discussed in A3 in 2.2.1.1. On the other hand, $T_{Passive}$ is supposed to stop the hip abduction angle from reaching its end of ROM with a high velocity. So we defined its value by the relation ($T_{Passive} = -b(\theta_2) \times \dot{\theta}_2$), where b acts as a damping coefficient for the angular velocity of the stance hip ($\dot{\theta}_2$). We set b to be close to zero in the middle of the ROM and increase exponentially near the two ends of ROM. We use a combination of error function to create the function for b as seen in Figure 44.

Ankle ROM

If we consider the foot to be glued to the ground, then θ_1 is the ankle eversion angle. We used the end of ankle ROM as the termination criterion for the integration algorithm. This was based on the simple notion that given the narrow range of θ_1 values seen in the FBR, should θ_1 reach such high deviations, the balance should already passed recovery by any strategy.

II. Criterion for Considering an Initial Quasistatic OLB State as Recoverable

Starting from each quasistatic state within the hip and ankle ROM, we ran the simulations twice: once with maximum ankle inversion and maximum hip abduction

moments to induce the maximum medial acceleration of the COM. On the second run, we reversed the ankle and hip moment signs to create the maximum lateral acceleration of COM. In terms of our criterion for recoverability of an initial OLB state, we considered if a person could make himself/herself fall both laterally and medially from an initial state, then there should have been a control strategy in the middle which could have brought the COM over the ankle. In terms of our simulations results, this translates to the sign of θ (the angle of the line connecting the stance ankle to the COM of the whole body) being different between the two different simulation runs.

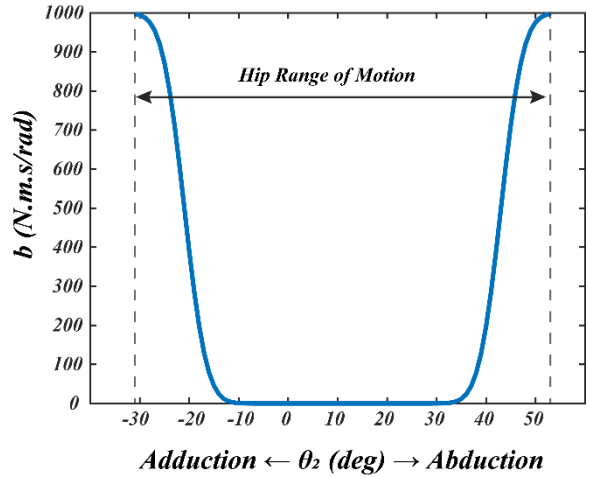


Figure 44- Coefficient of Damping ($b(\theta_2)$) considered for calculating $T_{Passive} = -b(\theta_2) \times \dot{\theta}_2$, which enforced the end of hip ROM. Our choice of 1000 for the maximum b and 20 degrees for the start of the rise of b value was arbitrary. However, we checked for the sensitivity of the recoverable OLB states to these choices (1000 vs 500, and 20 degrees vs 10 degrees) and did not observe a noticeable change in results.

Appendix III

Quantifying the Sensitivity of the Calculated Mean Intensity of the Hip Abduction Moment Demand to Potential Biases in the Calculations

I. Assumptions

Three assumptions were made for this analysis:

Quasistatic hip abduction moment can be used to estimate the mean hip abduction moment demand during OLB

Figure 45 shows the mean hip abduction moment demand estimated from the full dynamics equations of motion for the subject specific 3-link double inverted pendulum model parameters and recorded states during the OLB trial vs. the static estimate of hip abduction moment calculated from mean value for the parameters of the same model and mean value of the states. We can see that the two parameters are close to a one-to-one match ($R^2 = 99\%$, $\text{slop} = 1.01$). In other words, the subjects' OLB states were not dynamic enough to render a quasistatic estimate of the hip abduction moment demand incorrect. So in the remainder of this section, we will use the parameters in the quasistatic formula for the hip abduction moment to analyze the sensitivity of our estimates for the intensity of the hip abduction moment to different sources of error.

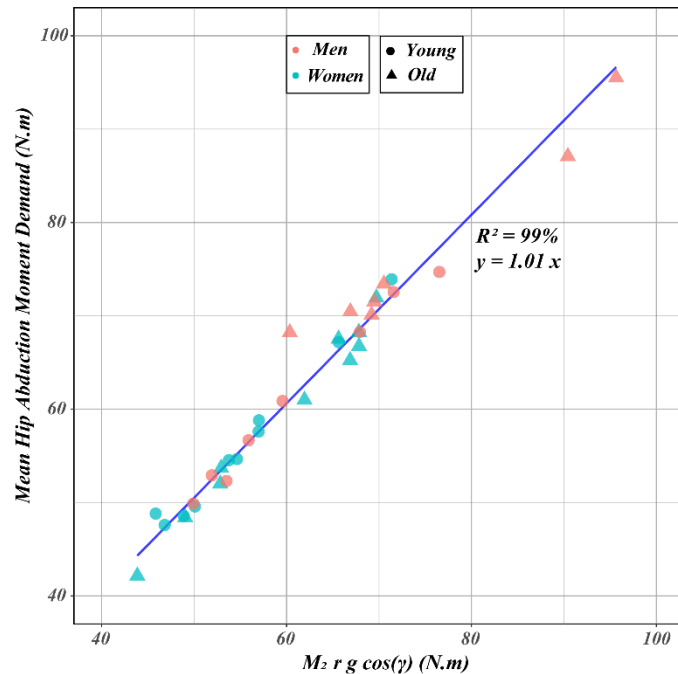


Figure 45- Mean hip abduction moment demand (estimated from inverse dynamic calculations) vs. quasistatic estimate of the hip abduction moment (calculated from mean value of r , $\cos(\gamma)$, and M_2). We can see that both estimates are in close agreement with each other ($R^2 = 99\%$). Please see 3.2.3.1 for definitions of the parameters and 2.2.1 for the calculations that show why $M_2.r.\cos(\gamma)$ is the quasistatic hip abduction moment).

Young subjects only

Since more data in the literature for younger subjects, we will use only the data from our young subjects as well. This allows us to make a comparison between our measurements and those of the literature to find any biases that could affect our calculation of the intensity of the hip abduction moment demand during OLB.

II. Applying biases in the direction that would reduce the estimated mean intensity of hip abduction moment demand

Here, we are quantifying the effect of biases in our measurement to examine if our estimations of the intensity are exaggerated.

Methods

The formula for calculating the intensity of hip abduction moment demand during OLB (%MVS) can be seen below:

$$\begin{aligned} \% MVS &= \frac{M_2 \times g \times r \cos \gamma}{\text{Max Voluntary Hip Abduction Strength}} = \frac{\frac{M_2}{\text{Body Mass}} \times r \cos \gamma}{\frac{MVS}{\text{Body Mass} \times g}} \\ &= \frac{m_2 \times r \cos \gamma}{MVS_{\text{normalized by weight}}} \end{aligned}$$

Equation 12- Equation for quasistatic estimation of the intensity of the hip abduction moment demand during OLB. M_2 is the mass of the body without the stance leg, r is the distance between the stance hip and the center of mass of M_2 , and γ is the horizontal inclination angle of the line connecting the stance hip to the center of mass of M_2 .

We can separate sources of bias in the calculation of intensity into three categories: m_2 , moment arm of M_2 , and hip abduction strength. Overestimating first two parameters and underestimating the hip abduction strength can lead to an exaggerated estimation of the intensity.

m₂ (percent body weight of the mass being balanced over the stance hip)

Table 15- Comparison of our estimate of *m₂* (percent body weight of the mass balancing over the stance leg) in young men (YM) and young women (YW) with the literature.

<i>First Author</i>	<i>m₂ (% Body Weight)</i>	
	<i>YM</i>	<i>YW</i>
<i>Winter, D. A. [65]</i>	83.9	83.9
<i>Dumas R. [96]</i>	81.7	79.9
<i>Kingma I. [97]</i>	78	78
<i>De Leva P. [98]</i>	80.1	79.1
<i>Norton J. [99]</i>	81.5	80.4
<i>This Study</i>	82.4	81.1

We reviewed our method for estimating the mass distribution for each subject in 3.2.2.4. For our young subjects the mean value for *m₂* was not significantly different between men and women ($p = 0.19$) and equal to 81.7% ([80.7, 82.7 %], 95% Mean Confidence Interval). Table 15 shows our estimates for *m₂* along with well cited publications in the literature. The largest difference between the mean values for *m₂* compared to our study was the *Kingma I.* with 3.7% difference. This will be the bias that we will use in our calculations ($\partial m_2 = -3.7\%$).

Moment Arm of M₂ (r cos(γ))

We could not find reported values in the literature for the moment arm of *M₂* during. Estimating it from the anthropometry data also require making extra assumptions. For example the pelvis inclination angle affects γ , and the amount of the lateral bending of the trunk affect both *r* and γ . In 3.3.4 we showed that for our subjects, the pelvis inclination angle and lateral bending of the trunk did not change significantly during their OLB trial. So using an averaged value for each person was the logical choice. However, we also showed that the starting value for each of these variables was slightly different between groups and therefore different subjects. To quantify the potential bias in the calculations of the moment arm of *M₂* then, we separate the sources of error in our estimations into two separate groups:

1) *Locating the hip joint centers (SCORE_{RMSE})*: Unless there are x-rays of each subject’s pelvis [24, 25], the location of the hip joint centers cannot be located without inherent error. We estimated the RMSE for our functional method during the OLB trial to be between 2 to 20 mm with a mean value of 10 mm (3.2.2.3). This is the spatial error for the left hip joint center. To be

conservative we will assume all 10 mm mean RMSE to be in the lateral direction which would increase the moment arm by the same amount.

2) *Locating the center of mass of M_2 (COG_{RMSE}):* We do not have a direct measurement of the error that we could have in locating the COM of the M_2 . This is because we do not have the real location of the COM for each person. For the whole body, we resorted to using an optimization algorithm that minimized the COG location calculated from the force data from the force plates with those calculated from the 3-link double inverted pendulum model. For the OLB trial, the RMSE between the two methods for all subjects ranged from 1.5 mm to 14 mm with a mean value of 5 mm. It will be a conservative estimate to use the RMSE and assume all of it is due to a bias of the location of M_2 in the medial direction.

The two error sources above are not independent of each other. However, here we will treat them as independent and also assume both of them are in the direction that increases our estimate of the moment arm. This means we assume the stance hip was calculated to be more lateral than it actually is and the location of the M_2 was closer to the stance hip in reality. Our assumption of independence also implies that we can just add the two assumed sources of bias to estimate a potential bias in the moment arm which would be: $\partial(r \cos \gamma) = SCORE_{RMSE} + COG_{RMSE} = -0.010 - 0.005 = -0.015 m$

Hip Abduction Strength Measurement

Table 16- Comparison of the hip abduction strength measured in this study versus published data. If the reported strengths were not normalized by weight, we used the reported mean height and weight in each paper to change it to the normalized by weight format.

<i>First Author</i>	<i>Hip Abduction Strength (N.m/N)</i>	
	<i>YM</i>	<i>YW</i>
<i>Crossley K.M. [100]</i>	0.167	0.167
<i>Johnston R.C. [57]</i>	0.122	-
<i>Cahalan T.D. [38]</i>	0.150	0.125
<i>Johnson M.E. [101]</i>	-	0.137
<i>Measured Strength in this Study</i>	0.157	0.131
<i>Adjusted Strength in this Study</i>	0.157	0.152

Table 16 shows a comparison of the measurements of the hip abduction strength in this study vs. published literature data. We can see that only one source in the reviewed literature reports higher hip abduction strengths. Then: $\partial(MVS) = 0.015 N.m/m$

III. Anticipated Effect of Bias in Parameter Estimations on the Calculated Intensity of Hip Abduction Moment Demand during OLB

Table 17 shows the calculated effect of possible biases in estimation of m_2 , $r \cos(\gamma)$, and maximum voluntary hip abduction strength on the calculated intensity of the hip abduction moment demand. *We can see that even if we assume all sources of error in the calculation of the intensity act as biases in the direction to increase the estimated intensity of the hip abduction moment demand, still the adjusted value for the calculated intensity is a substantial value (38% and 45% in younger men and women respectively).* It should also be noted that the small discrepancy between the reported intensity between Table 11 and Table 17 is due to the first assumption in this section.

Table 17- Calculated effect of possible biases in estimation of m_2 , $r \cos(\gamma)$, and maximum voluntary hip abduction strength on the calculated intensity of the hip abduction moment demand. m_2 is the percent body weight of the mass being balance over the stance leg, $r \cos(\gamma)$ is the moment arm of m_2 . We can see that biases in the calculation of the moment arm can create the biggest change in the calculated intensity. The highlighted cells are the unlikely event that all three possible sources of bias act in the wrong direction at the same time.

		Mean	Possible Bias	Adjusted Intensity (%MVS)
m_2 (%)	Men	82.4	-3.7	49.6
	Women	81.1		56.5
$r \cos(\gamma)$ (m)	Men	0.099	-0.015	44.1
	Women	0.111		51.2
MVS (N.m/m)	Men	0.157	0.015	47.4
	Women	0.152		53.9
Intensity (%MVS)	Men	52	13.5	38.4
	Women	59	14.7	44.5

Appendix IV

Deriving the Equations of Motion for a Single Inverted Pendulum with a Moving Base

I. Kinematics

$$\vec{r}_M = \vec{r}_S + L \begin{Bmatrix} \sin \theta \\ \cos \theta \end{Bmatrix},$$

$$\vec{v}_M = \vec{v}_S + L\dot{\theta} \begin{Bmatrix} \cos \theta \\ -\sin \theta \end{Bmatrix},$$

$$\begin{aligned} \vec{a}_M &= \vec{a}_S - L\dot{\theta}^2 \begin{Bmatrix} \sin \theta \\ \cos \theta \end{Bmatrix} + L\ddot{\theta} \begin{Bmatrix} \cos \theta \\ -\sin \theta \end{Bmatrix} \\ &\approx \ddot{x}_S - L\dot{\theta}^2 \begin{Bmatrix} \sin \theta \\ \cos \theta \end{Bmatrix} + L\ddot{\theta} \begin{Bmatrix} \cos \theta \\ -\sin \theta \end{Bmatrix} \end{aligned}$$

II. Dynamics

$$\sum F_x = Ma_{Mx} \rightarrow F_x = M\ddot{x}_S - ML\dot{\theta}^2 \sin \theta + ML\ddot{\theta} \cos \theta,$$

$$\sum F_z = Ma_{Mz} \rightarrow F_z = Mg - ML\dot{\theta}^2 \cos \theta - ML\ddot{\theta} \sin \theta,$$

$$\sum T_{COM} = I\ddot{\theta} \rightarrow T_1 + F_z L \sin \theta - F_x L \cos \theta = I\ddot{\theta},$$

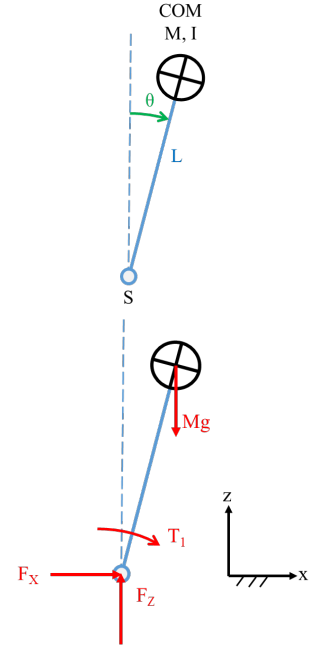
$$T_1 + (Mg - ML\dot{\theta}^2 \cos \theta - ML\ddot{\theta} \sin \theta)L \sin \theta - (M\ddot{x}_S - ML\dot{\theta}^2 \sin \theta + ML\ddot{\theta} \cos \theta)L \cos \theta = I\ddot{\theta},$$

$$\rightarrow T_1 + MgL \sin \theta - ML \cos \theta \ddot{x}_S = (I + ML^2)\ddot{\theta}$$

$$\rightarrow \ddot{\theta} = \frac{MgL}{I+ML^2} \sin \theta + \frac{T_1}{I+ML^2} - \frac{ML}{I+ML^2} \cos \theta \ddot{x}_S$$

Since all our analyses starts with a quasistatic OLB, then θ is small and we can simplify the above equation further:

$$\ddot{\theta} \approx \frac{MgL}{I + ML^2} \theta + \frac{T_1}{I + ML^2} - \frac{ML}{I + ML^2} \ddot{x}_S$$



Appendix V
Diagnostic Plots for the Linear Mixed-Effect Model Fitted to Primary Outcome Capacity of the HTS Experiment (DTH)

In the three following plots, you can see the diagnostic plots for the LMM fitted to the DTH measurements during the lateral and medial HTS experiments. We could not see a clear trend in the diagnostic plots to clearly violate the assumptions of the fitted mixed-effect model. So believe the model is a good enough model for drawing the conclusions in 4.3.2.

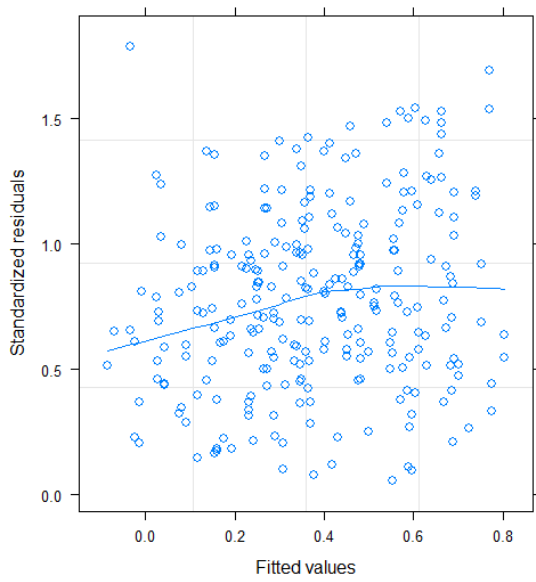


Figure 46- Absolute value of the normalized residuals vs. the fitted values for the LMM fitted to DTH measurements in 4.3.2.

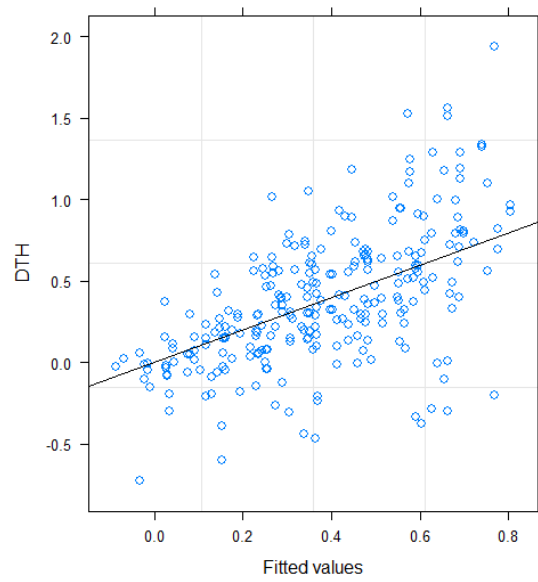


Figure 47- Experimentally measured DTH vs. the fitted values from the LMM in 4.3.2.

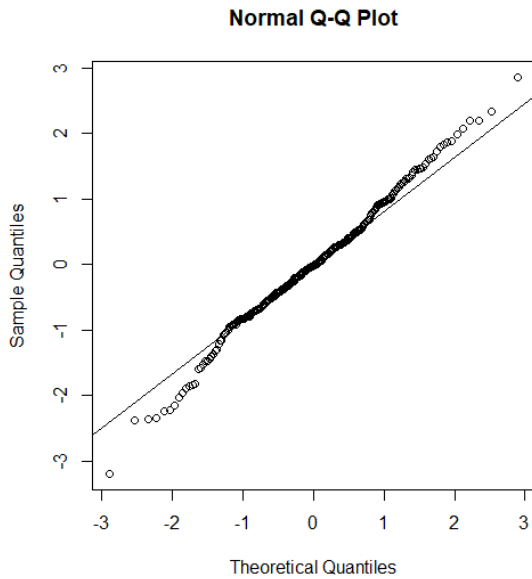


Figure 48- QQ-plot for checking the normality of the normalized residuals of the fitted LMM to DTH measurements in 4.3.2.

Appendix VI

Details of the Linear Mixed-Effect Model Fitted to the Combined Outcome Measures of the Lateral HTS Experiment

To statistically compare DTA and DTH during the lateral trials in 4.3.4, we combined them into one variable (*DT*) with a factor indicator variable (*Strategy*). We also made a new variable for the interaction of Age Group and Step Type factors and called it *InterGroups*. This allowed us to set up the contrasts for the comparison of DTA and DTH across each of the four groups. Given the boxplots in Figure 41, we assigned two random intercepts for each Subject: one for the DTA measurements and another for the DTH in a positive definite symmetric variance covariance matrix format. It also seemed obvious that the residuals of the DTA measurements would be different than the DTH measurements. So we allowed for different residual variations per group of measurements using the `varIdent` function in the `nlme` package in R. Finally, the structure of the fixed effects were defined using the formula below:

$$DT \sim -1 + InterGroup + InterGroups: Strategy$$

Using Likelihood Ratio test, we tested the null hypothesis that one random effects to just one random intercept per subject was sufficient for characterizing the random effects. The null hypothesis was rejected (LR = 10.4, $p = 0.005$). We then tested the null hypothesis that one group residual variation was enough for the model. This null hypothesis was also rejected (LR = 441, $p < 0.001$).

After fitting the LMM to the lateral HTS trials, the estimated standard deviation of the residuals in the DTH group was 0.36 rad/s ([0.312, 0.415] 95% confidence interval). This value for the DTA group was 0.069 of the DTH group ([0.056, 0.084] 95% confidence interval). So our original hypothesis that the variations in the DTH measurements are higher than the DTA was confirmed.

I. Diagnostic Plots

In the three following plots, you can see the diagnostic plots for the LMM fitted to the DT measurements. We could not see a clear trend in the diagnostic plots to clearly violate the

assumptions of the fitted mixed-effect model. So believe the model is a good enough model for drawing the conclusions in 4.3.4.

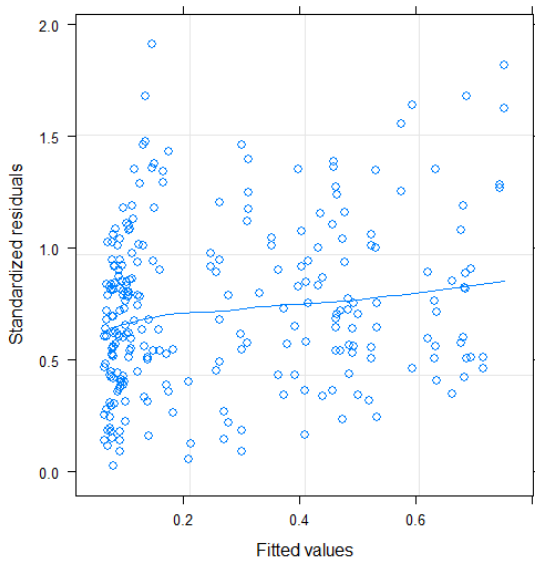


Figure 49- Absolute value of the normalized residuals vs. the fitted values for the fitted LMM to DT measurements in 4.3.4.

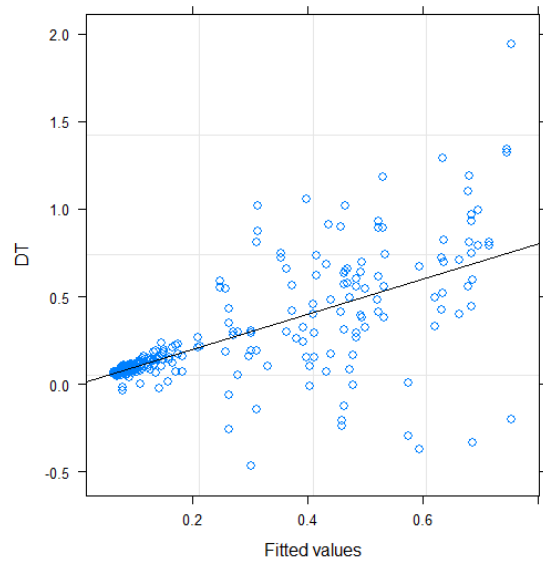


Figure 50- Experimentally measured DT values vs. the fitted values for LMM in 4.3.4.

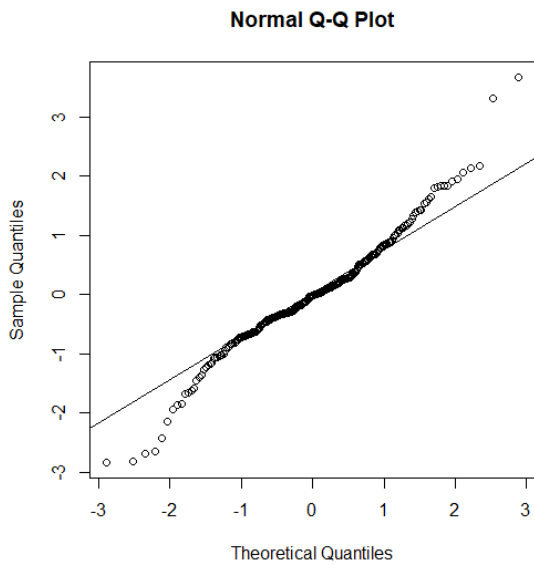


Figure 51- QQ-plot for checking the normality of the normalized residuals of the fitted LMM to DT measurements in 4.3.4.

Appendix VII Telephone Screening Form for Subject Recruitment

The Subject must answer “**yes**” to the following **general** screening questions in order to be considered a potential subject.

1. Are you either between 21 and 30 or 65 to 80 years of age? (Circle one)
2. Can you stand on One Leg for more than 10 seconds?(Y/N)
3. May I ask your Weight _____ lbs and Height _____ ft/in and calculate BMI _____ kg/m² (Y/N)
4. Are you able to stand or walk without a cane or walker for more than 30 minutes? (Y/N)
5. Do you exercise at least twice a week? (Y/N)
6. Are you free of any chronic diseases? (Y/N)
7. Can you communicate in simple English? (Y/N)
8. Are you willing to participate in a series of tests in a lab on North Campus that could take up to 3 hours if we provide a parking pass for you? (Y/N)

The subject must answer “**no**” to the following **general** screening questions in order to be considered a potential subject.

1. Do you take any medication other than aspirin or Tylenol? (Y/N)
2. Have you fallen or gotten injured in the last month? (Y/N)
3. Do you have a history of stroke or spinal surgery? (Y/N)
4. Do you have a history of muscle disease? (Y/N)
5. Do you have a history of amputation or foot deformity (Charcot foot)? (Y/N)
6. Have you had knee or hip replacement within the last 12 months? (Y/N)

7. Does your vision prevent you from walking safely? (Y/N)

Have you had a sore anywhere on your feet in the last 12 months? (Y/N)

REFERENCES

1. Centers for Disease Control and Prevention, National Center for Injury Prevention and Control. Web-based Injury Statistics Query and Reporting System (WISQARS) [Jan 15th 2018]. <https://www.cdc.gov/injury/wisqars/>. Accessed 15 Jan 2018
2. Tinetti ME, Williams CS (1998) The Effect of Falls and Fall Injuries on Functioning in Community-Dwelling Older Persons. *Journals Gerontol Ser A Biol Sci Med Sci* 53A:M112–M119
3. Tennstedt S, Howland J, Lachman M, Peterson E, Kasten L, Jette A (1998) A Randomized, Controlled Trial of a Group Intervention to Reduce Fear of Falling and Associated Activity Restriction in Older Adults. *Journals Gerontol Ser B Psychol Sci Soc Sci* 53B:P384–P392
4. Scheffer AC, Schuurmans MJ, Van Dijk N, Van der Hooft T, De Rooij SE (2018) Fear of falling : measurement strategy , prevalence , risk factors and consequences among older persons. 19–24
5. Deandrea S, Lucenteforte E, Bravi F, Foschi R, La Vecchia C, Negri E (2010) Risk factors for falls in community-dwelling older people: A systematic review and meta-analysis. *Epidemiology* 21:658–668
6. Ambrose AF, Paul G, Hausdorff JM (2013) Risk factors for falls among older adults: A review of the literature. *Maturitas* 75:51–61
7. Berg K, Wood-Dauphinee S, Williams JI, Gayton D (1989) Measuring balance in the elderly: Preliminary development of an instrument. *Physiother Canada* 41:304–311
8. Vellas BJ, Wayne SJ, Romero L, Baumgartner RN, Rubenstein LZ, Garry PJ (1997) One-leg balance is an important predictor of injurious falls in older persons. *J Am Geriatr Soc* 45:735–738
9. Winter DA (1995) Human balance and posture control during standing and walking. *Gait Posture* 3:193–214
10. Fujimoto M, Bair WN, Rogers MW (2015) Center of pressure control for balance

- maintenance during lateral waist-pull perturbations in older adults. *J Biomech* 48:963–968
11. Runge CF, Shupert CL, Horak FB, Zajac FE (1999) Ankle and hip postural strategies defined by joint torques. *Gait Posture* 10:161–170
 12. Henry SM, Fung J, Horak FB (2001) Effect of Stance Width on Multidirectional Postural Responses Effect of Stance Width on Multidirectional Postural Responses. *J Neurophysiol* 85:559–570
 13. Wing AM, Clapp S, Burgess-Limerick R (1995) Standing stability in the frontal plane determined by lateral forces applied to the hip. *Gait Posture* 3:38–42
 14. Hof AL (2007) The equations of motion for a standing human reveal three mechanisms for balance. *J Biomech* 40:451–457
 15. Frey-Law LA, Avin KG (2010) Endurance time is joint-specific: A modelling and meta-analysis investigation. *Ergonomics* 53:109–129
 16. Frey-Law LA, Looft JMJ, Heitsman J (2012) A three-compartment muscle fatigue model accurately predicts joint-specific maximum endurance times for sustained isometric tasks. *J Biomech* 45:1803–1808
 17. Avin KG, Tumuluri A, Looft JM, Frey-Law LA (2015) Strength Loss Counteracts Age-related Improvements in Muscle Fatigue Properties when Considering Functional Task Endurance A Modeling Study. *J Gerontol Geriatr Res.* doi: 10.4172/2167-7182.1000218
 18. Dorfman LJ, Bosley TM (1979) Age-related changes in peripheral and central nerve conductaon man. *Neurology* 29:38–44
 19. Norris AH, Shock NW, Wagman IH (1953) Age Changes in the Maximum Conduction Velocity of Motor Fibers of Human Ulnar Nerves. *J Appl Physiol* 5:589–593
 20. Allet L, Kim H, Ashton-Miller JA, De Mott T, Richardson JK (2012) Frontal plane hip and ankle sensorimotor function, not age, predicts unipedal stance time. *Muscle Nerve* 45:578–585
 21. Richardson JK, DeMott TK, Allet L, Kim H, Ashton-Miller JA (2014) Hip strength: Ankle proprioceptive threshold ratio predicts falls and injury in diabetic neuropathy. *Muscle Nerve* 1–6
 22. Morioka S, Fukumoto T, Hiyamizu M, Matsuo A, Takebayashi H, Miyamoto K (2012) Changes in the equilibrium of standing on one leg at various life stages. *Curr Gerontol Geriatr Res.* doi: 10.1155/2012/516283

23. Rubenstein LZ, Josephson KR (2006) Falls and Their Prevention in Elderly People: What Does the Evidence Show? *Med Clin North Am* 90:807–824
24. Inman VT (1947) Functional aspects of the abductor muscles of the hip. *J bone Jt Surg* 29:607–619
25. McLeish RD, Charnley J (1970) Abduction forces in the one-legged stance. *J Biomech.* doi: 10.1016/0021-9290(70)90006-0
26. Prior S, Mitchell T, Whiteley R, O’Sullivan P, Williams BK, Racinais S, Farooq A (2014) The influence of changes in static single leg standing posture on hip and thigh muscle activation in a pain free population. *BMC Sport. Sci. Med. Rehabil.*
27. Son J (2006) Unipedal Balance: Biomechanical Analyses of the Effects of Age and Disease. Thesis Univ. Michigan
28. Hoogvliet P, Van Duyl WA, De Bakker J V., Mulder PGH, Stam HJ (1997) A model for the relation between the displacement of the ankle and the center of pressure in the frontal plane, during one-leg stance. *Gait Posture* 6:39–49
29. Tropp H, Odenrick P (1988) Postural control in single-limb stance. *J Orthop Res* 6:833–839
30. Horak FB, Nashner LM (1986) Central programming of postural movements: adaptation to altered support-surface configurations. *J Neurophysiol* 55:1369–1381
31. King MB, Judge JO, Wolfson L (1994) Functional base of support decreases with age. *Journals Gerontol* 49:258–263
32. King DL, Zatsiorsky VM (2002) Periods of extreme ankle displacement during one-legged standing. *Gait Posture* 15:172–179
33. Otten E (1999) Balancing on a narrow ridge: biomechanics and control. *Philos Trans R Soc Lond B Biol Sci* 354:869–75
34. Rubenstein LZ (2006) Falls in older people: Epidemiology, risk factors and strategies for prevention. *Age Ageing* 35:37–41
35. Ashton-Miller JA, Wojtys EM, Huston LJ, Fry-Welch D (2001) Can proprioception really be improved by exercises? *Knee Surgery, Sport Traumatol Arthrosc* 9:128–136
36. Rohmert W, Wangenheim M, Mainzer J, Zipp P, Lesser W (1986) A study stressing the need for a static postural force model for work analysis. *Ergonomics* 29:1235–1249
37. Burke RE, Levine DN, Tsauris P, Zajac FE (1973) Physiological Types and

- Histochemical Profiles in Motor Units of the Cat Gastrocnemius. *J Physiol* 723–748
38. Cahalan TD, Johnson ME, Liu S, Chao EY (1989) Quantitative measurements of hip strength in different age groups. *Clin Orthop Relat Res* 136–145
 39. Ottaviani RA, Ashton-Miller JA, Wojtys EM (2001) Inversion and eversion strengths in the weightbearing ankle of young women. Effects of plantar flexion and basketball shoe height. *Am J Sports Med* 29:219–225
 40. Project YS (Ohio). AR, Army US, Force USA, Navy US, Committee T-SARPT-S (1988) Anthropometry and Mass Distribution for Human Analogues: Military Male Aviators. Anthropology Research Project
 41. Neumann DA, Soderberg GL, Cook TM (1988) Comparison of maximal isometric hip abductor muscle torques between hip sides. *Phys Ther* 68:496–502
 42. Hardcastle P, Nade S (1985) The significance of the Trendelenburg test. *J Bone Joint Surg Br* 67:741–746
 43. Milton JG, Cabrera JL, Ohira T, Tajima S, Tonosaki Y (2009) The time-delayed inverted pendulum : Implications for human balance control The time-delayed inverted pendulum : Implications for human. *Chaos* 19:1–30
 44. Thelen DG, Schultz AB, Alexander NB, Ashton-Miller JA (1996) Effects of age on rapid ankle torque development. *J Gerontol* 51:M226–M232
 45. Schultz AB, Ashton-Miller JA (1991) “Biomechanics of the Human Spine” in *Basic Orthopaedic Biomechanics*, 1st ed. Raven Press, New York
 46. Sepic SB, Murray MP, Mollinger LA, Spurr GB, Gardner GM (1986) Strength and range of motion in the ankle in two age groups of men and women. *Am J Phys Med* 65:75–84
 47. Boone DC, Azen SP (1979) Normal range of motion of joints in male subjects. *J Bone Joint Surg Am* 61:756–759
 48. Burdet C, Rougier P (2007) Analysis of center-of-pressure data during unipedal and bipedal standing using fractional Brownian motion modeling. *J Appl Biomech* 23:63–69
 49. Pai Y, Patton JL (1997) Center of Mass Velocity-Position for Balance Control Predictions. *Phys Ther* 30:347–354
 50. Yang F, Espy D, Pai Y (2009) Feasible stability region in the frontal plane during human gait. *Ann Biomed Eng* 37:2606–2614
 51. Hof AL, Gazendam MGJ, Sinke WE (2005) The condition for dynamic stability. *J*

Biomech 38:1–8

52. McIlroy WE, Maki BE (1993) Changes in early “automatic” postural responses associated with the prior-planning and execution of a compensatory step. *Brain Res* 631:203–211
53. Van Der Kooij H, Jacobs R, Koopman B, Grootenboer H (1999) A multisensory integration model of human stance control. *Biol Cybern* 80:299–308
54. Eckner JT, Richardson JK, Kim H, Lipps DB, Ashton-Miller JA (2012) A novel clinical test of recognition reaction time in healthy adults. *Psychol Assess* 24:249–254
55. Nishtala PS, Narayan SW, Wang T, Hilmer SN (2014) Associations of drug burden index with falls, general practitioner visits, and mortality in older people. *Pharmacoepidemiol Drug Saf.* doi: 10.1002/pds.3624
56. Richardson JK (2002) The clinical identification of peripheral neuropathy among older persons. *Arch Phys Med Rehabil* 83:1553–1558
57. Olson VL, Smidt GL, Johnston RC (1972) The maximum torque generated by the eccentric, isometric, and concentric contractions of the hip abductor muscles. *Phys Ther* 52:149–158
58. Widler KS, Glatthorn JF, Bizzini M, Impellizzeri FM, Munzinger U, Leunig M, Maffiuletti NA (2009) Assessment of hip abductor muscle strength. A validity and reliability study. *J Bone Jt Surg - Ser A* 91:2666–2672
59. Lawrence RK, Kernozek TW, Miller EJ, Torry MR, Reuteman P (2008) Influences of hip external rotation strength on knee mechanics during single-leg drop landings in females. *Clin Biomech* 23:806–813
60. Malliaras P, Hogan A, Nawrocki A, Crossley K, Schache A (2009) Hip flexibility and strength measures: Reliability and association with athletic groin pain. *Br J Sports Med* 43:739–744
61. Delp SL, Loan P, Hoy MG, Zajac FE, Topp EL, Rosen JM (1990) An Interactiv Gaphics-Based Model of the Lower Extremity to Study Orthopaedic Surgical Procedures. *IEEE Trans Biomed Eng* 37:757–67
62. Ehrig RM, Taylor WR, Duda GN, Heller MO (2006) A survey of formal methods for determining the centre of rotation of ball joints. *J Biomech* 39:2798–2809
63. Ehrig RM, Heller MO, Kratzenstein S, Duda GN, Trepczynski A, Taylor WR (2011) The SCoRE residual: A quality index to assess the accuracy of joint estimations. *J Biomech*

44:1400–1404

64. Zatsiorsky VM, King DL (1997) An algorithm for determining gravity line location from posturographic recordings. *J Biomech* 31:161–164
65. Winter DA (2009) *Biomechanics and Motor Control of Human Movements*. John Wiley & Sons
66. Chandler RF, Clauser CE, McConville JT, Reynolds HM, Young JW (1975) Investigation of inertial properties of the human body. *Traffic Saf* 1–169
67. Harry G. Armstrong Aerospace Medical Research Laboratory (1988) *Anthropometry and Mass Distribution for Human Analogues: Military Male Aviators. I:*
68. Yeadon MR, Morlock M (1989) The appropriate use of regression equations for the estimation of segmental inertia parameters. *J Biomech* 22:683–689
69. Woltring HJ (1985) On optimal smoothing and derivative estimation from noisy displacement data in biomechanics. *Hum Mov Sci* 4:229–245
70. van den Bogert AJ, Su A (2008) A weighted least squares method for inverse dynamic analysis. *Comput Methods Biomech Biomed Engin* 11:3–9
71. Arnold A, Komattu A, Delp SL (1997) Internal rotation gait : a compensatory mechanism to restore abduction capacity deformity ? *Dev Med Child Neurol* 39:40–4
72. Širca A, Sušec-Michieli M (1980) Selective type II fibre muscular atrophy in patients with osteoarthritis of the hip. *J Neurol Sci* 44:149–159
73. Johnson MA, Polgar J, Weightman D, Appleton D (1973) Data on the distribution of fibre types in thirty-six human muscles. An autopsy study. *J Neurol Sci* 18:111–129
74. Wang TG, Jan MH, Lin KH, Wang HK (2006) Assessment of Stretching of the Iliotibial Tract With Ober and Modified Ober Tests: An Ultrasonographic Study. *Arch Phys Med Rehabil* 87:1407–1411
75. Ober FR (1936) The role of iliotibial band and fascia lata as a factor in the causation of low-back disabilities and sciatica. *J Bone Jt Surg* 105–110
76. Putz R, Pabst R (eds) (2006) *Sobotta Atlas of Human Anatomy, Volume 2: Trunk, Viscera, Lower Limb*. URBAN & FISCHER
77. Birnbaum K, Siebert CH, Pandorf T, Schopphoff E, Prescher A, Niethard FU (2004) Anatomical and biomechanical investigations of the iliotibial tract. *Surg Radiol Anat* 26:433–446

78. Hammer N, Lingslebe U, Aust G, Milani TL, Hädrich C, Steinke H (2012) Ultimate stress and age-dependent deformation characteristics of the iliotibial tract. *J Mech Behav Biomed Mater* 16:81–86
79. Darwin KA, Baker AR, Spragg RK, Leigh DR, Farhat W, Iannotti JP (2006) Regional variability, processing methods, and biophysical properties of human fascia lata extracellular matrix Kathleen. *J Biomed Mater Res*. doi: 10.1002/jbm.a
80. Zwirner J, Babian C, Ondruschka B, Schleifenbaum S, Scholze M, Waddell NJ, Hammer N (2019) Tensile properties of the human iliotibial tract depend on height and weight. *Med Eng Phys* 69:85–91
81. Steinke H, Lingslebe U, Böhme J, Slowik V, Shim V, Hädrich C, Hammer N (2012) Deformation behavior of the iliotibial tract under different states of fixation. *Med Eng Phys* 34:1221–1227
82. Eng CM, Arnold AS, Lieberman DE, Biewener AA (2015) The capacity of the human iliotibial band to store elastic energy during running. *J Biomech* 48:3341–3348
83. Davis BL, Grabiner MD (1996) Modeling effects of muscle fatigue on unilateral postural control. *J Appl Biomech* 12:173–184
84. Cabrera JL, Milton JG (2002) On-off intermittency in a human balancing task. *Phys Rev Lett* 89:158702
85. Vellas BJ, Rubenstein LZ, Ousset PJ, Faisant C, Kostek V, Nourhashemi F, Allard M, Albarede JL (1997) One-leg standing balance and functional status in a population of 512 community-living elderly persons. *Aging Clin Exp Res* 9:95–98
86. Rogers MW, Mille M-L (2003) Lateral stability and falls in older people. *Exerc Sport Sci Rev* 31:182–187
87. Greenspan SL, Myers ER, Kiel DP, Parker RA, Hayes WC, Resnick NM (1998) Fall direction, bone mineral density, and function: Risk factors for hip fracture in frail nursing home elderly. *Am J Med* 104:539–545
88. Hayes WC, Myers ER, Morris JN, Gerhart TN, Yett HS, Lipsitz LA (1993) Impact near the hip dominates fracture risk in elderly nursing home residents who fall. *Calcif Tissue Int* 52:192–198
89. Gutierrez EM, Helber MD, Dealva D, Ashton-Miller JA, Richardson JK (2001) Mild diabetic neuropathy affects ankle motor function. *Clin Biomech* 16:522–528

90. Rossi M, Lyttle A, El-Sallam A, Benjanuvatra N, Blanksby B (2013) Body segment inertial parameters of elite swimmers using DXA and indirect methods. *J Sport Sci Med* 12:761–775
91. Villareal DT, Banks M, Siener C, Sinacore DR, Klein S (2004) Physical frailty and body composition in obese elderly men and women. *Obes Res* 12:913–920
92. Kingma I, Toussaint HM, Commissaris DACM, Hoozemans MJM, Ober MJ (1995) Optimizing the determination of the body center of mass. *28:1137–1142*
93. Vaughan CL, Andrews JG, Hay JG (1982) Selection of body segment parameters by optimization methods. *J Biomech Eng* 104:38–44
94. Dempster WT, Gabel WC, Felts WJ (1959) The anthropometry of the manual work space for the seated subject. *Am J Phys Anthropol* 17:289–317
95. Isman R, Inman VT, Poor P (1969) Anthropometric studies of the human foot and ankle. *Bull Prosthet Res*
96. Dumas R, Chèze L, Verriest JP (2007) Adjustments to McConville et al. and Young et al. body segment inertial parameters. *J Biomech* 40:543–553
97. Kingma I, Toussaint HM, De Looze MP, Van Dieën JH (1996) Segment Inertial Parameter Evaluation in Two Anthropometric Models by Application of a Dynamic Linked Segment Model. *J Biomech* 29:693–704
98. De Leva P (1996) Adjustments to zatsiorsky-seluyanov’s segment inertia parameters. *J Biomech* 29:1223–1230
99. Norton J, Donaldson N, Dekker L (2002) 3D whole body scanning to determine mass properties of legs. *J Biomech* 35:81–86
100. Crossley KM, Zhang WJ, Schache AG, Bryant A, Cowan SM (2011) Performance on the single-leg squat task indicates hip abductor muscle function. *Am J Sports Med* 39:866–873
101. Johnson ME, Mille M-LL, Martinez KM, Crombie G, Rogers MW (2004) Age-related changes in hip abductor and adductor joint torques. *Arch Phys Med Rehabil* 85:593–597